Hydrodynamic Modeling in Support of Franks Tract Restoration Feasibility Study, Delta Resiliency Strategy

Eli Ateljevich PE, Ph.D.
Kijin Nam PE, Ph.D.
Bay-Delta Office
Delta Modeling Section
California Department of Water Resources

December 2017

STATE OF CALIFORNIA
Edmund G. Brown Jr., Governor

THE NATURAL RESOURCES AGENCY
John Laird, Secretary for Resources

DEPARTMENT OF WATER RESOURCES
Grant Davis, Director

Cindy Messer
Chief Deputy Director

Michelle Banonis
Assistant Chief Deputy Director

Joel Ledesma Deputy Director	Kathie Kishaba Deputy Director	Taryn Ravazzini Deputy Director	Christy Jones Deputy Director

Erin Mellon Assistant Director, Public Affairs	Kasey Shimke Assistant Director, Legislation	Spencer Kenner Chief Counsel

BAY - DELTA OFFICE
Francis Chung, Chief

This report was prepared under the supervision of

Nicky Sandhu ....Supervising Engineer, Water Resources
Tara Smith ....Principle Engineer, Water Resources

by

Eli Ateljevich…………………………………………………… Senior Engineer, Water Resources
Kijin Nam…………………………………………………… Senior Engineer, Water Resources

with assistance from

Rueen-Fang Wang……………………………………………………Engineer, Water Resources

Table of Contents

Table

Figures

Acronyms and Abbreviations

CDEC	California Data Exchange Center
CDFW	California Department of Fish and Wildlife
cfs	cubic feet per second
cm	centimeters
CTD	conductivity-temperature-depth
CVP	Central Valley Project
D-1641	California State Water Resources Control Board Decision 1641
Delta	Sacramento-San Joaquin Delta
DWR	California Department of Water Resources
EC	electric conductivity (used often for specific conductance)
EDB	West False River emergency drought barrier
ESA	Environmental Science Associates
ft/s	feet per second
NAVD88	North American Vertical Datum of 1988
NOAA	National Oceanic and Atmospheric Administration
RMA	Resource Management Associates
SAV	submerged aquatic vegetation
SCHISM	Semi-implicit Cross-scale Hydroscience Integrated System Model
SWP	California State Water Project
µS/cm	micro-Siemens per centimeter
USGS	U.S. Geological Survey

Chapter 1. Project Description and Methods

1.1 Summary

This report summarizes 3-D hydrodynamics modeling performed by the Bay-Delta Office of the California Department of Water Resources (DWR) for the California Department of Fish and Wildlife (CDFW), in support of the *Franks Tract Feasibility Study*. The study is a component of the *Delta Smelt Resiliency Strategy*, and examines the feasibility and impact of partially restoring Franks Tract to a mostly intertidal marsh.

The modeling work in this report includes:

1. Analyzing velocities in and around the restoration site during and after construction, to help determine materials and construction requirements.
2. Describing the likely need or benefits of hydraulic structures in remnant channels to control velocities outside the main body of Franks Tract.
3. Predicting changes in tidal and net flows caused by the project.
4. Anticipating salinity impacts of the project and one alternative design relative to current conditions.
5. Sensitivity of regional salinity results to the presence of submerged aquatic vegetation (SAV), including refinement of SAV formulation to satisfy the modeling requirements of this and other smelt resiliency projects.
6. Analyzing synergy between this project and three additional restoration projects that were considered most likely to cause an interaction (Dutch Slough, Prospect Island, and McCormack-Williamson Tract).

The main conclusions of model simulations of project impacts are:

1. The restoration causes local changes in flow, particularly tidal flow. The most substantial increases occur in Fisherman's Cut and on Old River between the San Joaquin River and Franks Tract.
2. Restoring Franks Tract reduces salinity intrusion into the mid-Sacramento-San Joaquin Delta (Delta). It potentially increases salinity on the main stems of the San Joaquin River, particularly between Jersey Point and San Andreas Landing. The project may increase the water cost of California State Water Resources Control Board Decision 1641(D-1641) compliance at San Andreas Landing, but this is more likely in conjunction with other projects that affect Delta Cross Channel flow.
3. SAV inhibits circulation on Franks Tract but does not limit freshening of the mid-Delta as it did during the 2015 West False River emergency drought barrier (EDB) installation.

1.2 Site Characterization

Franks Tract is a flooded island located near the confluence of the Sacramento and San Joaquin rivers (Figure 1). Just to the northwest lies Little Franks Tract, a smaller flooded island adjacent to Franks Tract, which is also included in the restoration designs.

Figure 1 Franks Tract Location in the Sacramento-San Joaquin Delta

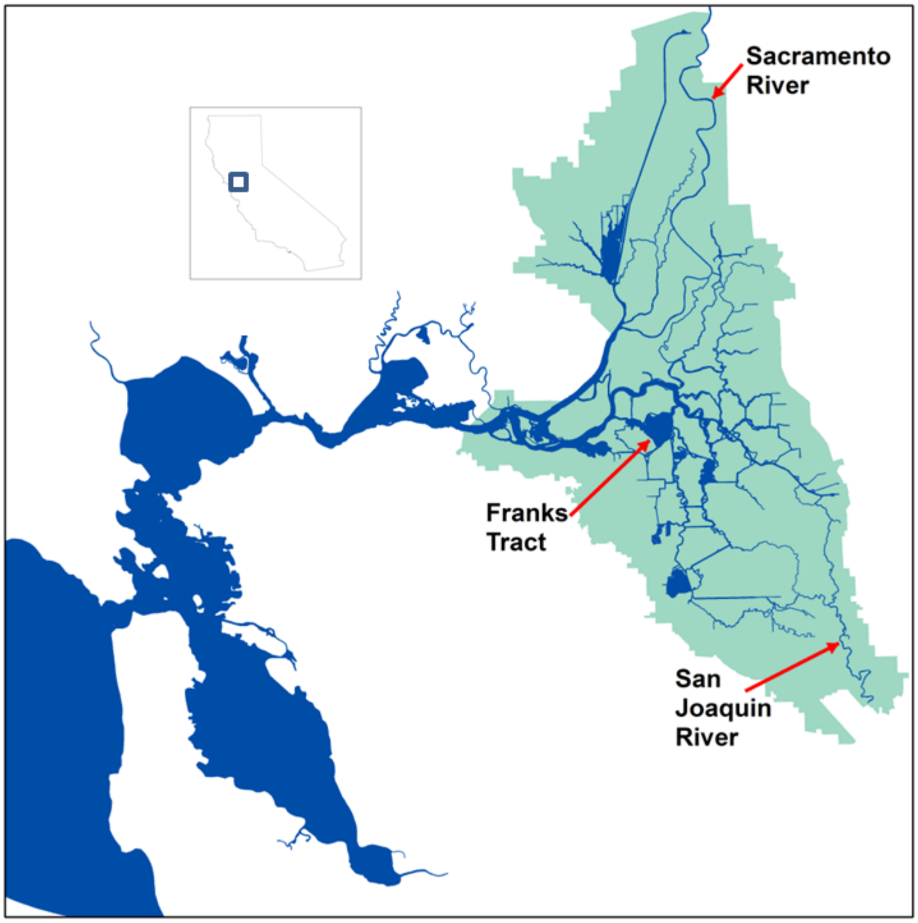

Figure 2 shows the existing bathymetry in Franks Tract and Little Franks Tract, and some of the physical features around them. Levees, in many cases deteriorated, remain along much of the perimeter, with numerous breaches leading to the interior of the tract. The island is shallow, generally less than 8 feet deep. Local mean sea level is approximately 3.75 feet NAVD88 (North American Vertical Datum of 1988). The tidal range is approximately 3.5 feet. The channels and remnant channels at its perimeter are deeper. Several of the perimeter breaches are scoured.

Labels have been added to a number of frequently discussed features. The *nozzles* are places water enters the tract from False River through relatively narrow breaches. The water enters as a jet, like a firehose discharging into a swimming pool. The *2015 drought barrier site* is the location of the EDB temporary rock barrier was placed in 2015. It produced changes that are the closest historical analog available to the present project. *OSJ* is the USGS monitoring station Old River at Franks Tract, which lies on a short reach of Old River between Franks Tract and the San Joaquin River. It is included because it is ubiquitous in discussions of Franks Tract dynamics. Finally, research for this report revealed a naming ambiguity in the northern channel. Some maps refer to "False River" and others to "Washington Cut." In this report, it is referred to as False River.

Figure 2 Franks Tract Bathymetry and some Physical Features

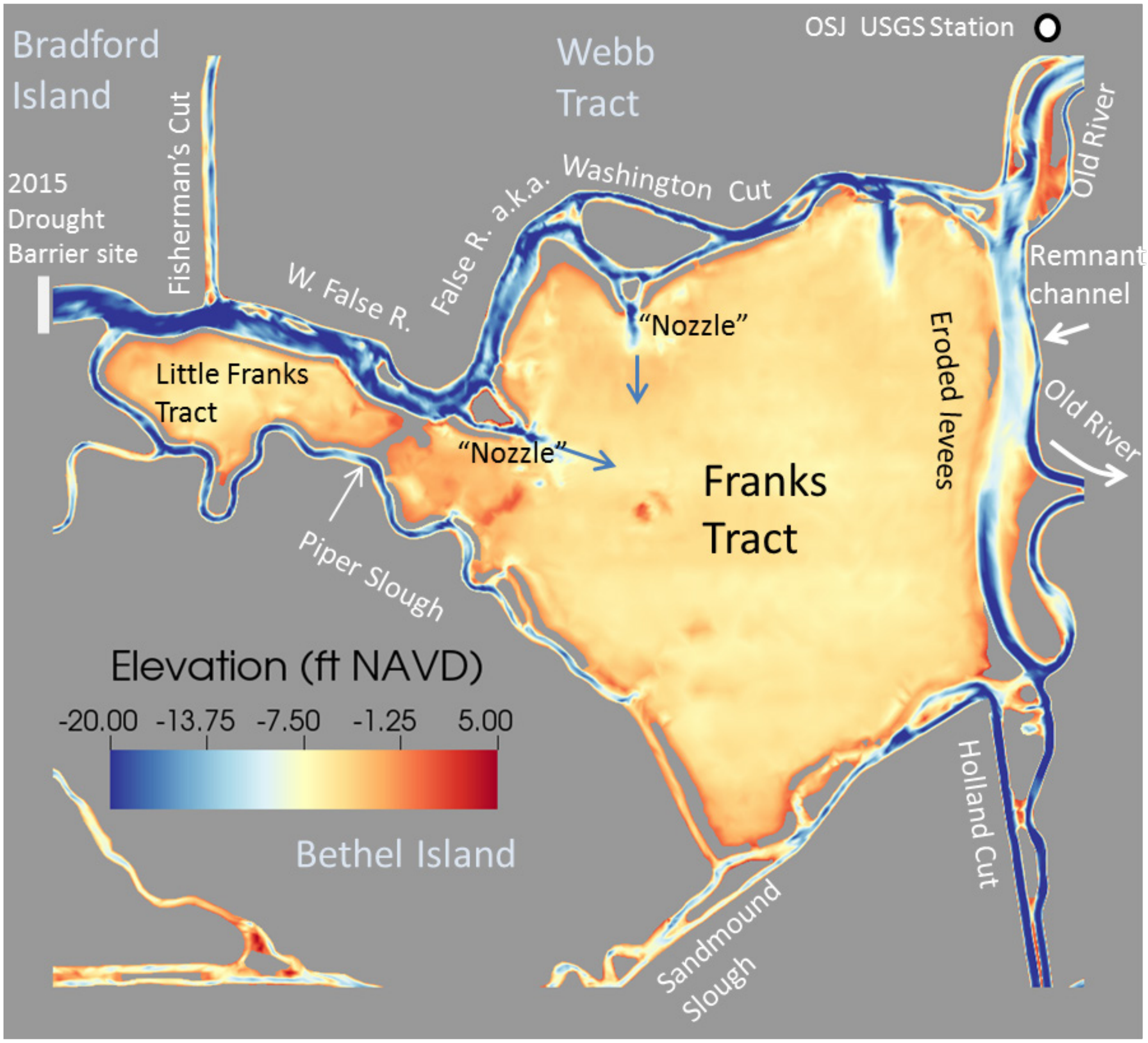

Note: NAVD = North American Vertical Datum, OSJ = California Data Exchange Code for Old River at Franks Tract, USGS = U.S. Geological Survey

Franks Tract is heavily vegetated. The vegetation has been noted to increase in recent years. Figure 3 is a map of the Normalized Difference Vegetation Index from 2015. The index has been binned to highlight the presences/absence of submerged species. The year 2004 was originally chosen as a model of typical patterns, because it has a starker contrast between the main channel through the vegetation and the vegetation canopy. But monitoring and accounts from the authors (Khanna pers. comm. 2017) suggest that the new, denser vegetation with a vague main channel has recurred.

Figure 3 September 2015 Binned Normalized Difference Vegetation Index

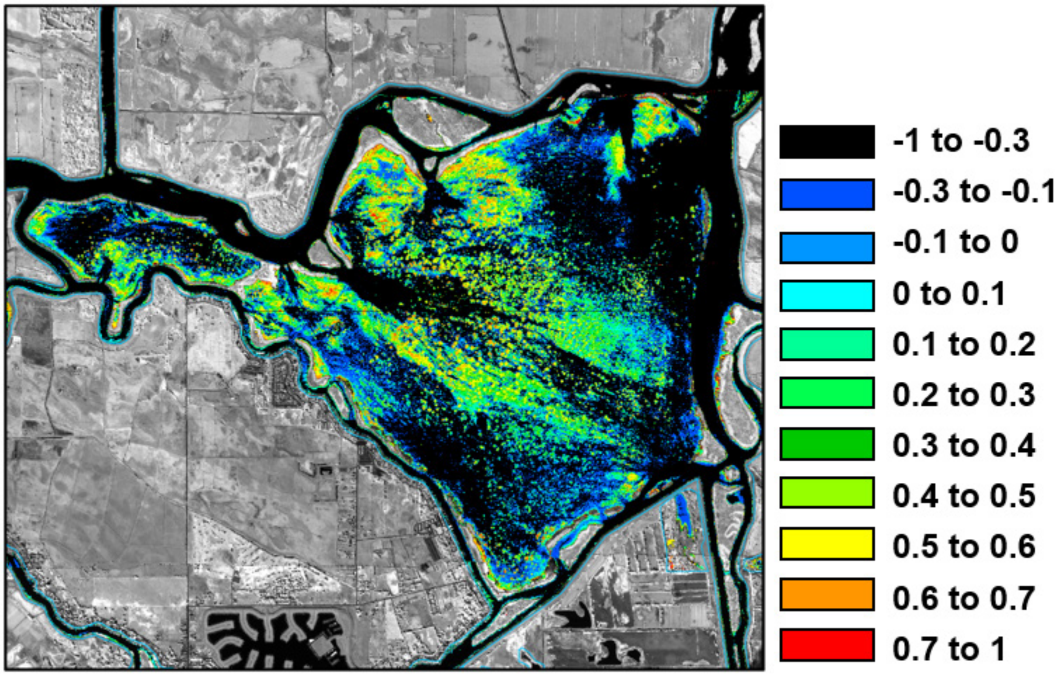

Source: Ustin et al. 2016.
Note: Higher values suggest higher density of vegetation.

1.3 Conceptual Plan for Restoration

The conceptual plan for restoring Franks Tract and Little Franks Tract is indicated in Figure 4, which was provided by CDFW. An earlier alternative with a levee set further east is shown Figure 5 and including a much larger fraction of Franks Tract. This variant was modeled and produced changes in tides and regional salinity similar to the results presented here for the preferred design, but in terms of habitat was regarded by most stakeholders as less advantageous to smelt.

The conceptual design uses a large barrier to divide Franks Tract into a western restored side and an eastern unperturbed side. Within the restoration area, the bed is graded to intertidal elevations. Some higher areas are included in the design to accommodate for sea level rise. A small region near the main berm is designated high marsh. The implementation of the channels followed the conceptual plan closely, though two channels are slightly longer and more sinuous than in the original conceptual plan to provide better drainage and less sheet flow, which was found to dominate velocity patterns in an early iteration of the modeling. Guidelines from the Dutch Slough design by Environmental Science Associates (ESA) were used to size the channels for Franks Tract, but the design included only the two highest orders of channels (the mesh is shown in Figure 8). The bed of the tidal channels was positioned at existing grade almost everywhere, which reduced costs, maintained some variability, and produced elevations that are typical of restoration designs. By comparison, the restoration design for Little Franks Tract is relatively simple, with existing bathymetry near the breaches and gradual slopes upward toward the northeast and southwest.

Figure 4 Draft Conceptual Design as Delivered by California Department of Fish and Wildlife

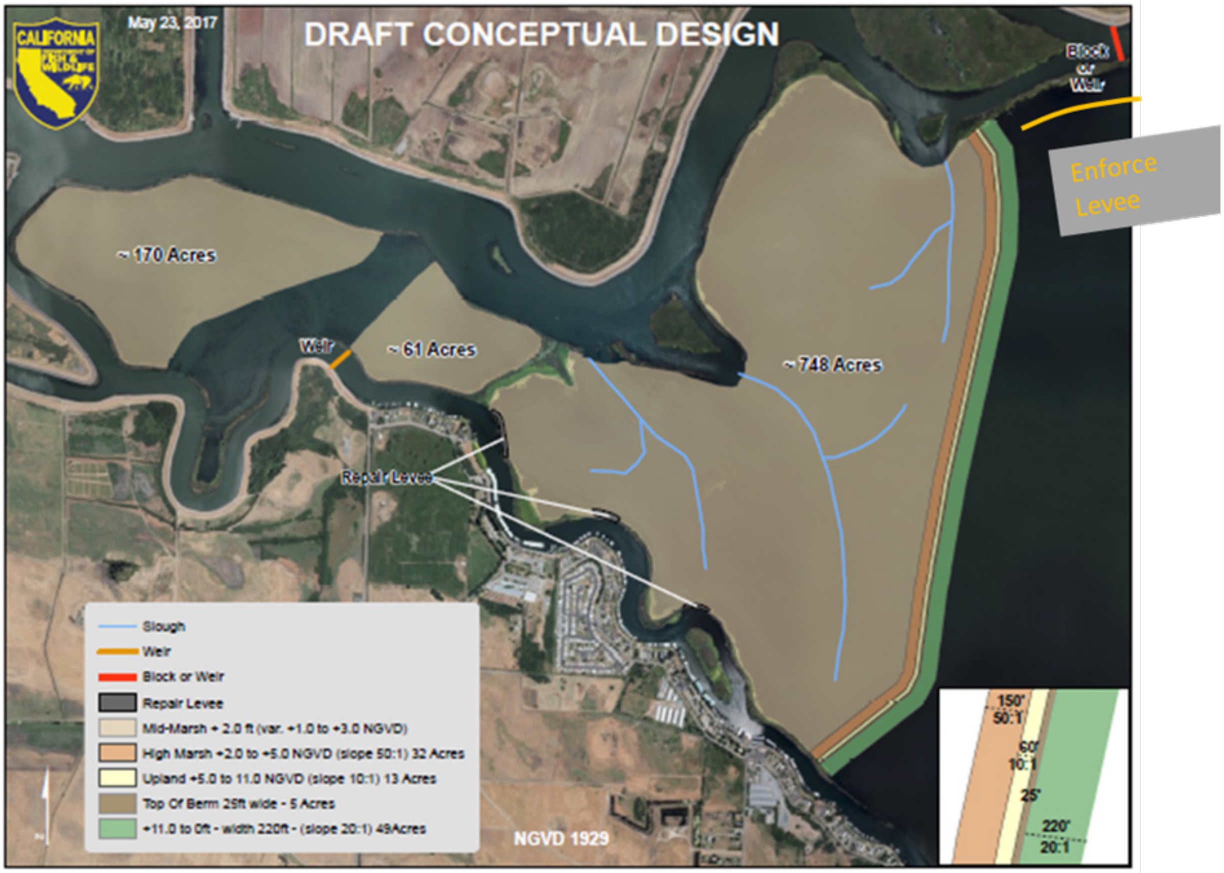

Note: One levee requiring enforcement has been annotated.

The restoration design included a small stretch of levee, annotated in orange in Figure 4, which is expected to experience higher-than-historical head differences because it separates waters that are hydraulically connected to the two “sides” of the main project, which will be tidally out of phase. Given the added stresses on this levee, it is recommended that this levee be reinforced to a similar standard as the main berm.

Some model simulations reported in this document include other regional restoration sites, including Dutch Slough, Prospect Island, and McCormack-Williamson Tract. The meshing and modeling for these projects is described briefly in the sensitivity section of Chapter 3, but the projects themselves are not described in detail in this report.

1.4 Model Description

The model used in this study is Bay-Delta SCHISM, which is based on the Semi-Implicit Cross-scale Hydroscience Integrated System Model (SCHISM, Zhang et al. 2016), which in turn is derived from the semi-implicit Eulerian-Lagrangian finite-element (SELFE) model (Zhang and Baptista 2008). SCHISM is an open-source community-supported modeling system, whose origins were to serve as a second-generation model (following ELCIRC, a Eulerian–Lagrangian algorithm used to solve shallow water

Figure 5 Prior Draft of Conceptual Plan with Restoration Encompassing most of Franks Tract

equations) for use in the Columbia River estuary by the Center for Coastal Margin Observation and Prediction (CMOP). The model has subsequently been enhanced by the Virginia Institute of Marine Sciences and used in basins throughout the world in applications as diverse as reservoir temperature, estuarine transport of salinity, morphology, and near-coast tsunami response. The model has participated in numerous regional benchmarks. A list of peer-reviews papers is maintained on the model website (http://ccrm.vims.edu/schismweb). The larger SCHISM suite includes modules for sediment transport, ecology/biology, wind-wave interaction, ice, oil spill, and marsh evolution, listed approximately in order from greatest to least maturity.

The SCHISM hydrodynamic algorithm is based on mixed triangular-quadrangular unstructured grids in the horizontal and a flexible coordinate system in the vertical (localized sigma coordinates with shaved cells, or LSC^2, Zhang et al. 2015). The modeling system utilizes a semi-implicit finite-element/finite-volume method together with a Eulerian-Lagrangian method (ELM) for momentum advection to solve the Reynolds-averaged Navier-Stokes and transport equations at ocean to creek scales. It has both a hydrostatic and non-hydrostatic option, but as explained in MacWilliams et al. (2016) non-hydrostatic modeling is not feasible at field scale in the Bay-Delta.

The formulation of the core SCHISM hydrodynamic module is based on the 3-D hydrostatic Reynolds-averaged shallow water equations, including mass conservation, horizontal momentum conservation and salinity transport:

$$\nabla \cdot \boldsymbol{u} + \frac{\partial w}{\partial z} = 0 \tag{1}$$

$$\frac{D\mathbf{u}}{Dt} = -f\mathbf{k} \times \mathbf{u} - \frac{\mathbf{1}}{\rho_0} \nabla p_A - \frac{g}{\rho_0} \int_z^{\eta} \nabla \rho \, d\xi - g\nabla\eta + \frac{\boldsymbol{\partial}}{\boldsymbol{\partial z}}\left(\nu \frac{\boldsymbol{\partial u}}{\boldsymbol{\partial z}}\right) + \nabla \cdot (\mu \nabla \boldsymbol{u}) \tag{2}$$

$$\frac{DS}{Dt} = \frac{\boldsymbol{\partial}}{\boldsymbol{\partial z}}\left(\kappa \frac{\boldsymbol{\partial u}}{\boldsymbol{\partial z}}\right) \tag{3}$$

Where

η is the elevation of the water surface,
vector **u** represents the (x,y) directional components of velocity,
w is vertical velocity,
S is salinity,
g is gravity,
f is the Coriolis force,
k is the unit vector in the vertical direction,
ρ_0 is a reference density for water,
∇p_A is atmospheric pressure,
$\rho(x, t)$ is density,
ξ is a dummy variable for integration,
μ is horizontal diffusivity,
ν is vertical eddy viscosity, and
κ is vertical eddy diffusivity.

Both the formulation and algorithm in SCHISM share many points in common with other 3-D models used in the estuary, including the use of an unstructured geometry, implicit treatment of certain destabilizing terms, and a splitting that features the efficient cointegration of mass conservation (equation 1) in vertically integrated form along with vertically integrated momentum conservation (equation 2). Technically, SCHISM departs from many of the other most common models in its use of a finite element method (FEM) representation of some of these steps. Because of the use of FEM, SCHISM is able to use a terrain-conforming vertical mesh and is more robust to skew mesh element shape so the grid can follow internal channels without requiring very high resolution. On the other hand, the FEM formulation does not promise local (i.e., per-element) mass conservation as do finite volume representations.

As with most well-resolved applications in the estuary, horizontal momentum diffusion was neglected (μ=0 m^2/s). The elimination of horizontal viscosity is justified on the assumption that a well-resolved horizontal grid captures mixing because the largest scales of circulation and a modest amount of numerical diffusion are sufficient to model horizontal mixing at smaller scales.

Boundary conditions for the water column are given by wind stresses at the free surface and shear at the bed. For wind, the boundary condition is

$$\nu \frac{\partial u}{\partial z} = \tau_w, \text{ at } z = \eta \tag{4}$$

using the wind stress (τ_w) formulation from Large and Pond (1981). The boundary condition at the bed ($z = -h$) is

$$\nu \frac{\partial u}{\partial z} = \tau_b, \text{ at } z = -h \tag{5}$$

with bottom stress (τ_b) derived from a quadratic formulation based on the velocity ($\boldsymbol{u}_b$) evaluated at the top of the bottom computational cell and is

$$\tau_b = C_D|\boldsymbol{u}_b|\boldsymbol{u}_b \tag{6}$$

The drag coefficient (C_D) of roughness is calculated dynamically from a roughness parameter by using standard boundary layer assumptions as described in Zhang (2008). The values of roughness used here vary from 0.1 millimeter in shallow areas to 10 millimeters at depth.

The turbulent eddy viscosity (ν) and eddy diffusivity (κ) is generated by using an independent set of turbulence closure equations, specifically the k-kl 2.5 equation closure with a background eddy viscosity of 0.00001 m^2s^{-1}. The closure is implemented in SCHISM by using the Generic Length Scale approach of Umlauf and Burchard (2003).

Entrainment is studied using a particle streamlines of neutrally buoyant particles. For purposes of this study, the equations of motion for each particle are accordingly advection with flow with a small amount of added diffusion.

$$\frac{d\boldsymbol{x}_i}{dt} = \boldsymbol{u}(\boldsymbol{x}_i, t) + \varepsilon d\boldsymbol{W}_t \tag{7}$$

where $\boldsymbol{x}_i$ is the position of the i'th particle and $\boldsymbol{u}(\boldsymbol{x}_i, t)$ is its 3-D velocity at time t. This formulation includes a uniform background diffusion parameter in the vertical direction, but not in the horizontal. The diffusion ϵ parameter is chosen to provide some minimum background diffusivity while still emphasizing mean flow processes. The chosen value (0.0001 m^2s^{-1}) is smaller than the spatially variable parameter that would be used to link the formulation with the SCHISM transport equation for dissolved species.

1.5 Discretization

The Franks Tract modeling is embedded within a larger domain encompassing the entire San Francisco Bay-Delta (Figure 6). The model domain spans from the Farallon Islands off the coast, to Vernalis on the San Joaquin River and Knights Landing on the Sacramento River. Horizontal resolution over the full domain varies from 5 meters in a small number of narrow small channels to 2 kilometers on the near coast. The most current version (version control label: v84_franksrestore) of the mesh used as the base condition for this study has 183,000 triangular and quadratic elements. The Franks Tract portion is shown in Figure 7. Resolution is 10 meters to 70 meters in Franks Tract, with higher resolution concentrated near inlets. The restoration cases involve higher resolution (elements 4 meters wide) than the base case within the channels on the marsh plain.

Figure 6 Bay-Delta SCHISM Full Mesh, Version 84_franksrestore

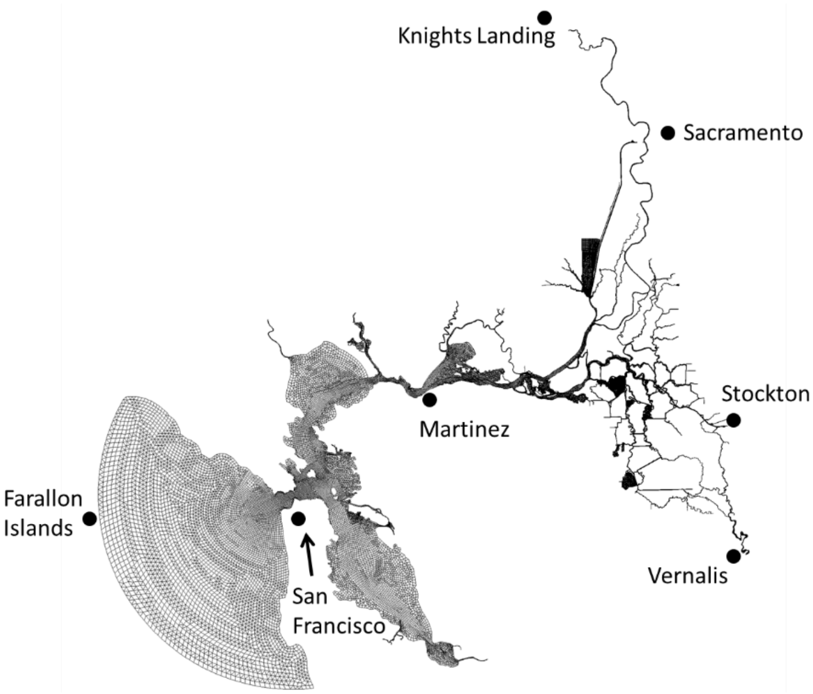

Figure 7 Franks Tract Portion of the Full Bay-Delta Mesh as used for the Base Geometry

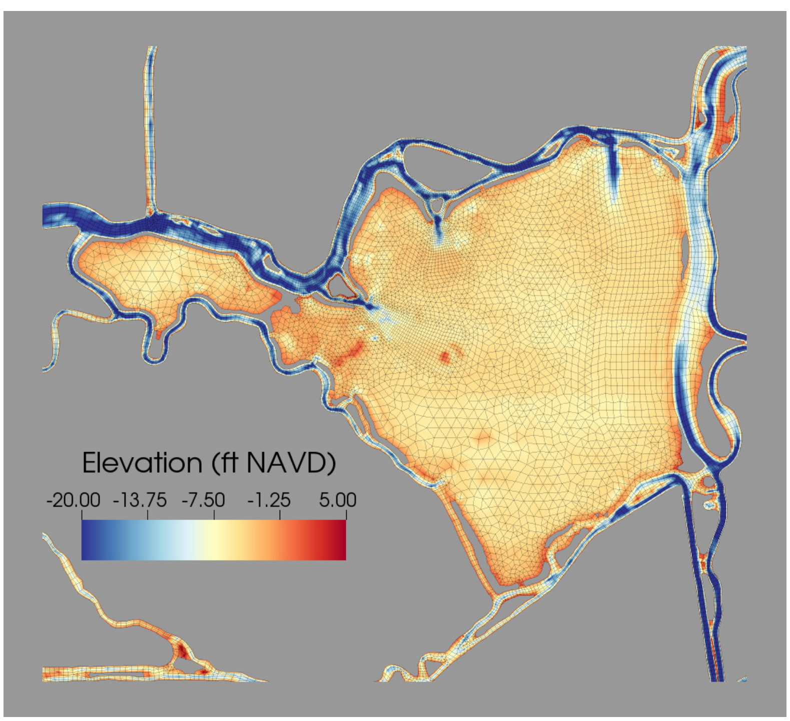

Note: The top elevation has been truncated at 5 feet NAVD88 to elicit contrasts.

Figure 8 Mesh and Bathymetry for the Restoration Study

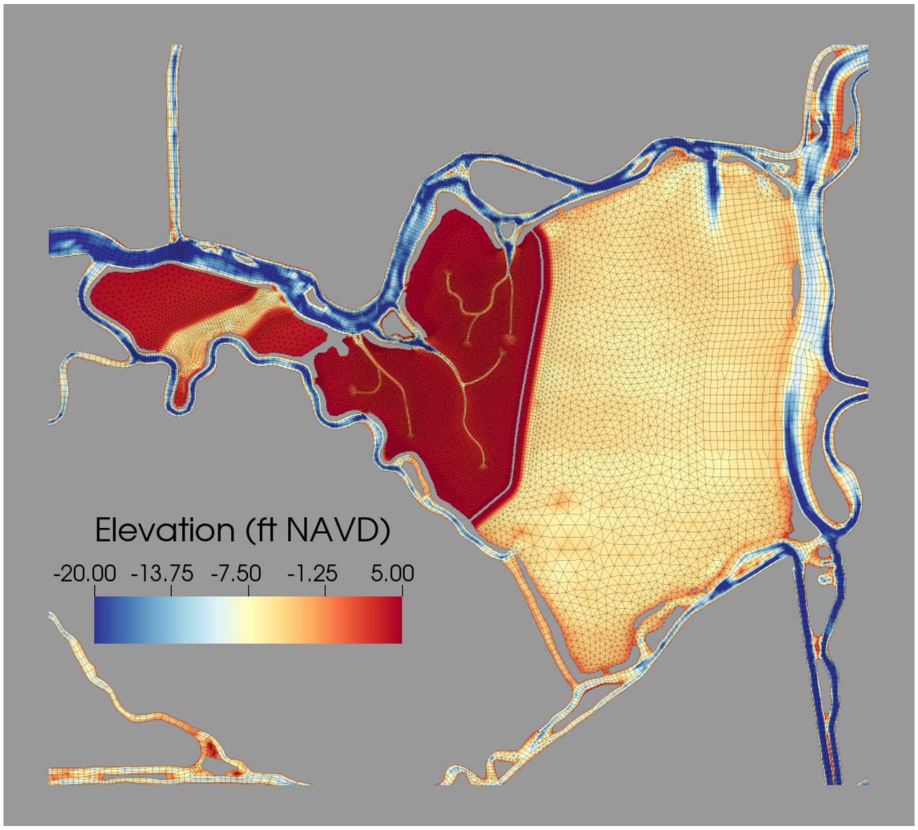

Note: The color scale has been truncated at 5 feet NAVD88 to elicit contrasts. Portions of the main berm are as high as 11 feet.

In the vertical, the model employs an adaptive, terrain conforming LSC^2 mesh ranging from 23 vertical levels in deep areas near the coast to a single (2-D) layer at the upstream reaches of the Sacramento and San Joaquin rivers. Within Franks Tract, there are 12 levels covering the approximate depth of 2 meters. Without vegetation or wind, Franks Tract is overwhelmingly 2-D. A well-resolved vertical mesh is needed either to resolve the wind boundary layer or to independently resolve the regions above and below the canopy. The use of an LSC^2 vertical grid represents a change from the original reporting of the application in Ateljevich (2014) when a 23-level terrain conforming "S" grid (Song and Haidvogel 1994) was used everywhere.

The model time step was 90 seconds for the work presented in this document. This is slightly shorter than the normal time step of 120 seconds needed to stabilize computations in small elements over the marsh plains.

1.6 Bathymetry

The project bathymetry comes from the maps prepared by Wang and Ateljevich (2012), with a number of regions updated by the preparation of new 2-meter maps. This map collated numerous collections; the majority of points in Franks Tract are attributed to a National Oceanic and Atmospheric Administration (NOAA) survey done in 1992. There is some slowness in updating bathymetry in the middle of Franks Tract region by Delta standards, which is the result, in part, of the thick vegetation and shallowness of Franks Tract, both of which make it difficult to conduct efficient multi-beam survey. In the channels proximate to Franks Tract, DWR has performed numerous additional multibeam surveys since 2013, many motivated by the 2015 EDB project, including collections at False River, Dutch Slough, Fisherman's Cut, Old River, and remnant channels along the eastern and northern rims of Franks Tract.

1.7 Model Inputs

Like any physically based flow models applied on an estuary, SCHISM requires an initial condition, bathymetry, and tidal and flow boundaries. As implemented, the model also requires wind and pressure fields, agricultural sources of mass and tracer concentration, gate and hydraulic structure timing, and in the case of SAV, vegetation parameters.

The nominal start date for all the work presented in this report is February 10, 2009, when the U.S. Geological Survey (USGS) Polaris cruise data (Schraga and Cloern 2017) were available to initialize salinity in the model by using conductivity-temperature-depth (CTD) vertical profiles or casts. For this project, which begins when the Delta is fresh, the simplest initialization practices was used: ocean salinity beyond the Golden Gate; Polaris CTD cast data in the bays for salinity, interpolating along the cruise route and vertically, and then extrapolating constant values laterally from the transect. A constant salinity value of 0.15 parts per thousand (equivalent to 300 µS/cm specific conductance) in the Delta represents fresh conditions. Water levels are initialized with a fixed elevation of 0.97 meter NAVD88 everywhere, and velocities are "cold started" from zero. To avoid misinterpretation of startup transients, there is no report for the first two weeks of hydrodynamic output, or the first three months of salinity or temperature.

The hydrodynamic forcing for the simulations comes from 2009 and 2010. Boundary conditions were implemented mostly in accordance with the practices described in Ateljevich et al. (2014), including upstream inflows from USGS gauges, pumping volumes from water project operators, and tide data along the near coast. The boundary data requirements are illustrated in Figure 9.

The modeling work presented in this report includes the major hydraulic structures in the Delta, including Delta Cross Channel, Montezuma Slough Salinity Control Structure, and South Delta agricultural barriers. Timing for most of the operable is shown in Figure 10 for 2009, and Figure 11 for 2010. Clifton Court radial gates are modeled using a radial gate rating, which is an improvement over earlier work. Details concerning the Clifton Court radial gate rating process as well as Harvey O. Banks Pumping Plant pumping data can be found in Ateljevich et al. (2015) and Shu and Ateljevich (2017), which elaborate on issues described by Smith (2011) and MacWilliams and Gross (2013). Unfortunately, the improvement is limited in 2009 because of missing data.

Another enhancement in the hydraulic structures introduced for this project was a better representation of the Sandmount Slough culverts and flap gates; previously, these were modeled as a complete blockage.

SCHISM also requires atmospheric forcing, including wind and air pressure as a minimum; other variables, such as air temperature, radiation, and specific humidity, are required for modeling temperature. One notable change in the modeling inputs since Ateljevich et al. (2014) is wind, which was formally based on climate reanalysis and weather products, but is now interpolated from 69 field stations operated by NOAA, Weatherflow, National Estuarine Research Reserve (NERR), California Irrigation Management Information System (CIMIS), Meteorological Terminal Aviation Routine (METAR) airports, DWR, and Bay Area Air Quality Management District (BAAQMD). One BAAQMD station

Figure 9 Flow, Water Level and Consumptive Use Inputs to Bay-Delta SCHISM

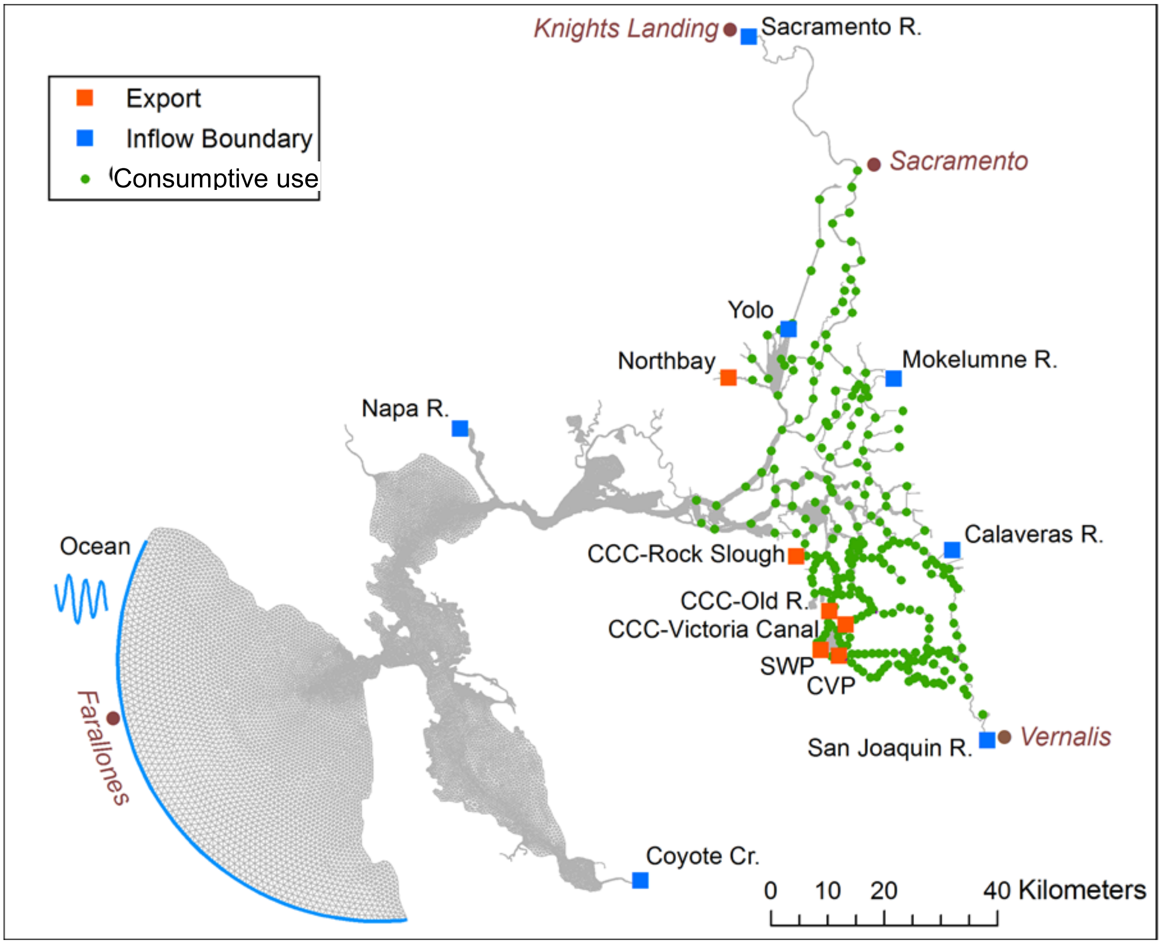

with a long historical wind record is situated on Bethel Island near Franks Tract. A newer DWR station was installed directly in Franks Tract (California Data Exchange Center [CDEC] code: FRK) in 2016.

Lastly, the model inputs for the present study used the Delta Evapotranspiration of Applied Water (DETAW) model as the basis of for channel depletions rather than the Delta Island Consumptive Use (DICU) that was used in Ateljevich (2015) and other earlier work. Channel depletions were adjusted to minimize seasonal discrepancies with USGS outflow, as described in Ateljevich (2015). Sandhu (2016) describes recent progress made by the Bay-Delta Office and other researchers on channel depletions and consumptive-use products for hydrodynamic modeling.

1.8 Model Period

The model simulations were carried out from February 10, 2009, through August 2010. Water Year 2009 was classified as dry; Water Year 2010 was classified as below normal. Most of the results are presented for August 2009 or November 2009. Some dates in March 2009 were used for velocity-only investigations. Some output dates were adjusted for locations near the Delta Cross Channel or South Delta Gates to investigate periods when those structures were in operation.

Figure 10 **Delta Hydraulic Structure Operations for 2009**

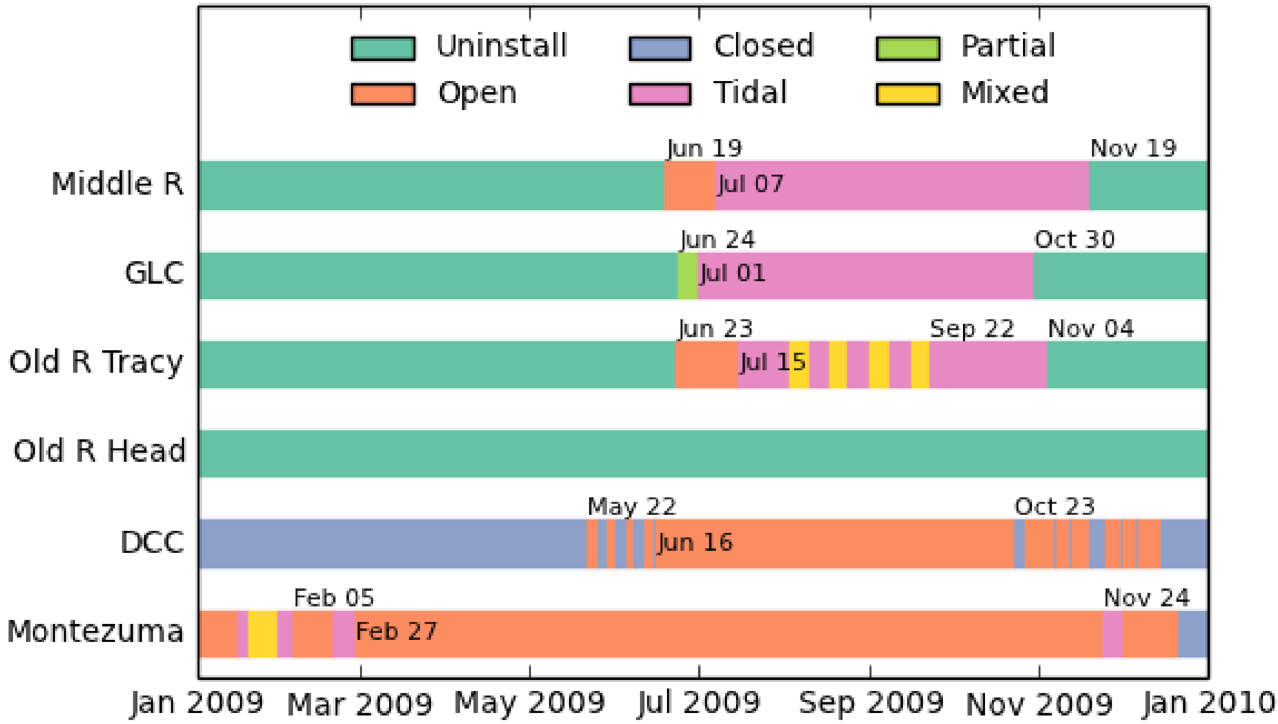

Figure 11 **Delta Hydraulic Structure Operations for 2010**

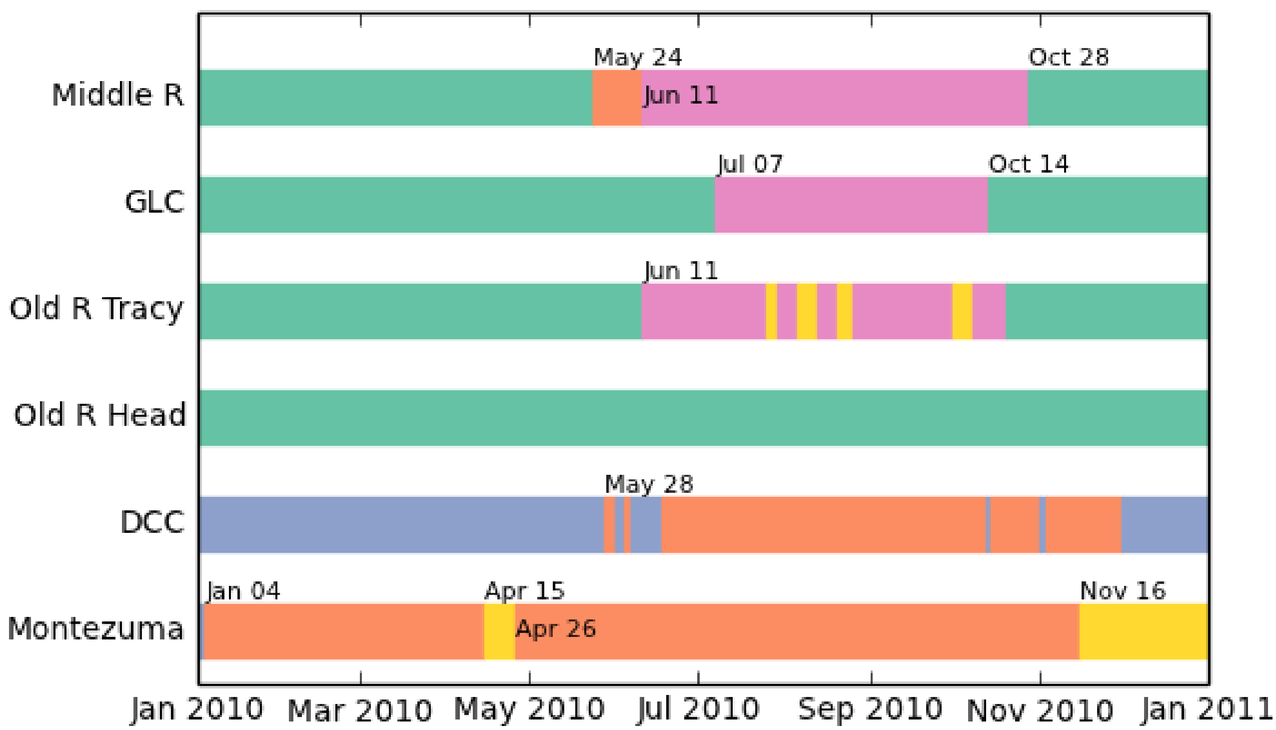

Chapter 2. Local Velocity Studies

Simulations were performed around the restoration site during peak tides in energetic periods to identify near-maximum tidal velocities for five purposes.

1. To identify velocities on the marsh plain and in the dendritic channels supplying them, to help determine stable fill materials.
2. To identify the largest currents in nearby waters that would affect construction and navigability.
3. To determine velocity changes post-project.
4. To identify peak velocities affecting closure of the main berm.
5. To determine whether barriers, weirs, or other structures were needed on False River and Piper Slough to control velocity, as suggested on the conceptual design of the description document.

Many of these were short simulations, utilizing energetic tidal periods near the beginning of March or around May 20.

As part of the materials selection and construction design objective, the peak tides of March 4, 2009, were found to exemplify energetic near-peak tides. One peak flood and two ebb snapshots of velocity were extracted to represent maxima at the site, as well as in nearby channels such as False River and Fisherman's Cut. These are shown in Figure 12 through Figure 14. Note that the velocity arrows only indicate general current directions. Magnitude plots include every element on the grid.

The study of closure velocity was undertaken with a specialty mesh of 8-meter, or finer, resolution along the length of the gap. Figure 15 provides an example of output. Snapshots were found to convey typical maximum conditions better than a mosaic of individual maxima collected from different times. Experiments were done at 100 feet, 500 feet, and 1,000 feet. Animations and stills were produced, concluding that typical tidal maxima are:

- 100-foot gap: 4 feet per second (ft/s).
- 500-foot gap: 2.9 ft/s.
- 1,000-foot gap: 2.5 ft/s.

These velocities were considerably lower than the 12 ft/s modeled during the closure of the 2015 EDB, which were confirmed informally by timing oranges thrown into the water. The lower values in Franks Tract were expected, given the expansion of flow as it enters the restoration area. Little dependence of closure velocity on tidal range was noted. As a result, there is little advantage to timing the closure to neap tide.

One-year simulations were used to examine permutations of "barrier," "weir," and "no structure" on Piper Slough, and "barrier" and "weir" on False River at the locations indicated (which lists False River as a barrier and Piper Slough as a barrier or weir). The original motive behind these structures was to prevent high velocities in the perimeter channels, and also to maintain hydraulic separation between False River and Old River for smelt. In the process of modeling Piper Slough, the list of goals included the need to promote some sort of through-flow to avoid very long residence times. It was discovered that velocities were somewhat elevated on Piper Slough with no structure (the maximum velocity snapshot in Figure 16, suggests velocities slightly more than 2 ft/s), but reasoned that they were probably within a tolerable range and had little effect on salinity over the greater region. Given that it is an economical combination, the combination of complete blockage on False River and no structure on Piper Slough was retained for all subsequent work.

Finally, velocities were also modeled in the stretch of Old River between the San Joaquin River and Franks Tract. The objectives in this case were twofold, to determine velocity patterns that construction crews might encounter in late-state construction of the main berm, and to examine navigability changes and scour potential in this channel following closure. Maximum velocities were found to be slightly stronger on flood than ebb. They reached 3 ft/s (Figure 17), which is lower than 2015, but higher than the 2.0–2.5 ft/s typical of base conditions.

Figure 12 Snapshot on March 4, 2009, 04:00, Showing Peak Flood Velocities in the Restoration Site

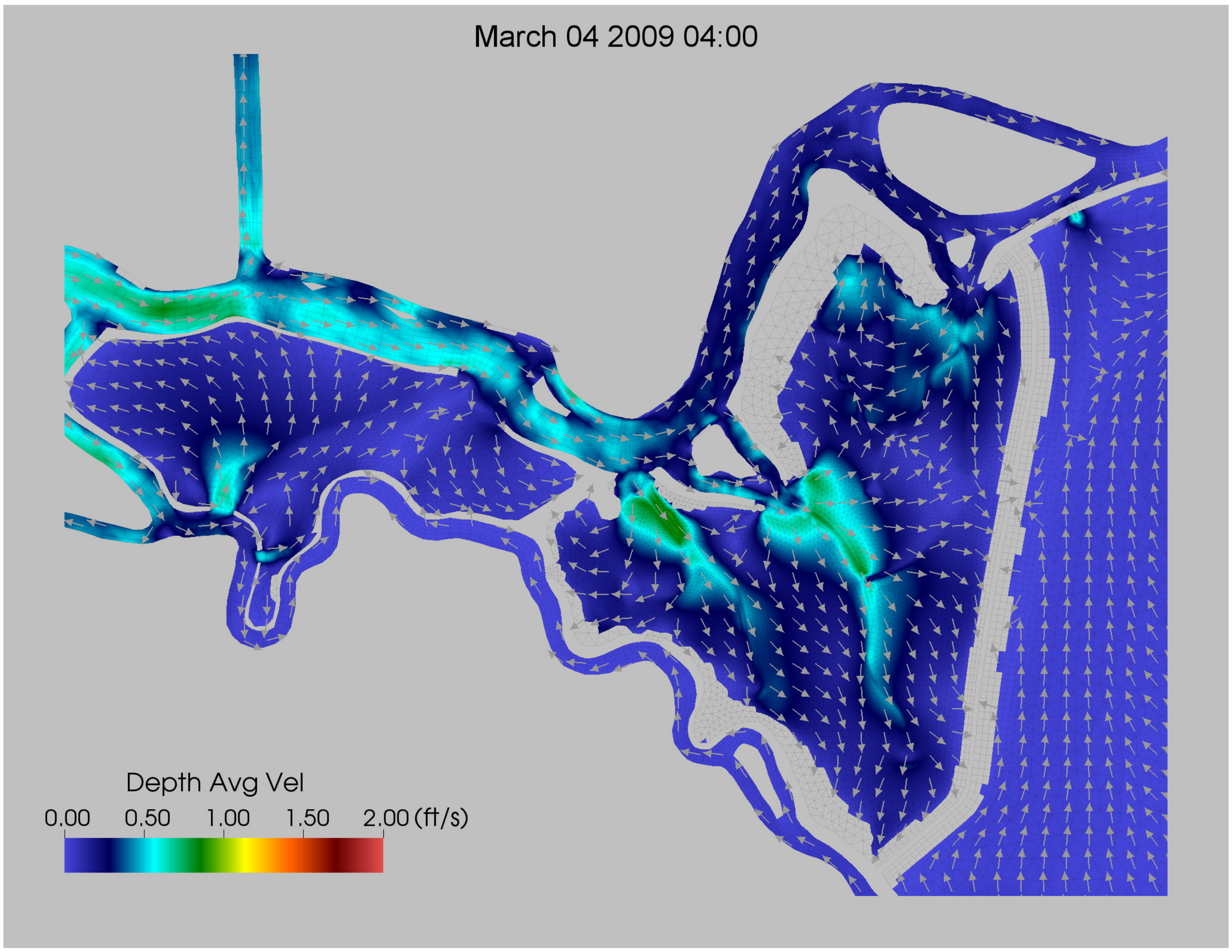

Note: Arrows show direction, colors show magnitude.

Figure 13 Snapshot on March 4, 2009, 06:30, Showing Peak Flood Velocity in Nearby Channels

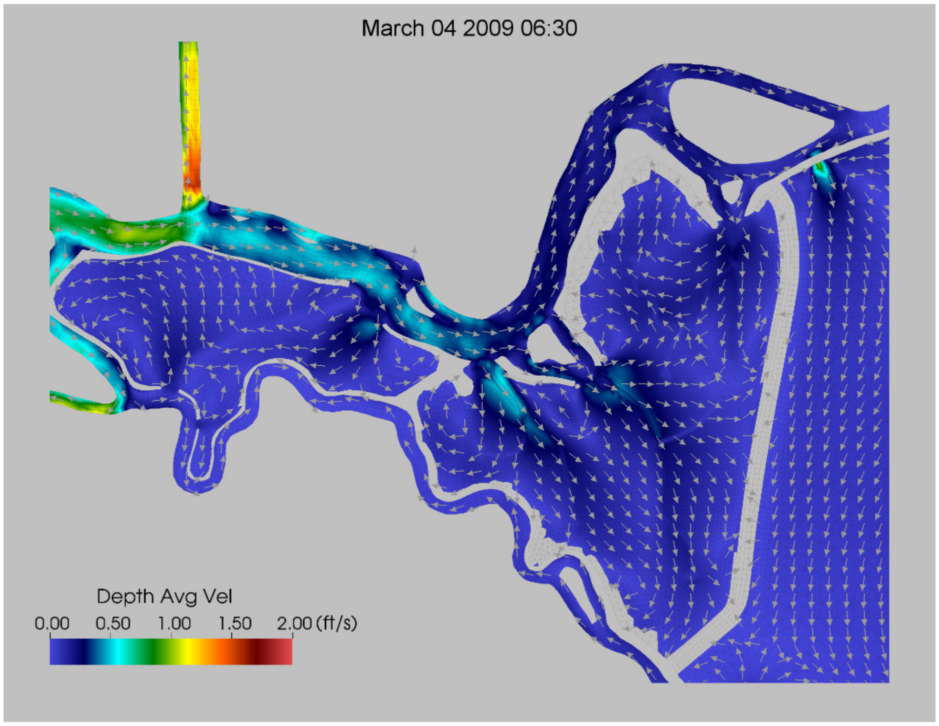

Note: Arrows show direction, colors show magnitude.

Figure 14 Snapshot on March 4, 2009, 13:00, Showing Peak Ebb Velocities in the Restoration Site and Surrounding Channels

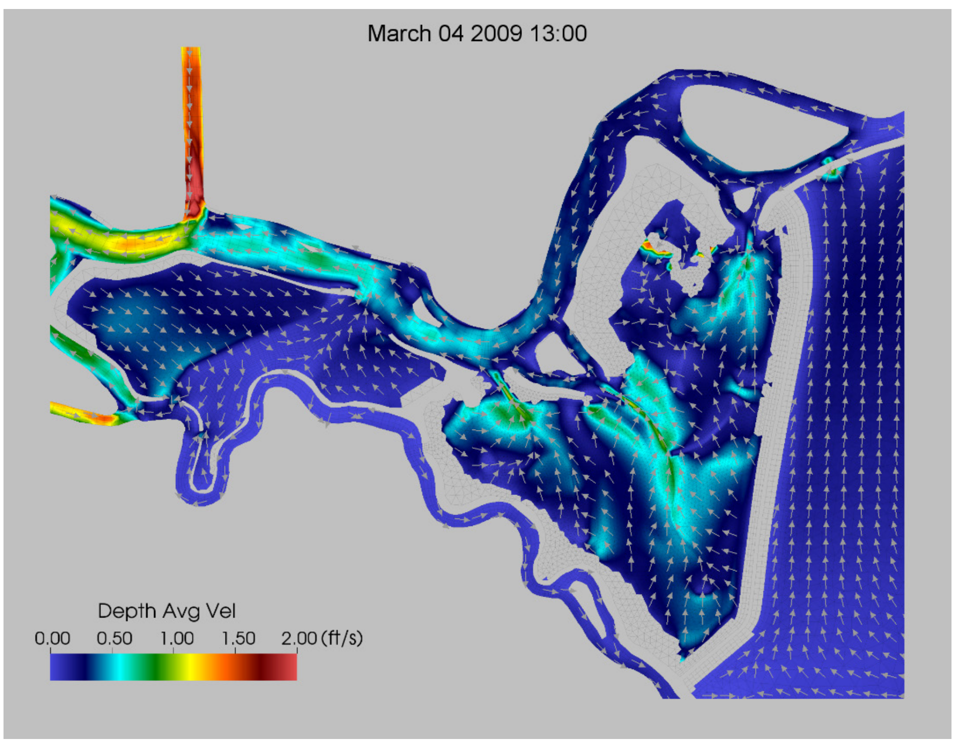

Figure 15 Peak Flow During Closure

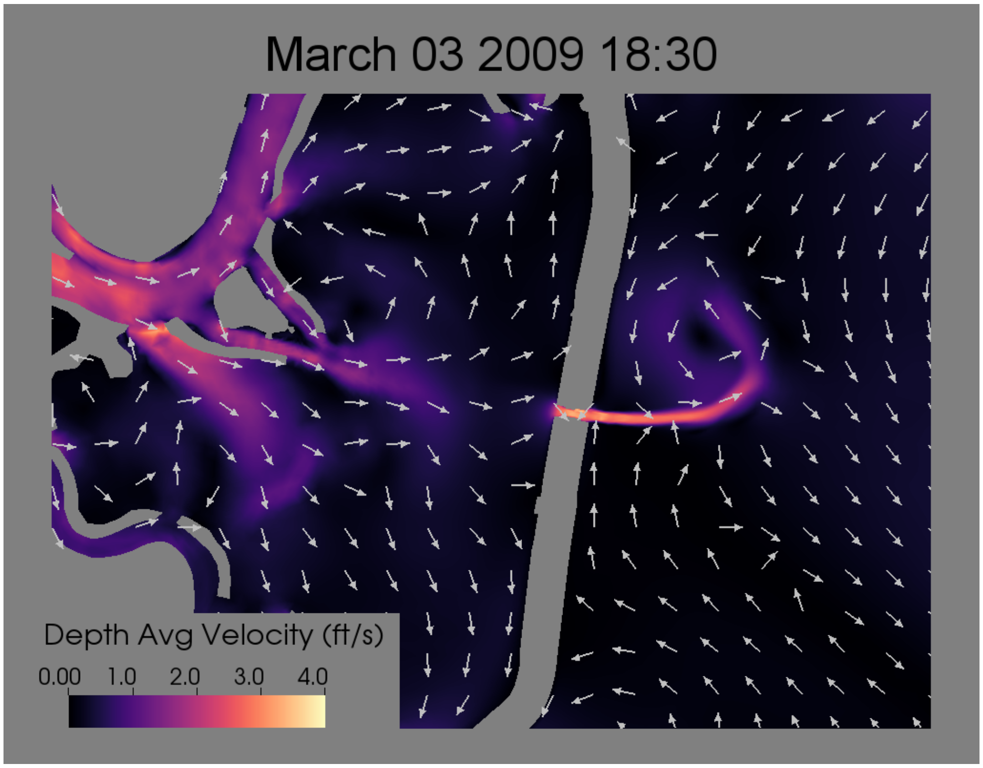

Figure 16 Velocity Snapshot of Peak Ebb Flow through a Breach to Piper Slough

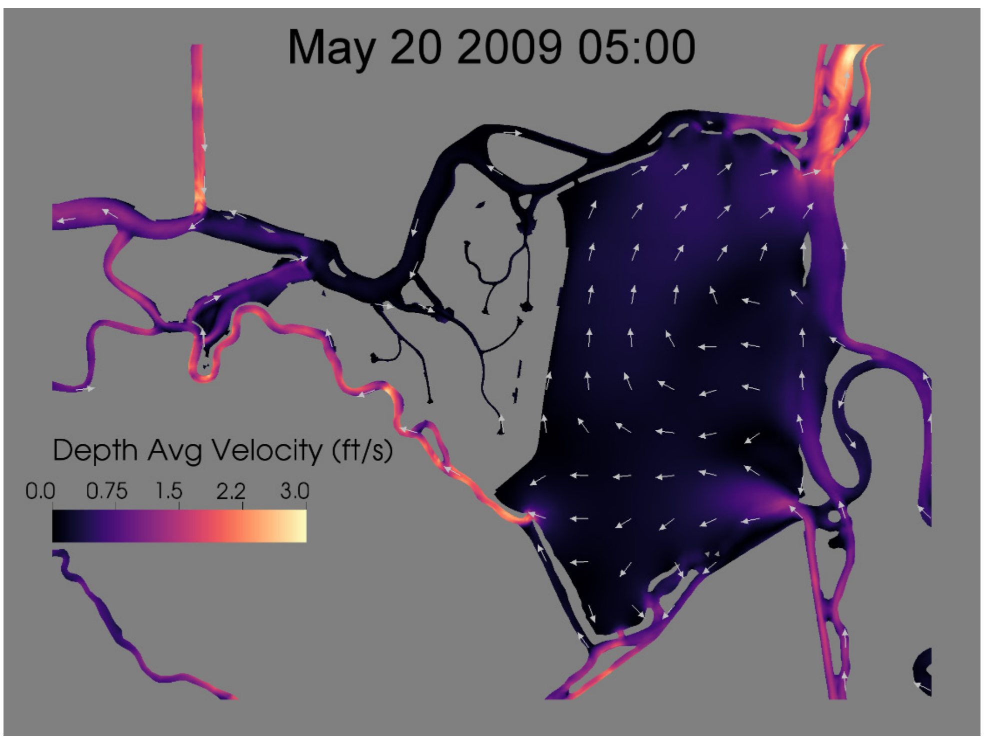

Note: In this simulation Piper Slough has no structure and False River has a complete blockage.

Figure 17 Peak Depth Averaged Flood Velocity March 2, 2009, on Old River between the San Joaquin River (top right of plot) and Franks Tract (bottom left)

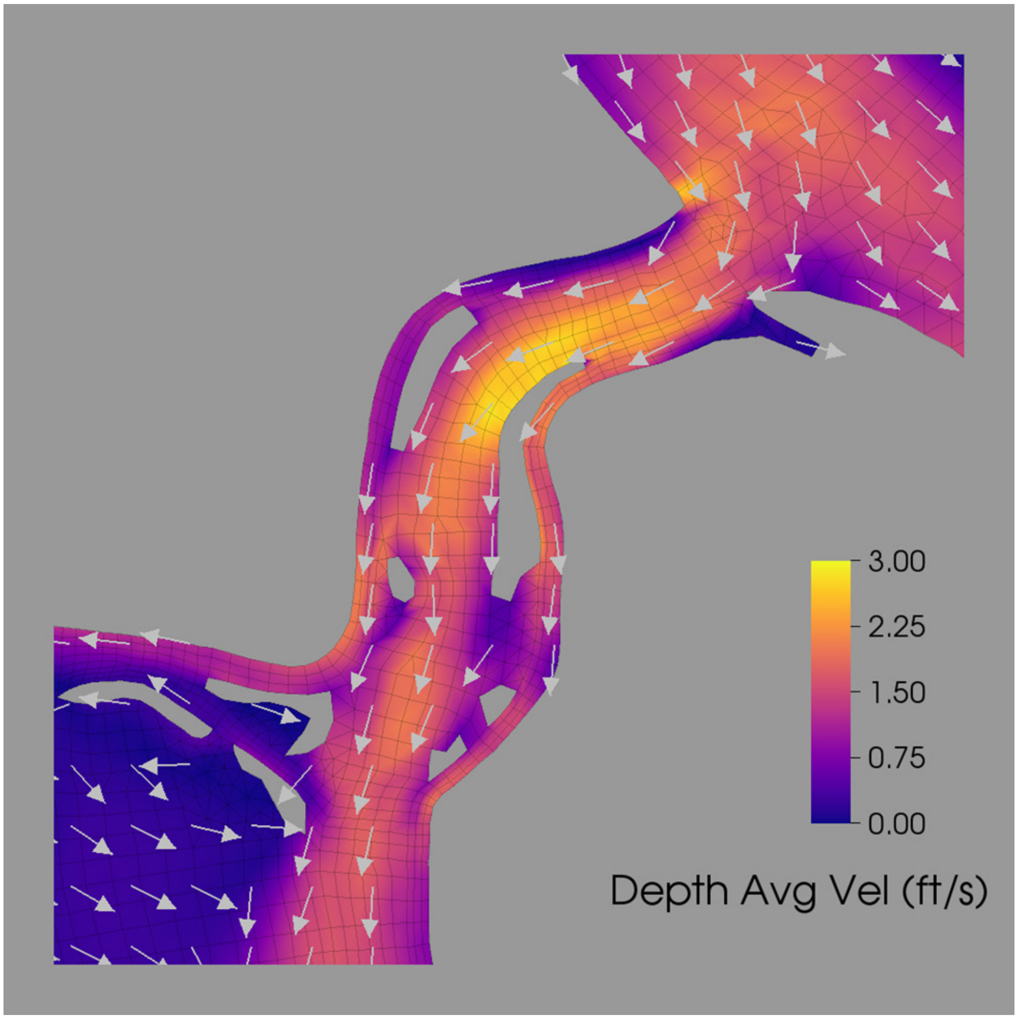

Chapter 3. Regional Impacts on Water Levels, Flow, and Salinity

The Franks Tract Restoration project affects tidal energetics in the area around Franks Tract and changes the ways that salinity intrudes into the mid-Delta. DWR performed 600-day simulations in 2009–2010 to probe the changes that would occur in hydrodynamics and salinity over a full salinity-intrusion season. The locations studied are shown in Figure 18.

3.1 Water Levels

Modeling analysis indicates the project will have only a small effect on tidal water levels. The change, such as it exists, will be on the order of 3 percent to 5 percent, and will be limited to stations near Franks Tract. Stations on the San Joaquin River upstream of Jersey Point, near Three Mile Slough, may experience small increases; most other areas may experience small decreases. Peak water levels will change in the same way.

Although amplitude and peaks will not change much, some locations will experience significant changes in phase (timing) because the tides have to take a more circuitous route around Franks Tract. Figure 19 shows a typical case at the station Old River at Bacon Island (CDEC code: BAC), which was chosen as an example because it is upstream of the restoration site. That ensures phase differences between the two cases (20 minutes) are fully developed. Additionally, the station is well surveyed.

Even larger (3-hour) phase lags will develop immediately at the restoration site. For instance, Figure 20 shows time series of water levels expected to develop on either side of the barrier proposed on False River at the perimeter of the restoration site and that would exist across the vulnerable levee flagged in Figure 4.

Figure 18 Stations Referred to in Description of Water Level, Flow and Salinity Impacts

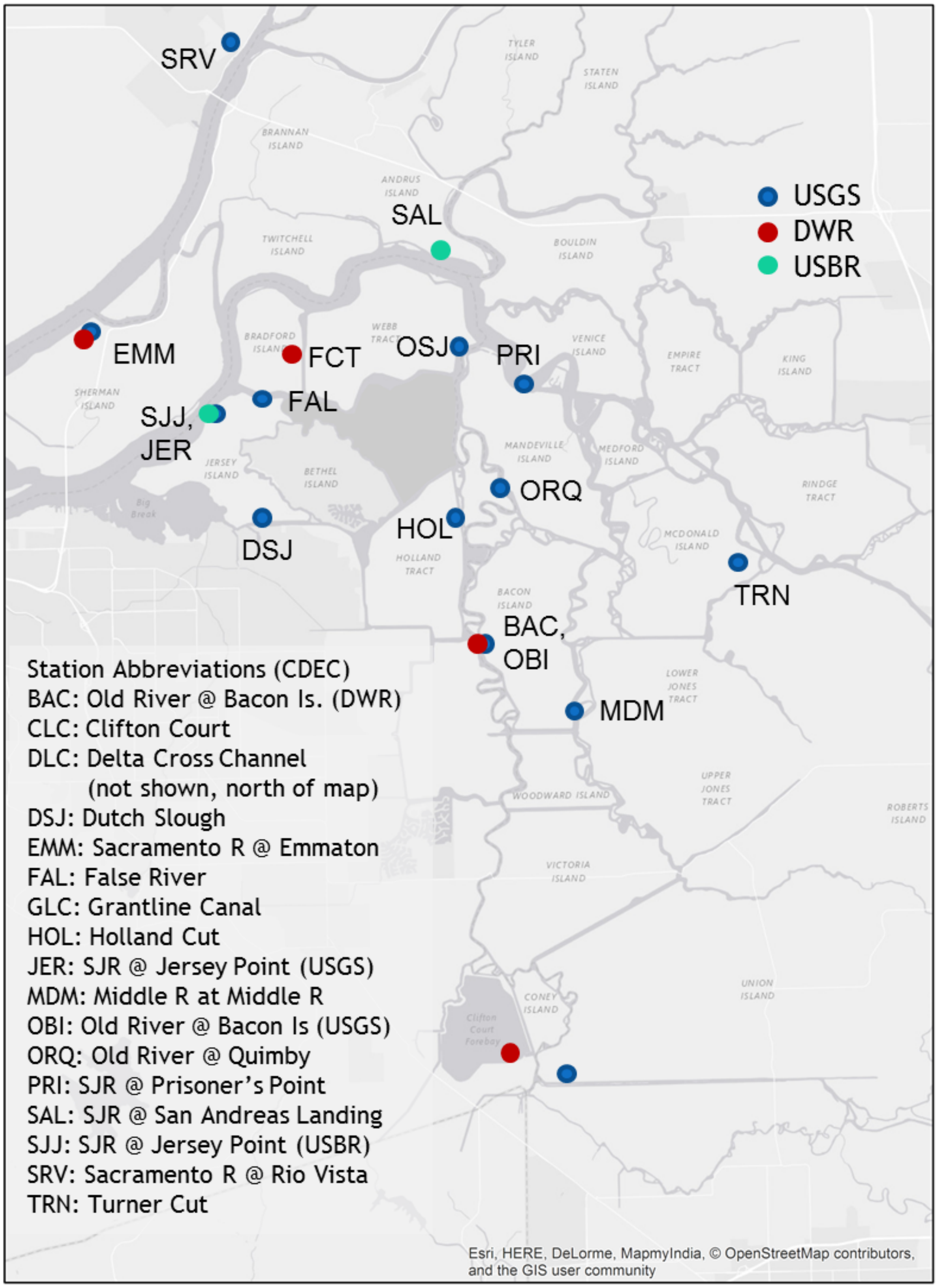

Note: CDEC = California Data Exchange Center, DWR = California Department of Water Resources, USBR = U.S. Bureau of Reclamation, USGS = U.S. Geological Survey

Figure 19 **Tidal Water Levels on August 5, 2000, for Base and Restoration Case**

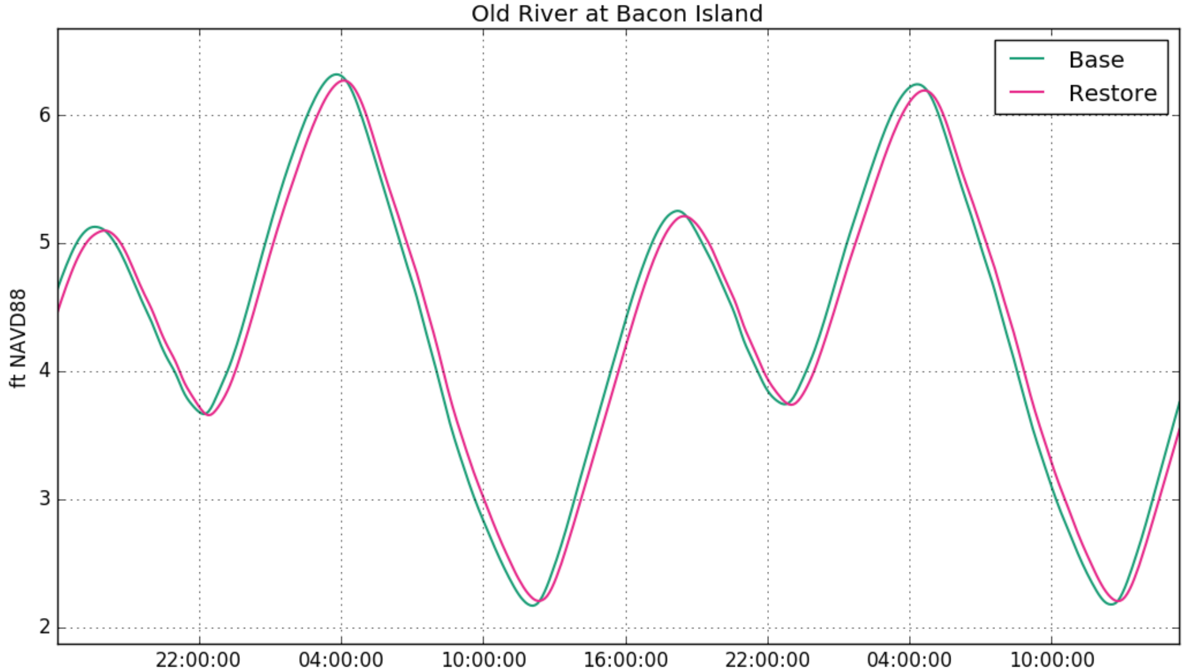

Figure 20 **Stage Differences Between the West (restoration) and East Side of Barriers on Old River**

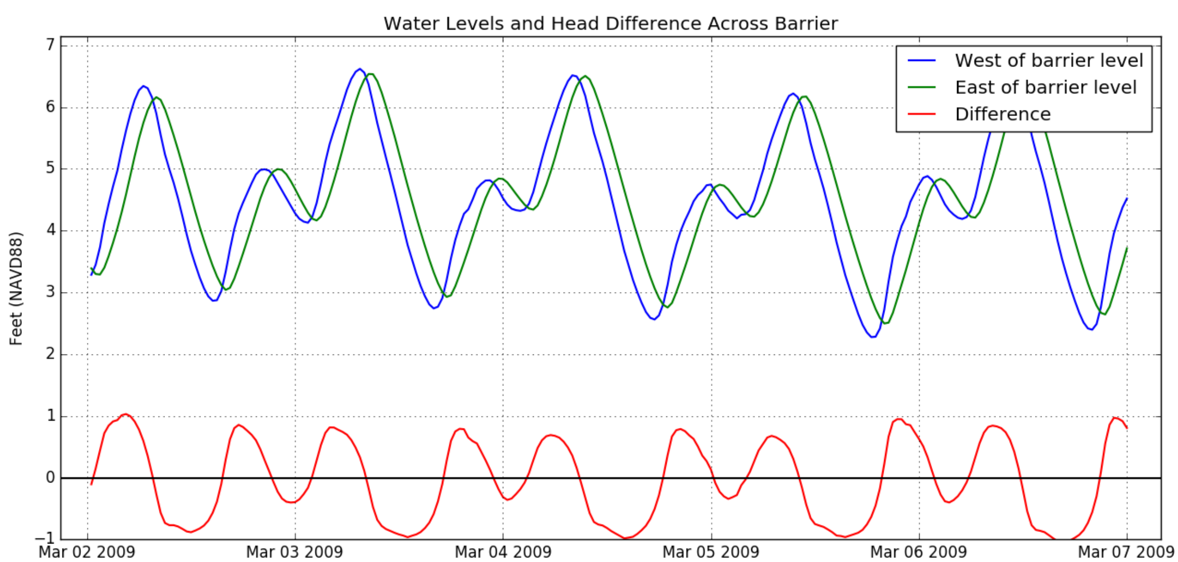

3.2 Flow

According to modeling analysis, the project is expected to affect tidal range and net flows in the region around Franks Tract. Figure 21 indicates the magnitude of these changes, with red arrows indicating locations of increase and blue arrows indicating locations of decrease. *Tidal range* is measured as the July 2009 to September 2009 average difference between tidal maximum and tidal minimum discharge. For instance, a location that averages -40,000 cubic feet per second (cfs) on ebb tide and +50,000 cfs on flood tide has a tidal range of 90,000 cfs. *Net flow* is the average of tidally filtered flow over a longer period (March 2009 to August 2010). The Delta Cross Channel, which is seasonal and has a very period-dependent mean flow, is excluded from the graphic; it is included in the time series that follow. Quantities described as *tidally filtered* are calculated using a squared Cosine-Lanczos filter with a 40-hour cutoff.

Figure 21 Modeled Tidal Range (left) and net Flow (right) Differences Between Restored and Unrestored Cases

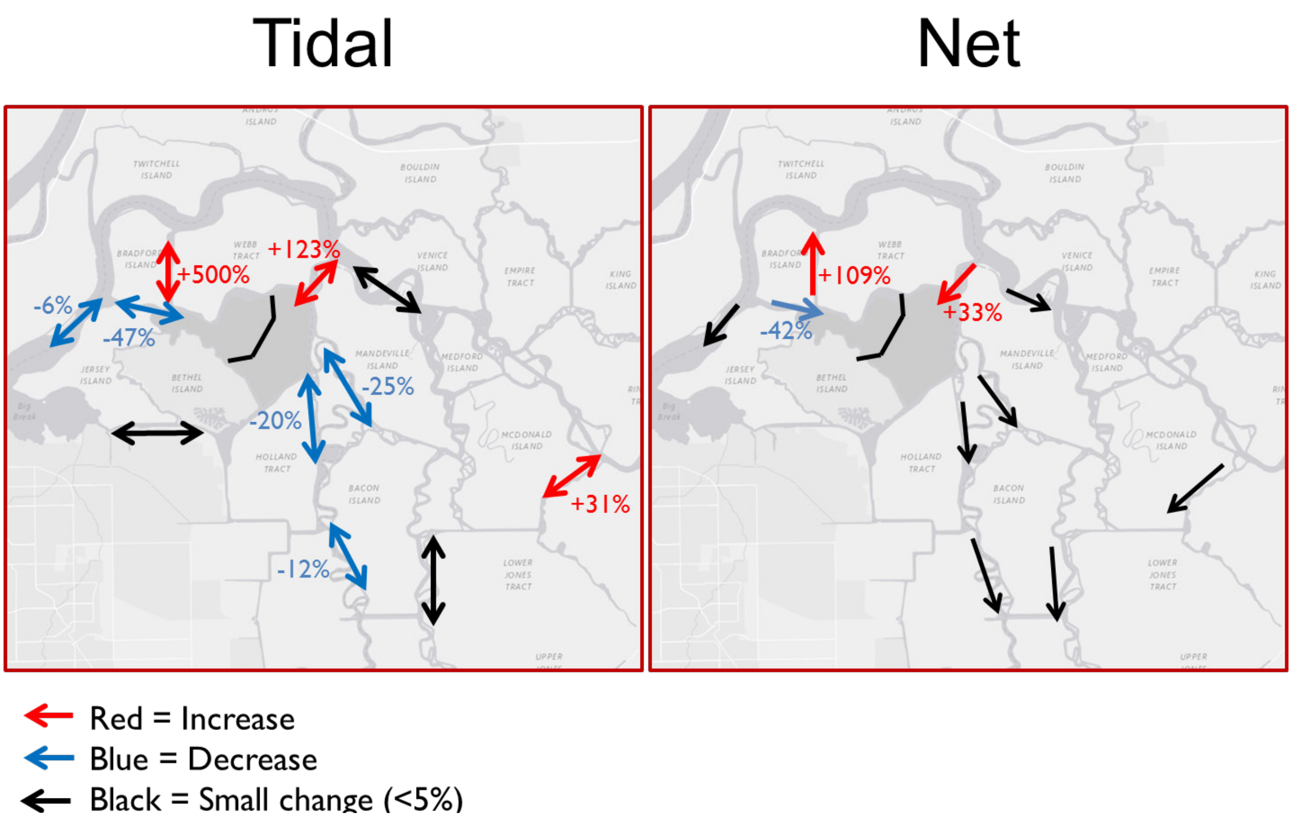

Note: Arrows are colored according to whether the magnitude increases or decreases. Net flow directions are valid for both the restored and unrestored cases and represent the direction of flow not the direction of change.

Figures 22 through 29 show modeled time series of flow at instantaneous (top) and tidally filtered (bottom) scales at stations that experience the greatest change, as well as time series of flow at the Delta Cross Channel and Grantline Canal, which help complete the narrative in the far field.

The changes at specific stations are described here.

False River (CDEC code: FAL, Figure 22): With the project, False River no longer supplies as much tidal flow to Franks Tract and the channels farther south. Tidal range of flow decreases from 104,000 cfs to less than 55,000 cfs.

Fisherman's Cut (CDEC code: FCT, Figure 23): With the project, some of the tidal energy that normally propagates from False River into Franks Tract is now directed through Fisherman's Cut. Tidal range in Fisherman's Cut is expected to increase from 2,600 cfs to 16,000 cfs. While this represents a large proportional change, the figure is considerably smaller than was experienced in 2015, with the installation of the West False River emergency drought barrier. Additionally, Fisherman's Cut does not experience the directional change (flood tide direction changed from northward to southward) that occurred that year. The change is nonetheless large relative to the more quiescent base case.

Old River at Franks Tract (CDEC code: OSJ, Figure 24): With the project, tidal range of flow through Old River in the northeast of Franks Tract is predicted to increase from 30,000 cfs to 68,000 cfs. Net flow through this route will increase, suggesting that Old River begins to supply more of exports. This is serendipitous, because, as noted in the next section, Old River is also the corridor enjoying the bigger salinity decrease. Velocities in this section of Old River are of interest because they have the potential to affect both late stage construction and navigability after the project is built. An example of peak velocity change on this section of Old River is shown in Figure 17, which maps the moment of maximum flood flow on March 2, 2009. Velocity of 3 ft/s occurs because of shoaling; velocities approach 2 ft/s over much of the channel. Ebb is similar, though slightly more muted. As with Fisherman's Cut, the changes are significant. The change is smaller in magnitude than in 2015 under the EDB project, when tidal range grew to exceed 90,000 cfs.

Holland Cut (CDEC code: HOL, Figure 25): Tidal range of flow from Franks Tract to Holland Cut is reduced under the project by approximately 25 percent, from 36,000 cfs to 29,000 cfs. Other connections between Franks Tract and the channels to the south Delta, such as Old River at Quimby (CDEC code: ORQ), are not shown but react similarly.

Turner Cut (CDEC code: TNC, Figure 26): Tidal flows from the San Joaquin River through Turner Cut are expected to increase from 7,200 cfs to 9,500 cfs under the project, or by approximately 31 percent. Other connections between the San Joaquin River and Middle River, and the San Joaquin River to the east, such as Empire Cut, are not shown but react similarly.

Delta Cross Channel (CDEC code: DLC, Figure 27): According to the model, the project has only a small effect on Delta Cross Channel and other stations in the North Delta. It increases net flow through the cross-channel flow by 100 cfs when it is open, which should be regarded as an increase in its efficacy. The cross-channel is also strongly affected (10-percent flow reduction) by other restoration projects in the area, which will be reconsidered below when project interactions are considered.

Grantline Canal (CDEC code: GLC, Figure 28): The restoration project has negligible effect on east-west flows in the south Delta. Figure 28 shows flows at Grantline Canal. The period of this plot has been shifted later in the years to include conditions after removal of the agricultural barrier.

Old and Middle River (CDEC code: OMR, Figure 29): The project has an insignificant impact on OMR flow. Figure 29 shows OMR, the sum of Old River flow at Bacon Island (CDEC code: OBI) and Middle River flow near Railroad Cut (CDEC code: MDM). Unlike the other plots, this calculation is based on a 14-day running average to match the computation under National Marine Fisheries Service (NMFS) stipulations. The four scenarios differ from one another by an average of less than 10 cfs and are indistinguishable visually.

Figure 22 Flow (top) and Tidally Filtered Flow (bottom) at False River Under Four Scenarios

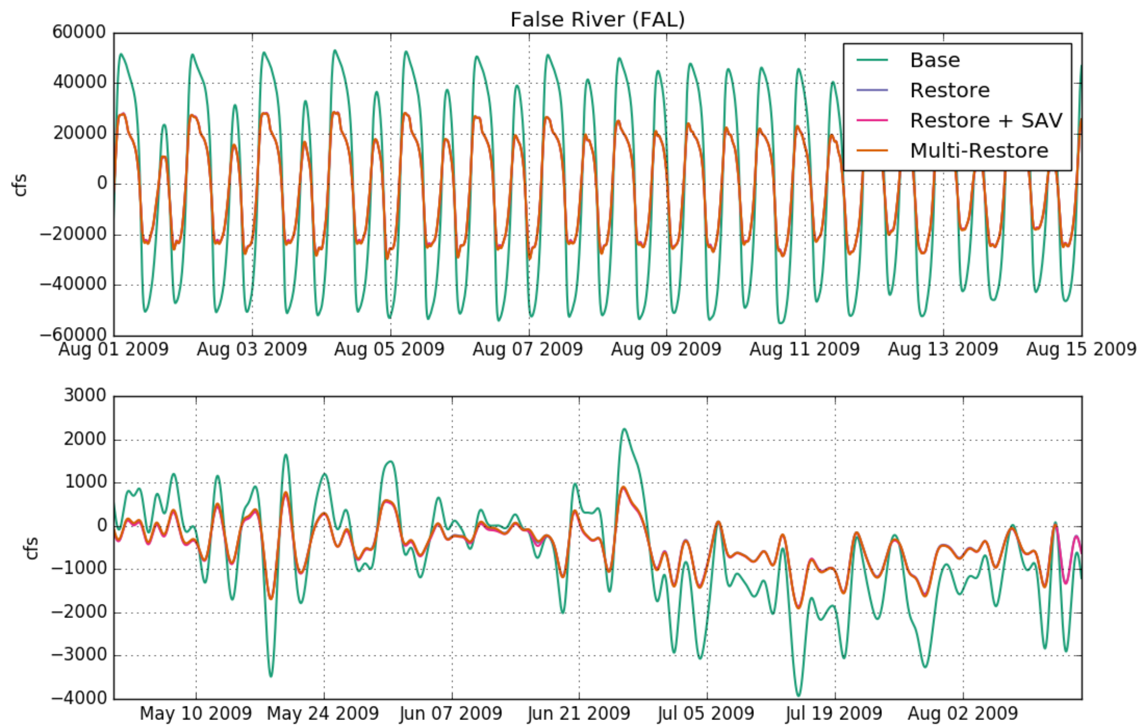

Notes: SAV = submerged aquatic vegetation

Figure 23 Flow (top) and Tidally Filtered Flow (bottom) at Fisherman's Cut Under Four Scenarios

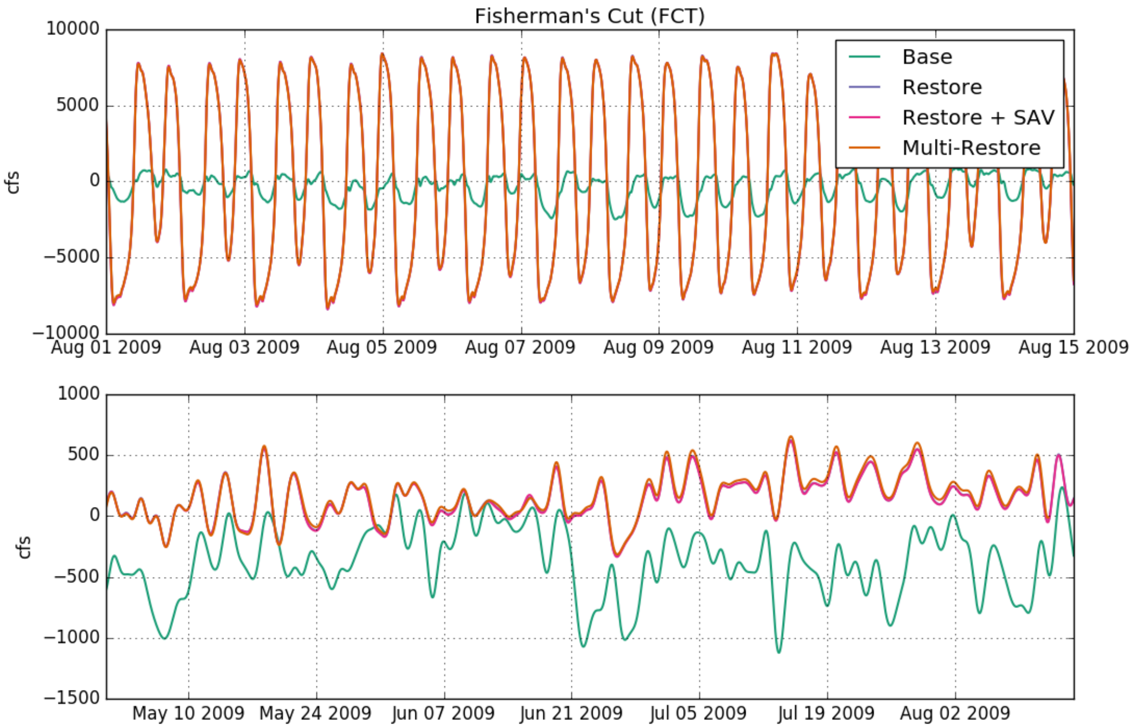

Notes: SAV = submerged aquatic vegetation

Figure 24 Flow (top) and Tidally Filtered Flow (bottom) at Old River near Franks Tract Under Four Scenarios

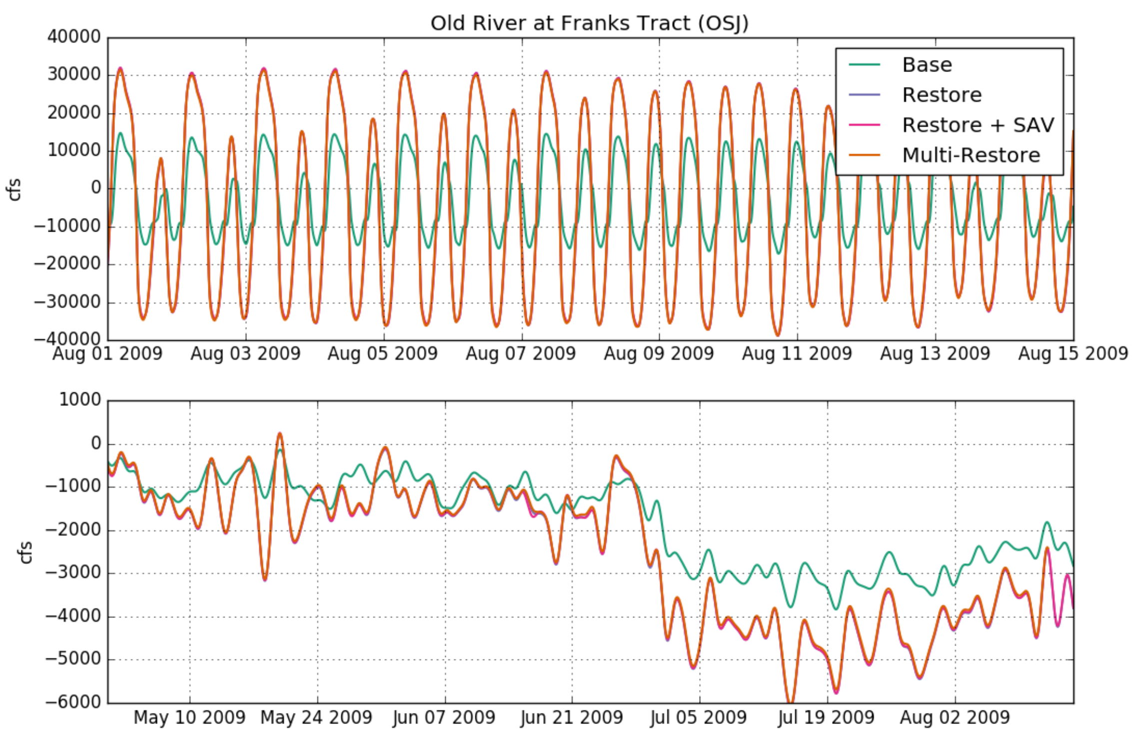

Notes: SAV = submerged aquatic vegetation

Figure 25 Flow (top) and Tidally Filtered Flow (bottom) at Holland Cut Under Four Scenarios

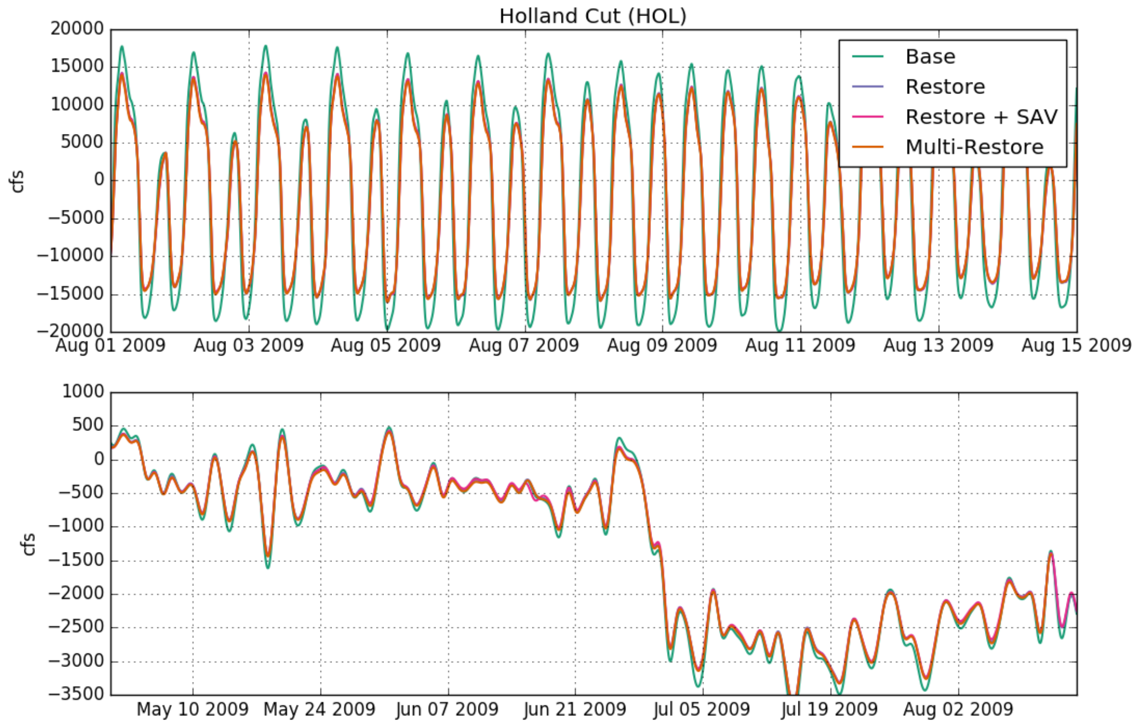

Notes: SAV = submerged aquatic vegetation

Figure 26 Flow (top) and Tidally Filtered Flow (bottom) at Turner Cut Under Four Scenarios

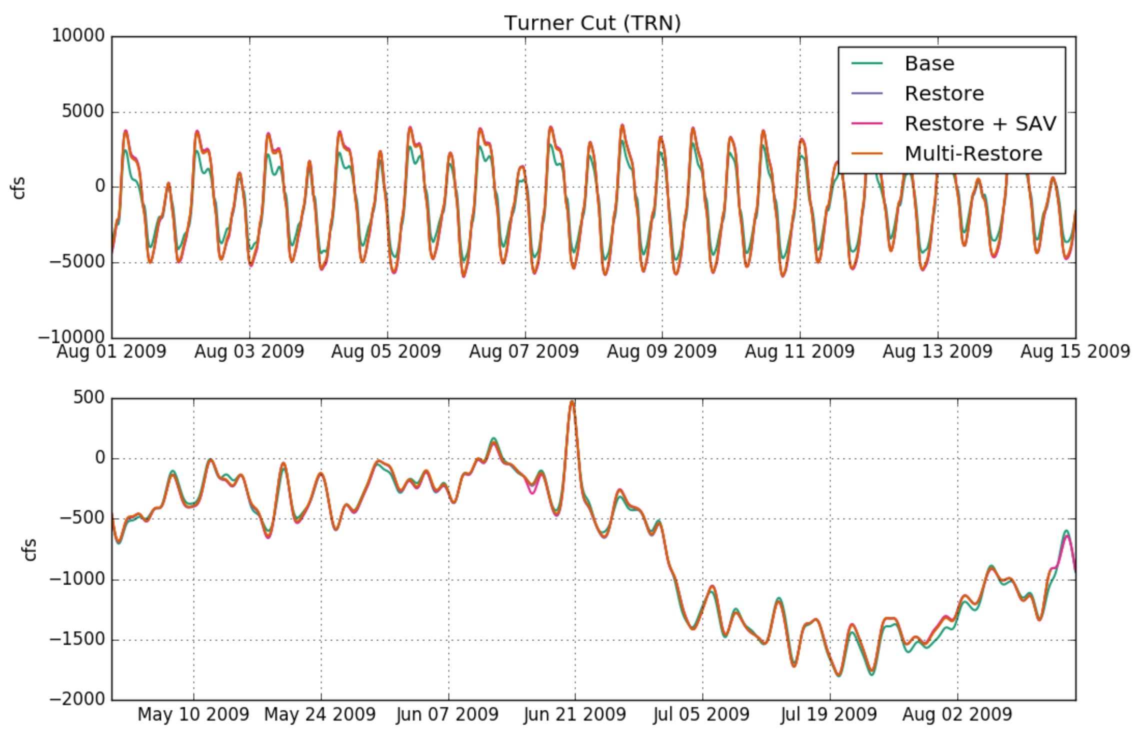

Notes: SAV = submerged aquatic vegetation

Figure 27 Flow (top) and Tidally Filtered Flow (bottom) Through the Delta Cross Channel Under Four Scenarios

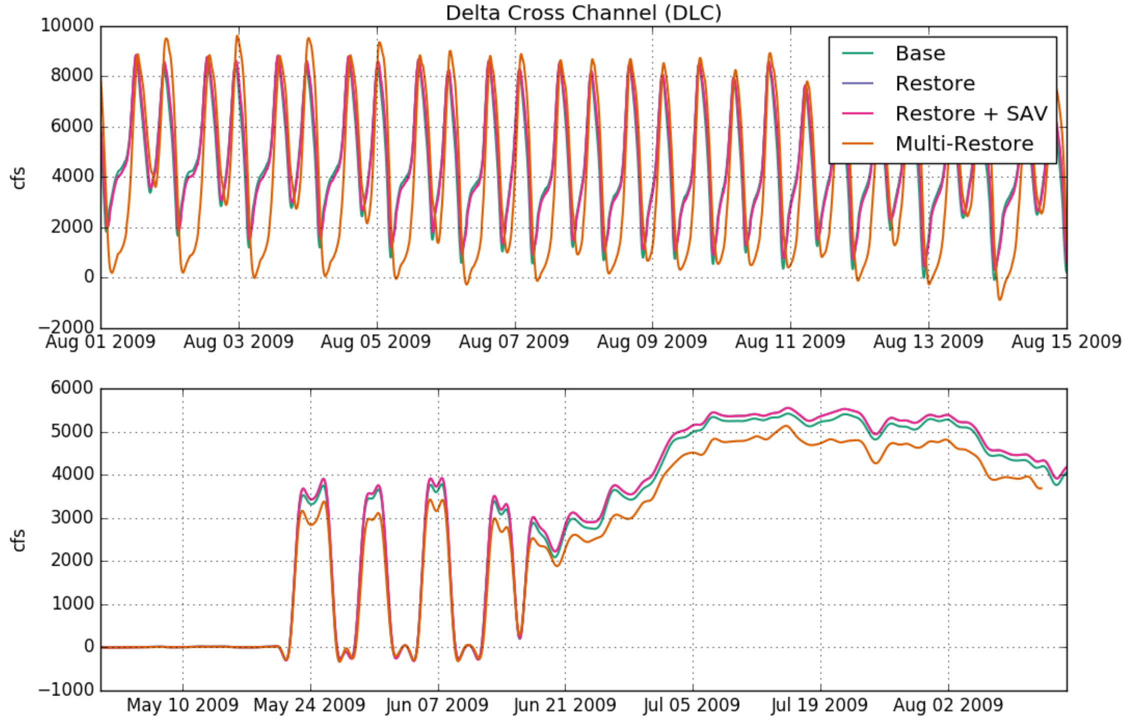

Notes: SAV = submerged aquatic vegetation

Figure 28 Flow (top) and Tidally Filtered Flow (bottom) Through the Grantline Canal Under Four Scenarios

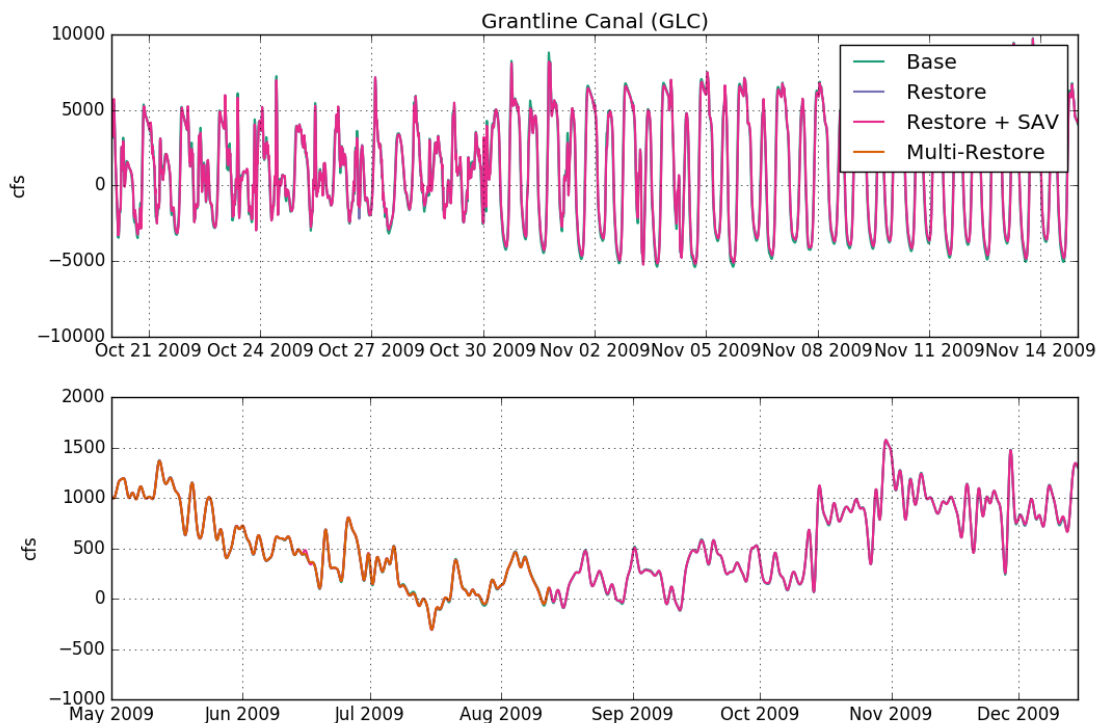

Note: Notes: SAV = submerged aquatic vegetation

The multi-restore case has a period of missing data.

Figure 29 **14-Day Running Average of Filtered Old Middle River Flow for Four Scenarios**

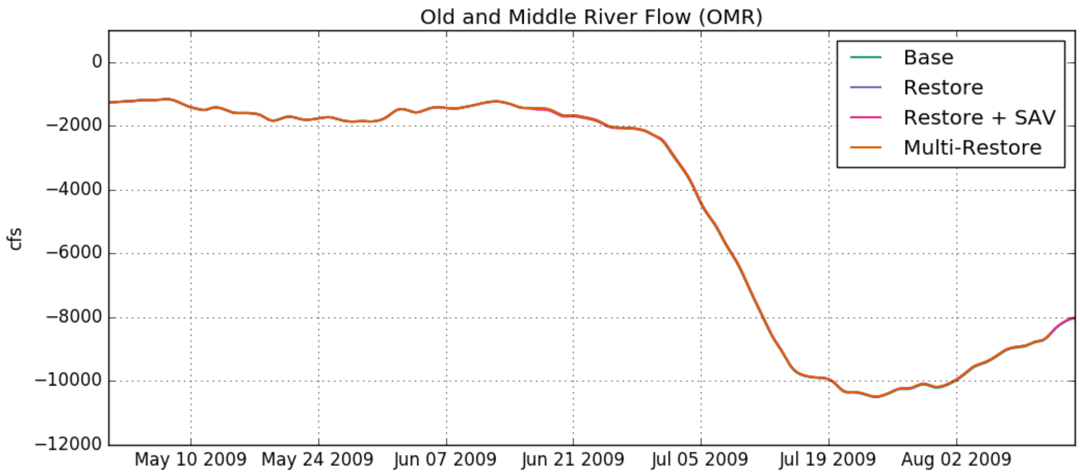

Note: Notes: SAV = submerged aquatic vegetation

Scenarios are indistinguishable because they are within 10 cubic feet per second of each another.

3.3 Salinity

The restoration design eliminates tidal pumping from False River, an important mechanism of salinity intrusion int)o the mid-Delta. Figure 30 is a conceptual illustration of how tidal pumping works based on model simulation results prepared during 2015 emergency barrier planning. On flood tide, a jet of higher salinity (red) water can be seen entering Franks Tract from False River on a flood tide through an aperture sometimes referred to as a nozzle. Water quality in this jet is heavily influenced by that of the San Joaquin River at Jersey Point which is saltier than most of the Delta and Franks Tract. The return flow from Franks Tract is fresher — the salty jet of water will have mixed out somewhat and the ebb flow is drawn radially from a broader area so it includes more of the ambient water in Franks Tract. Even if the volume of flow is the same in both directions, the asymmetry between a salty flood and fresher ebb adds up and causes a net transport of salt into the Delta — like a bus that travels both north and south, but carries many more passengers in the southern direction. The restoration project reduces False River flows and isolates the tidal pumping region from the Old River fresh water corridor.

Figure 30 Conceptual Illustration of Tidal Pumping

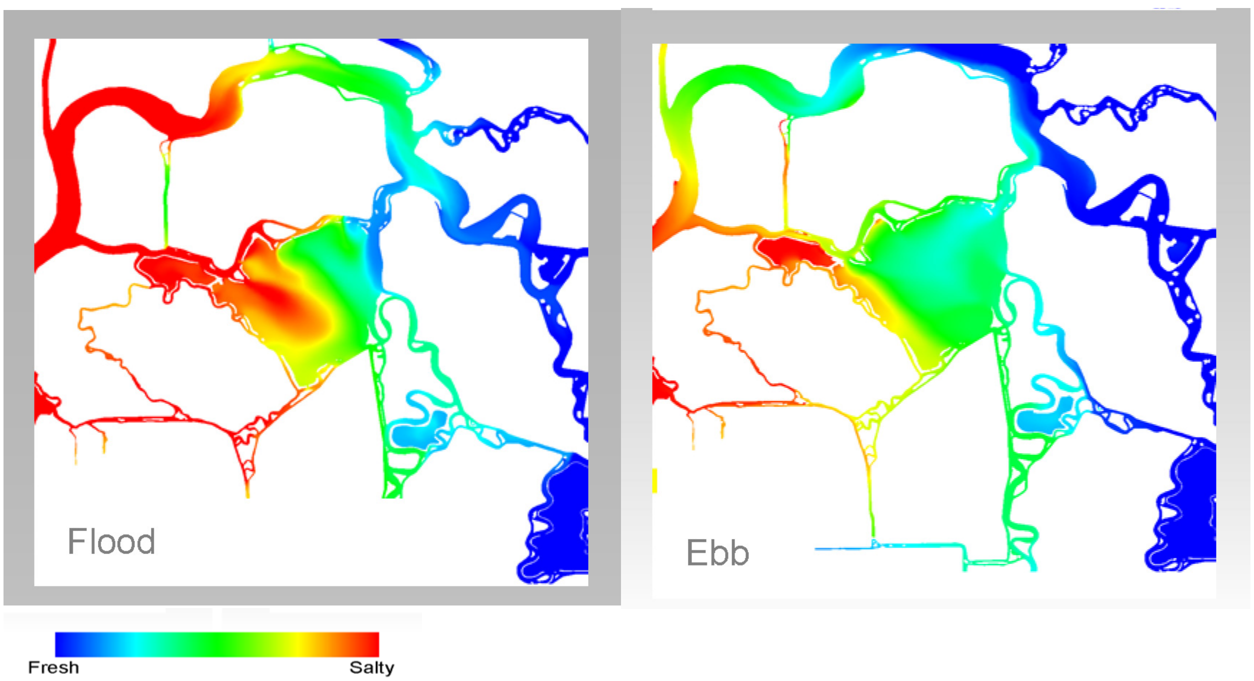

Source: Bay-Delta Semi-implicit Cross-scale Hydroscience Integrated System Model, 2015

Figure 31 shows a change map of 14-day averaged salinity (converted to units of specific conductance) during August 1–14, 2009. Figure 32 is an analogous map for the first 14 days of November 2009. The maps span the region where the project has a pronounced effect. Regions shown in red indicate salinity increases; regions shown in blue indicate where freshening occurs. Changes are larger in August primarily because salinity is higher in August. The project only impacts Sacramento salinity by more than 2 percent during November. This is, incidentally, a period when the Delta Cross Channel was toggled open and closed a number of times to meet Rio Vista outflow standards.

Figure 31 **14-Day Differences in Salinity, August 2009**

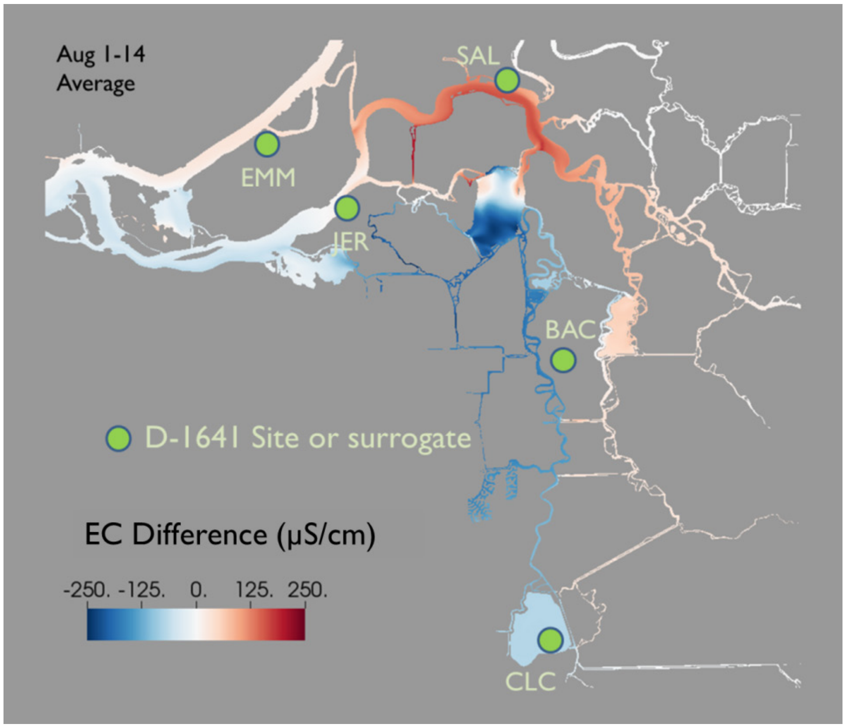

Note: EC = electrical conductivity (also referred to in text as specific conductance)
Salinity is converted to units of EC. Differences are between the restoration and base cases for August 1–14.

Figure 32 **14-Day Differences in Salinity in November 2009**

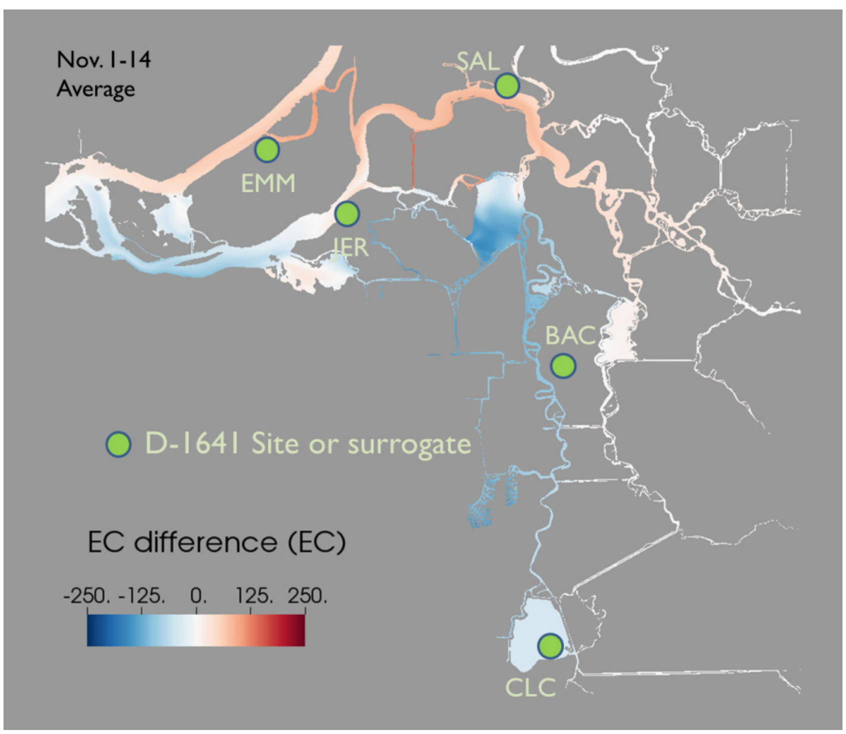

Note: EC = electrical conductivity (also referred to in text as specific conductance)
Salinity is converted to units of EC. Differences between the restoration and base cases for the first 14 days of November 1–14.

Regions upstream of the restoration site are shielded from ocean saltwater intrusion and the mid-Delta becomes fresher. The reduction in conductivity mid-Delta can be more than 100 micro-Siemens per centimeter (µS/cm), which is a large relative improvement for these channels. Downstream of the restoration site, and on the main stems of the Sacramento and San Joaquin rivers, the response varies between insignificant and degradation. Where increased salinity occurs, it is generally similar in scale absolute units to the upstream improvements, but smaller in relative terms. These changes can still be important if they occur at stations that are the “controlling” locations in California State Water Resources Control Board Decision 1641(D-1641) or contractual compliance.

To investigate the potential impact on D-1641 compliance, Figure 33 through Figure 37 show time-series plots of tidally filtered salinity at D-1641 locations, converted to units of specific conductance. The plots include the base case with no project (labeled “Base”), the case with restoration (“Restore”) and two sensitivity studies involving SAV (“Restore + SAV”) and interactions with other restoration sites (“Multi-Restore”). The sensitivity results will be discussed more in the following section.

Figure 33 through Figure 35 show salinity at Jersey Point (CDEC Code: JER), Emmaton (CDEC Code: EMM), San Andreas Landing (CDEC Code: SAL). In dry and critical years Emmaton and Jersey Point are also frequently the stations limiting D-1641 compliance. They are not situated in locations that would be expected to benefit in water quality. The neutrality of the project at these sites over several years is thus promising, and suggests that there may be little additional water cost arising from the project at these traditional limiting locations. On the other hand, San Andreas Landing, which usually is a fairly easy objective, becomes salty enough to warrant vigilance (the dry year objective is 580 µS/cm). The increase at San Andreas Landing becomes particularly important when considering interactions between Franks Tract and other projects that may alter cross-channel flow, a point taken up in the next section on sensitivity. It should be noted that if D-1641 objectives are exceeded, the treatment of salinity as a free variable is an oversimplification; what will really happen is that upstream releases will be increased, objectives will be met, and mid-Delta water quality will get even fresher.

Figure 36 and Figure 37 show tidally filtered specific conductance at Old River at Bacon Island and Clifton Court, respectively. They are used in this report as surrogates for Rock Slough and the State Water Project. These two stations lie upstream of the restoration site. As a result, they experience significant reductions in salinity. In the case of Old River at Bacon Island, the improvement is 200 µS/cm, or 25 percent. The improvement at Harvey O. Banks Pumping Plant is smaller and less uniform over the year because this site responds more to salinity from the San Joaquin River and South Delta sources.

Figure 33 Tidally Filtered Specific Conductance at Jersey Point

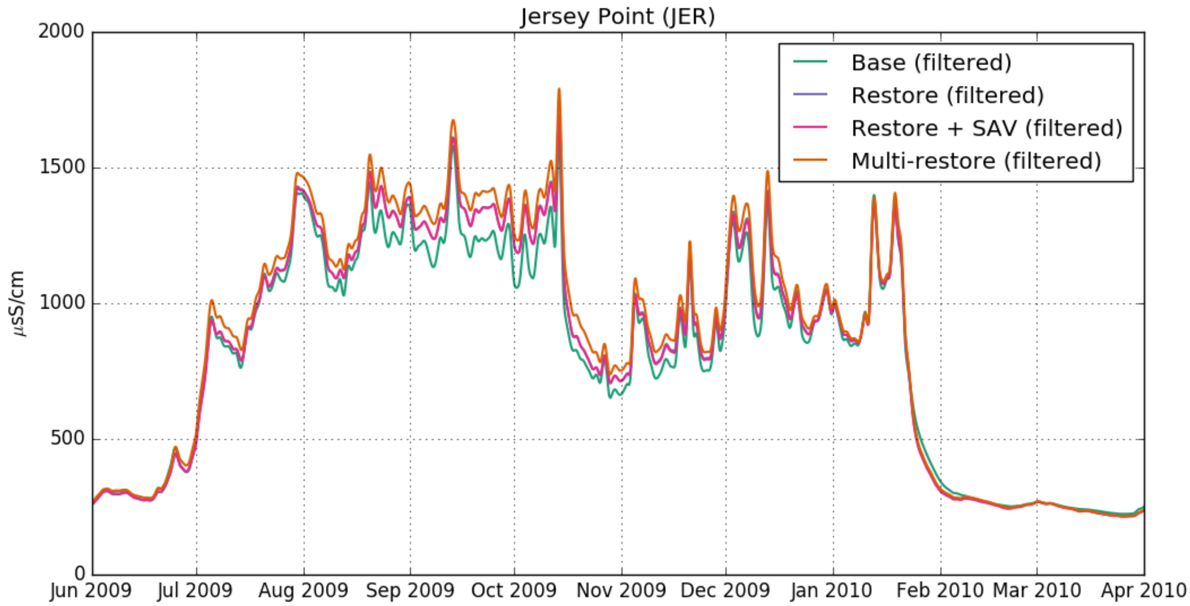

Note: SAV = submerged aquatic vegetation
Specific conductance is computed as salinity and converted to conductance at Jersey Point for four scenarios.

Figure 34 Tidally Filtered Specific Conductance at Emmaton

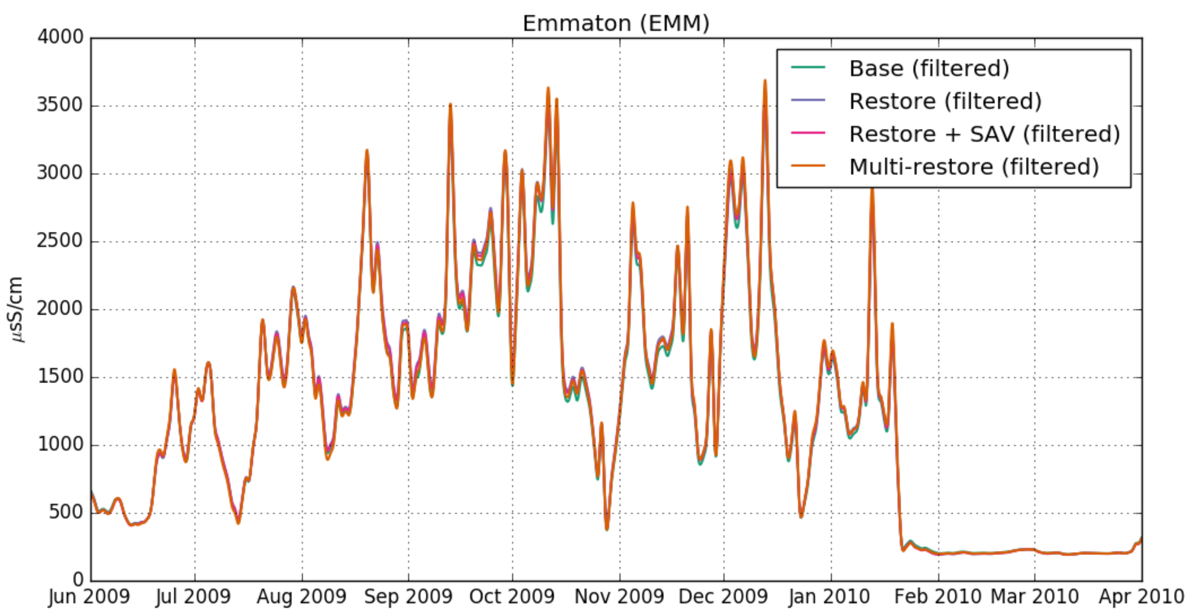

Note: SAV = submerged aquatic vegetation
Specific conductance is computed as salinity and converted to conductance at Emmaton for four scenarios.

Figure 35 Tidally Filtered Specific Conductance at San Andreas Landing

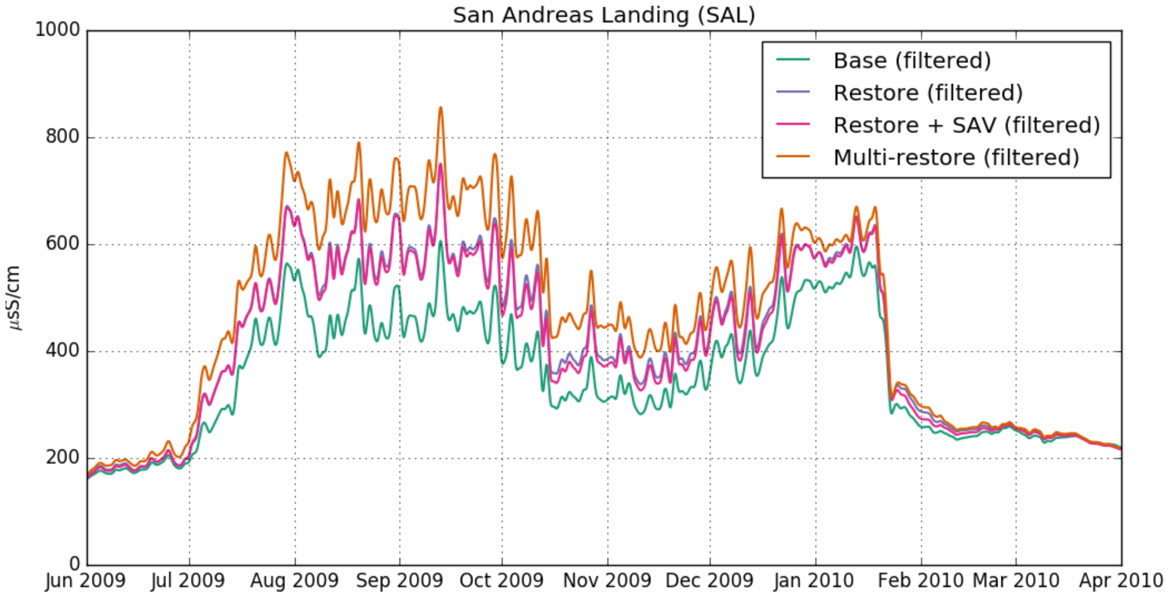

Note: SAV = submerged aquatic vegetation

Specific conductance is computed as salinity and converted to conductance at San Andreas Landing for four scenarios.

Figure 36 Tidally Filtered Specific Conductance on Old River at Bacon Island

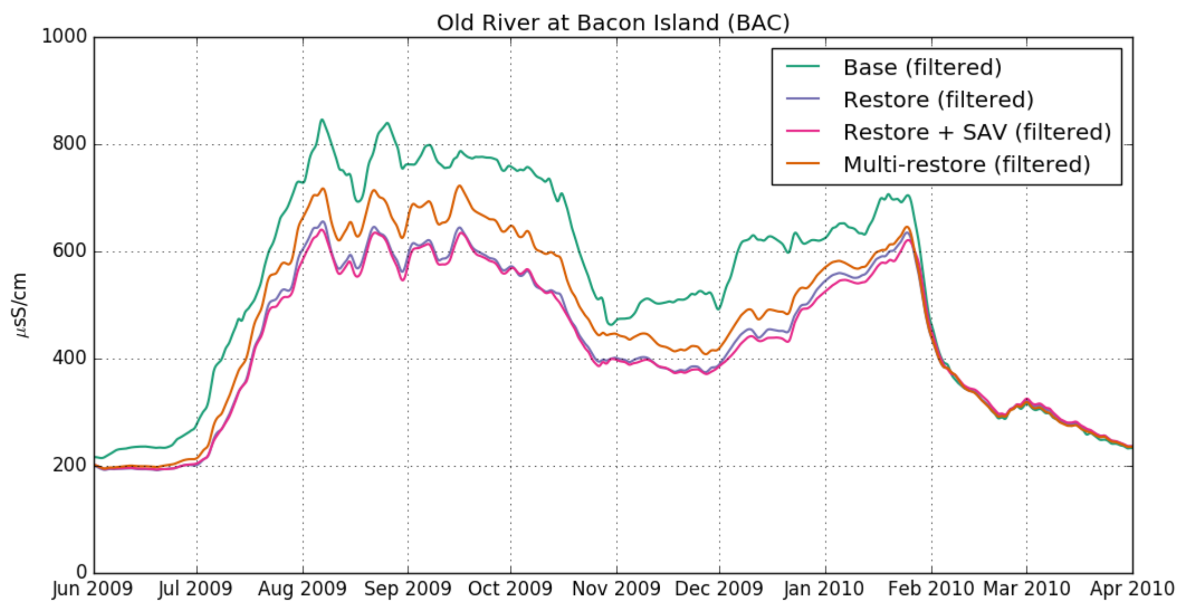

Note: SAV = submerged aquatic vegetation

Specific conductance is computed as salinity and converted to conductance on Old River at Bacon Island for four scenarios.

Figure 37 **Tidal Filtered Specific Conductance at Clifton Court**

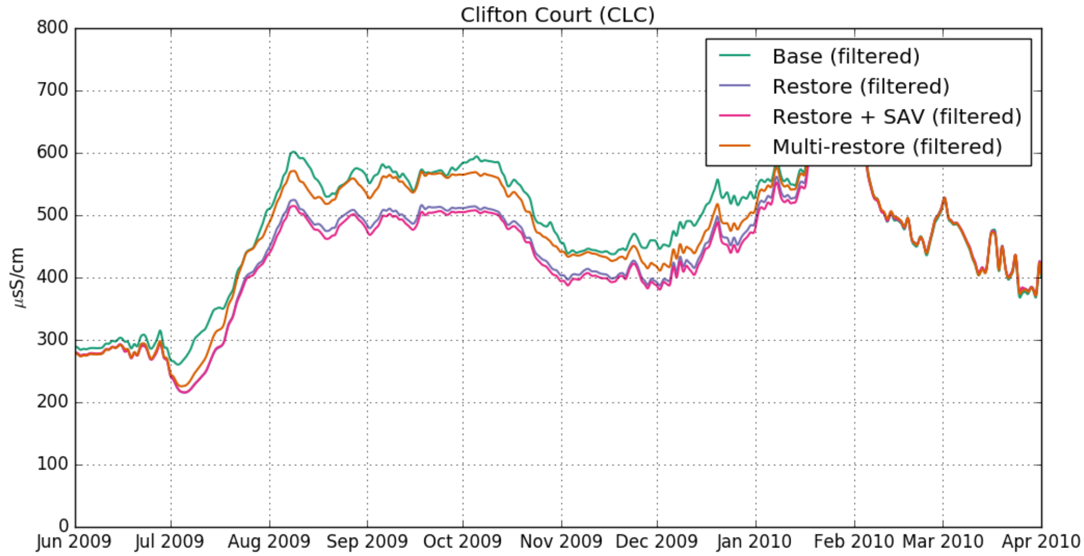

Note: SAV = submerged aquatic vegetation
Specific conductance is computed as salinity and converted to conductance at Clifton Court for four scenarios.

3.4 Entrainment

In order to explore the potential effect of the project on entrainment at State Water Project (SWP) and Central Valley Project (CVP) facilities, particle tracking simulations were performed under high and low export hydrologies from 19 sites around the Delta. The simulations confirm that the project reduces entrainment of particles originating from Jersey Point and other western sites, but not from locations upstream on the San Joaquin River east of Franks Tract. When particles are entrained, the route they take to the export locations is more circuitous and requires more time.

The release locations, as well as entrainment results, are shown in Figure 38 and Figure 39. The locations are taken from Kimmerer and Nobriga (2008). Particles were randomly injected in the top two-thirds of the water column over a rectangle 1,000 feet long, and 60 feet to 1,000 feet wide, depending what the local channel width would accommodate. Each batch comprised 8,000 neutrally buoyant particles. The releases were distributed over 24 hours on the first day of the month in June 2009 and July 2009. The releases were tracked for 30 days. These two months were chosen as the periods of study because they represented very different export levels, with combined average SWP and CVP exports of 1,800 cfs in June and 10,100 cfs in July. Despite the order of magnitude differences in exports between months, exports are relatively constant within each individual month, allowing a relatively stationary experiment for blocks of 30 days. This duration is sufficient for most particles near Franks Tract (75 percent to 85 percent at Jersey Point depending on the scenario) to reach a long-term fate, either entrained or exiting to the west, beyond Chipps Island.

The particle tracking results indicate that the project brings about an appreciable drop in entrainment from sites west of Franks Tract. For instance, in the lower export June case the fraction of neutrally buoyant particles injected at Jersey Point entrained at the export facilities drops from 8.75 percent to 3 percent. In the higher July case, entrainment is reduced from 53 percent to 44 percent. In contrast, entrainment goes up for particles starting at Franks Tract East (FTE), consistent with the increases in salinity and tidal

Figure 38 Percentage of Modeled Particles Entrained at State Water Project and Central Valley Project Export Sites within 30 days during a Low Export Month

Release	w/o project	w/ project
ANT	2.26	0.55
BAC	72.59	77.36
COL	1.21	0.51
FTE	17.80	21.98
FTW	13.63	5.69
GEO	8.28	13.85
HOO	3.63	2.76
JER	8.75	3.06
MED	16.46	27.32
MOS	50.79	51.81
NFM	7.64	12.06
POT	10.95	16.04
RIO	3.52	1.01
RYD	2.86	0.96
SFM	5.25	7.81
STO	3.05	5.39
TWI	13.89	7.89
VIC	90.30	90.47
X3M	9.28	3.17

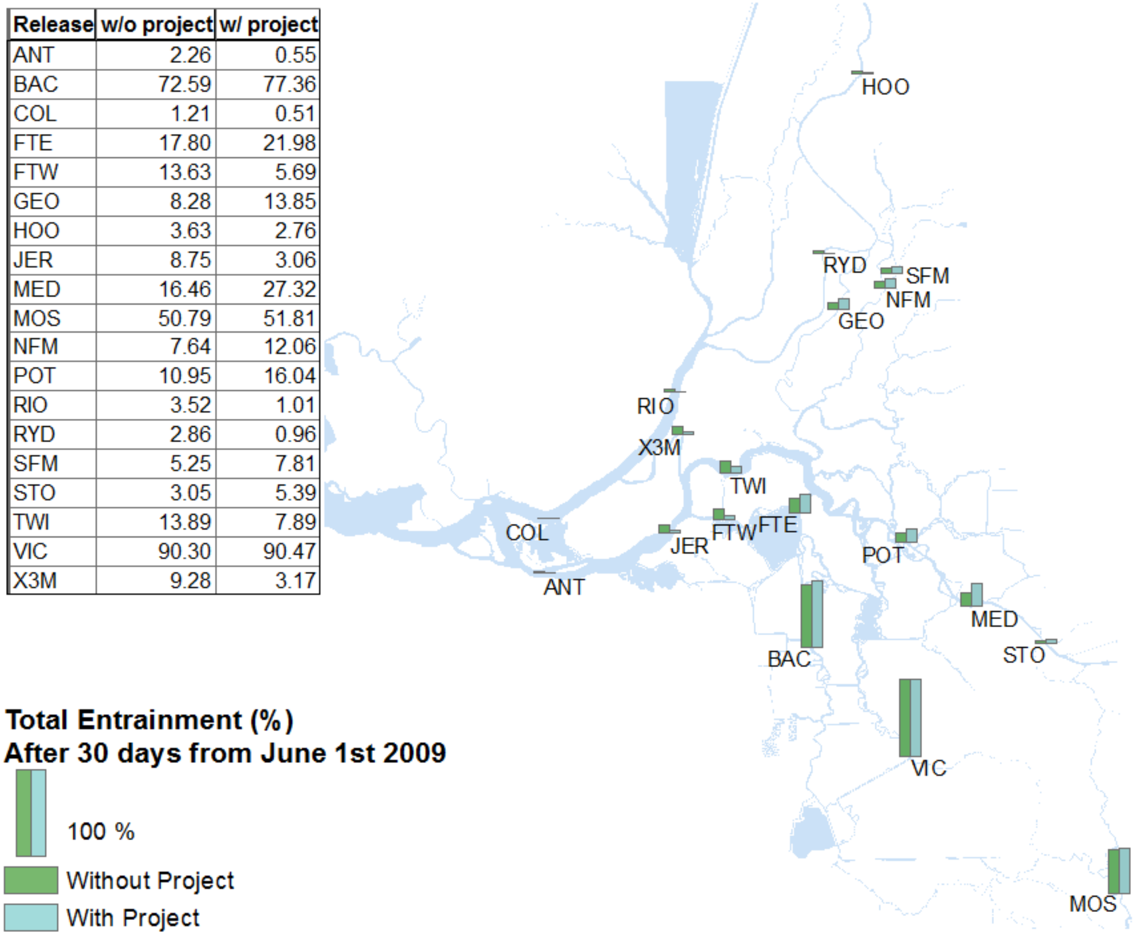

Note: Particles were released on June 1, 2009, from locations shown on the map.

range nearby. A modest increase in entrainment also occurs upstream on the San Joaquin River, although this is only detectable in the low-flow case. The increase is most likely because of the increased tidal range of flow through connections such as Turner Cut and Columbia Cut (Figure 26).

The changes in entrainment rates under the project are associated with the altered pathways particles must take to reach the export sites. Figures 40 (a) and 40 (b) show the particle trajectories from the Jersey Point (JER) injection site to the south Delta with and without the project. Each of the figures superimposes a large number of trajectories using lines of low transparency so that the paths that appear darkest are high traffic routes. The plot shows that in the base case, Franks Tract is the primary route for entrainment. In the restored case, the False River route is cut off and the main route to the export locations is clockwise around Bradford Island.

Note that in addition to cutting off movement through Franks Tract and increasing upstream movement along the San Joaquin River, the project also increases tidal exchange between the San Joaquin and Sacramento rivers through Three Mile Slough.

Figure 39 Percentage of Modeled Particles Entrained at State Water Project and Central Valley Project Export Sites within 30 days during a High Export Month

Release	w/o project	w/ project
ANT	20.26	16.86
BAC	97.85	97.53
COL	10.98	8.90
FTE	82.33	91.72
FTW	64.21	51.90
GEO	83.63	86.63
HOO	38.42	37.56
JER	53.34	43.69
MED	82.31	82.41
MOS	66.45	64.94
NFM	84.22	87.14
POT	91.19	91.17
RIO	23.86	19.00
RYD	25.59	20.85
SFM	72.26	61.20
STO	4.70	5.36
TWI	74.40	69.61
VIC	98.81	98.64
X3M	52.64	44.02

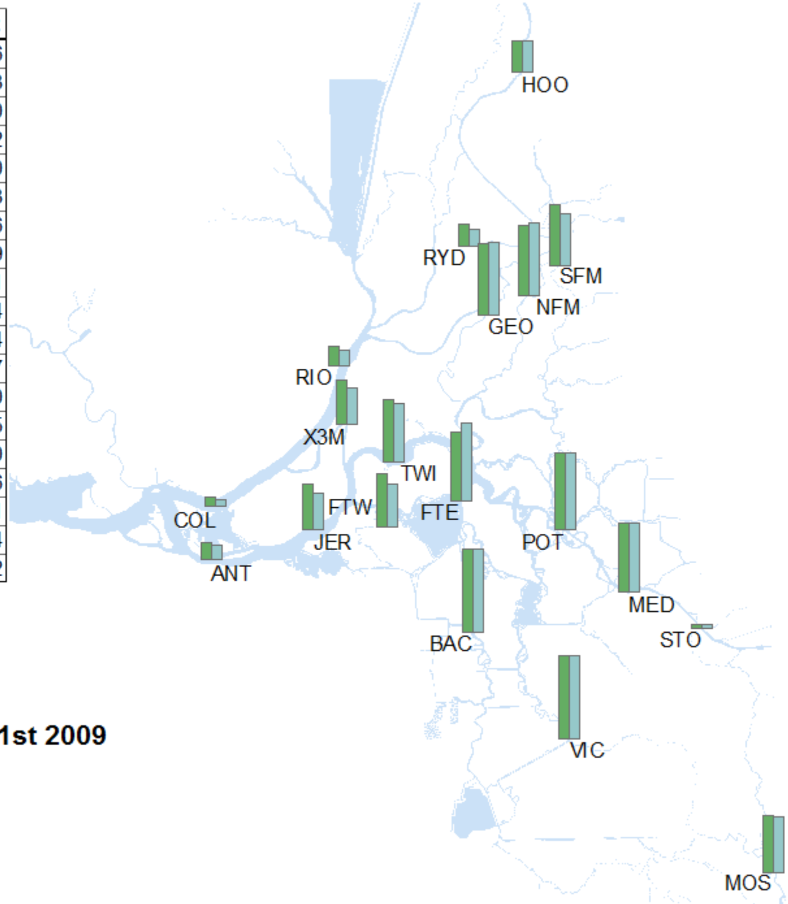

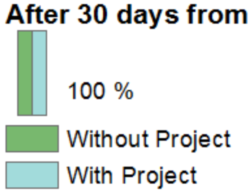

Note: Particles were released on July 1, 2009, from locations shown on the map.

Because of the more circuitous route particles must take to reach the pumps, transit time is also longer in the restored case. Figure 41 plots the distribution of transit times for particles injected at the Jersey Point (JER) site for both the low export June case and the high export July case. In the high-flow case, there is a 7-day horizontal shift between the restoration and base cases, representing additional time for particles to reach the export facilities from Jersey Point. In the low flow case, there is an even larger shift in age. It is less clear in the low flow case that the results are fully developed; 20 percent to 25 percent of the particles from Jersey Point area remain in the system at the end of the experiment.

Overall, the differences in entrainment rates and transit times between low and high exports are greater than the changes arising in entrainment from the restoration project.

Several simulations were performed to test the sensitivity of the modeling results to two potentially confounding factors, aquatic vegetation and other restoration sites.

Figure 40 Particle Trajectories for the Base (a) and Restored (b) Cases for Particles Released near Jersey Point, Showing the Main Routes

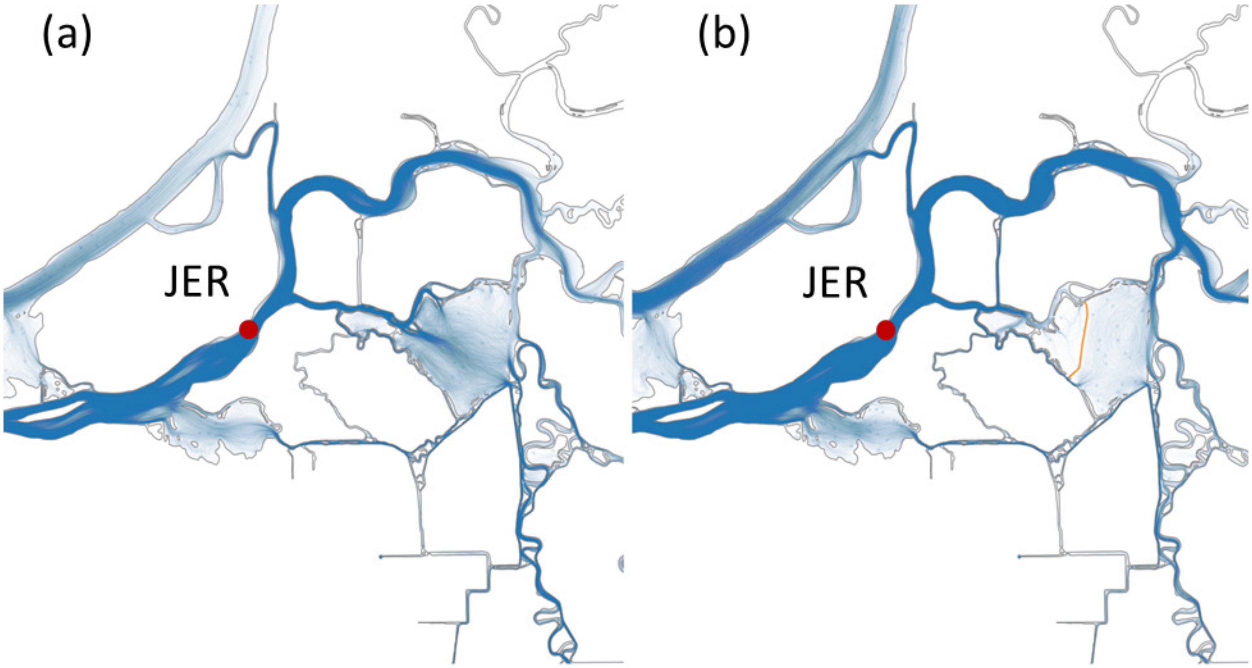

Note: JER = California Data Exchange Center Code for Jersey Point.
Trajectories are lines drawn with high transparency so that only major routes appear strongly.

Figure 41 Transit Time or Age of Neutrally Buoyant Particles Injected at Jersey Point (JER) that are Entrained at an Export Site

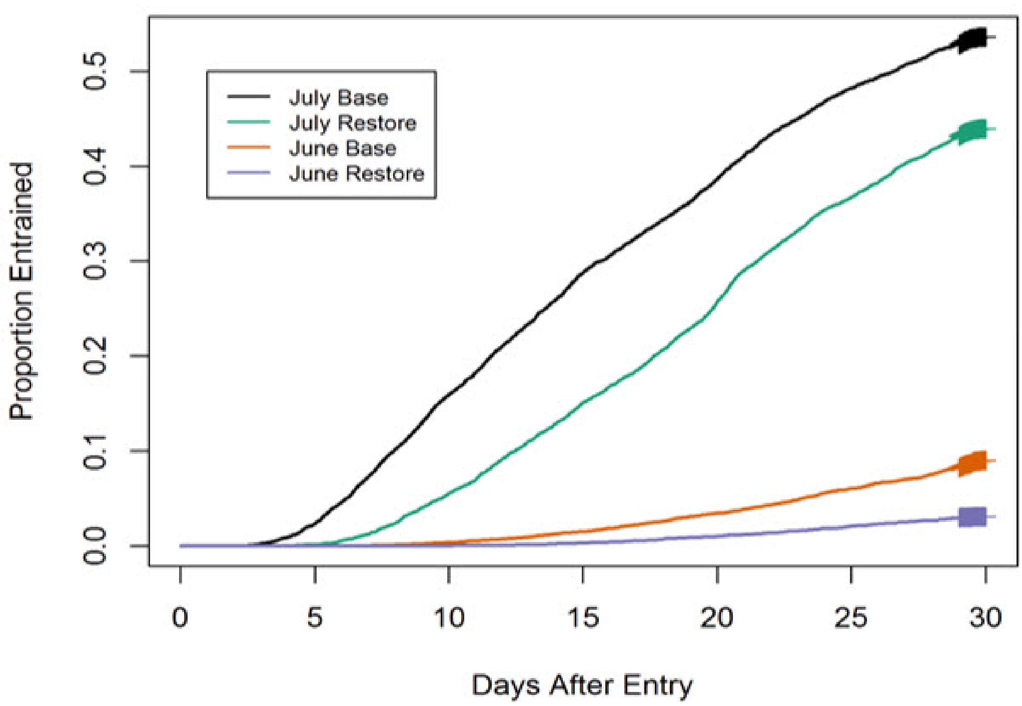

Note: Cross-hatching near day 30 indicates that the estimate was affected by data censorship as the experiment ended.3.5 Sensitivity

3.5.1 Submerged Aquatic Vegetation

There are two ways Franks Tract responds to SAV that might affect the feasibility study. One involves the system under the current geometry. The other affects the system more under the restoration.

First, under the base geometry, SAV produces drag on flow entering Franks Tract from False River, providing a sink for energy and dissipating tidal progression through Franks Tract. The resulting changes in tidal range and salinity are similar to the effects of the restoration project itself, but more moderate. As a result, if the project were assessed relative to a baseline that includes heavy vegetation, its incremental impact would be reduced.

Second, under any geometry SAV forms a curtain on the east side of Franks Tract where it meets the remnant channels to the east. The discontinuity can be discerned in the 2015 Normalized Difference Vegetation Index (NDVI) remote sensing map shown in Figure 3, although this map is even more “filled in” than prior years and the curtain has a break toward the north near the Old River entrance because of elevated velocities under the EDB. The curtain of SAV inhibits lateral (east-west) mixing between Old River water entering from the north and water in the body of Franks Tract. This potentially leads to a situation where fresher water enters from Old River and travels down the eastern remnant channels on flood tide, but then turns around and returns without influencing Franks Tract salinity. During the 2015 EDB installation, low lateral mixing in Franks Tract limited freshening of water moving into Holland Cut and points south (California Department of Water Resources 2017, in preparation).

Knowing that SAV had played a limiting role in the past, a model was done of a 2015 SAV field within the present project using additional drag and turbulent shear production caused by the canopy. The canopy was held at an elevation of 0.25 meters, stem density was 20 stems/square meter to 100 stems/square meter, spatially distributed according to the binned values of the NDVI from September 2015 (Figure 3) provided by Ustin et al (2016). Figure 42 is a velocity plot that shows the change in circulation strength resulting from SAV; velocity direction is marked by arrows and magnitude by color. Although the direction of circulation changes only slightly, its magnitude is reduced from a moderate to a very-low value away from the main channel. Based on the 3-mile diameter of Franks Tract, and typical remote velocities without (0.25 ft/s) and with (0.05 ft/s) vegetation, it appears SAV can increase the circulation time scale from less than one day to nearly one week.

Although SAV dampens circulation velocity in east Franks Tract, its impact on system-wide salinity remains low compared to the impact in 2015 with the emergency barrier, essentially undiscernible in the salinity plots of Figure 33 through Figure 37. One possible reason for this is that there are few other sources of salt reaching east Franks Tract from the west in the restoration project compared to the sources under the emergency barrier (e.g. leakage, Fisherman’s Cut). Another is that the eastern side is now smaller in volume and equilibrates with Old River more easily.

Figure 42 Ebb Velocity Without SAV (top left) and with SAV (bottom right)

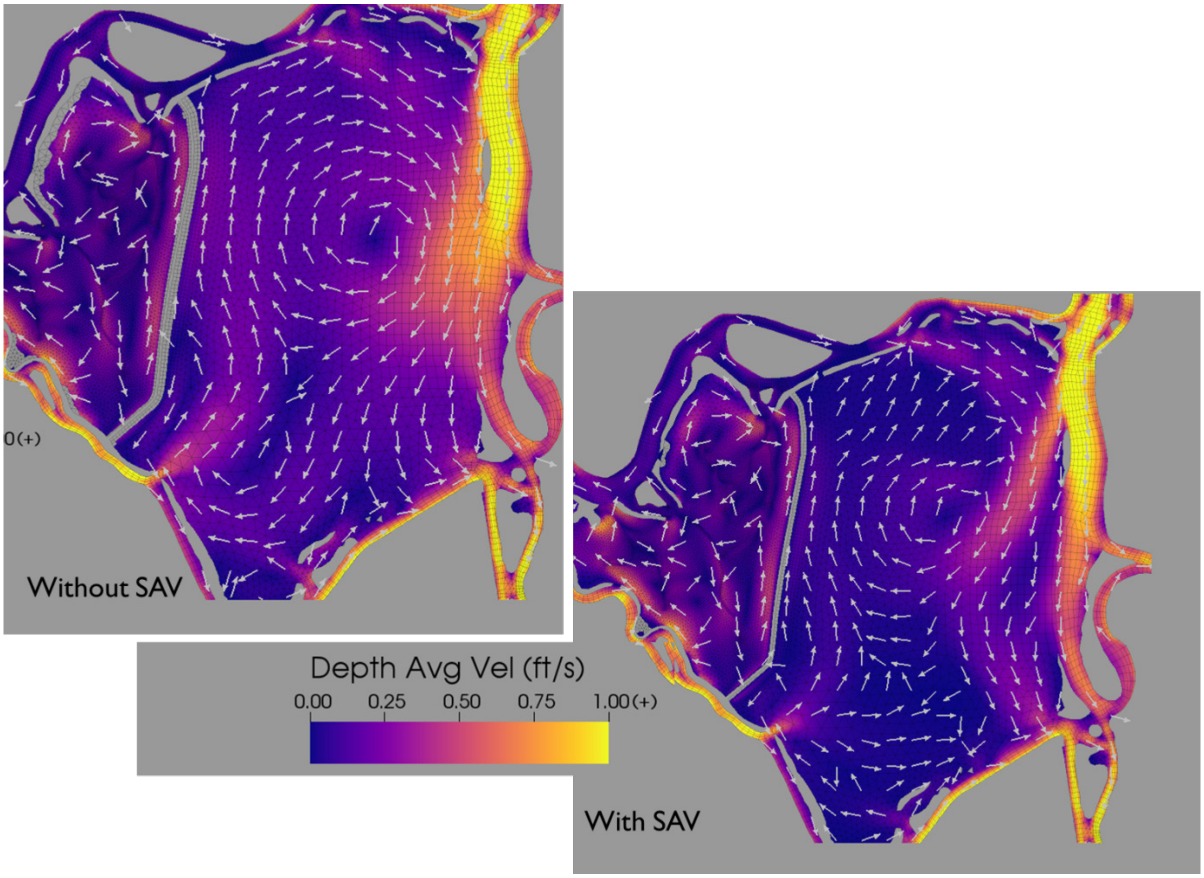

Note: SAV = submerged aquatic vegetation

3.5.2 Other Restoration Projects

A number of restoration projects are planned for the Delta in the near future. Stakeholders were interested in possible interactions between the proposed restoration in Franks Tract and several large projects that are in a more advanced state of design. For this sensitivity study, focus was placed on restoration proposals at Dutch Slough, Prospect Island, and McCormack-Williamson Tract. The selection of these three restoration projects was made based on the size of the projects, availability of design surfaces (sources listed in Table 1), and physical basis for interaction. In the case of Dutch Slough, interaction was expected based on size and proximity. In the case of Prospect Island and McCormack-Williamson Tract, modelers at Research Management Associates working on a regional salinity model had found that McCormack-Williamson Tract restoration had the potential to reduce Delta Cross Channel flow. That is important for the Franks Tract project because the Franks Tract restoration increases San Andreas Landing salinity. Delta Cross Channel flow is helpful for controlling this effect.

The modeling of the other projects mostly followed the same procedures as the Franks Tract site. All three additional sites were included with Franks Tract at once. For simplicity in tidal flow, the connection of Emerson Tract to Marsh Creek in the Dutch Slough project was omitted. Also omitted was an eastern breach on McCormack-Williamson Tract; both were designed for flood control. Within each restoration site, higher order channels were discretized down to a width of approximately 6 meters; lower order channels were ignored. This comment pertains mostly to the Dutch Slough design (the mesh in Figure 43), the design for which had an elaborate dendritic channel system.

Table 1 Sources of Design Surfaces for Projects in the Multiple Restoration Scenario

Project	Institution	Source of Design	Provider Version
Dutch Slough Tidal Restoration	DWR/RD 2137	ESA	95% Draft Grading Plans
Prospect Island	DWR/CDFW	DWR 2016	CEQA Alt 2
McCormack-Williamson Floodplain and Tidal Restoration	DWR/ Nature Conservancy	cbec eco engineering	Scenario 1

Note: CDFW = California Department of Fish and Wildlife, CEQA = California Environmental Quality Act, DWR = California Department of Water Resources, ESA =Environmental Science Associates, RD2137 = Reclamation District 2137

Figure 43 Dutch Slough Restoration Site, Emerson and Gilbert Tracts

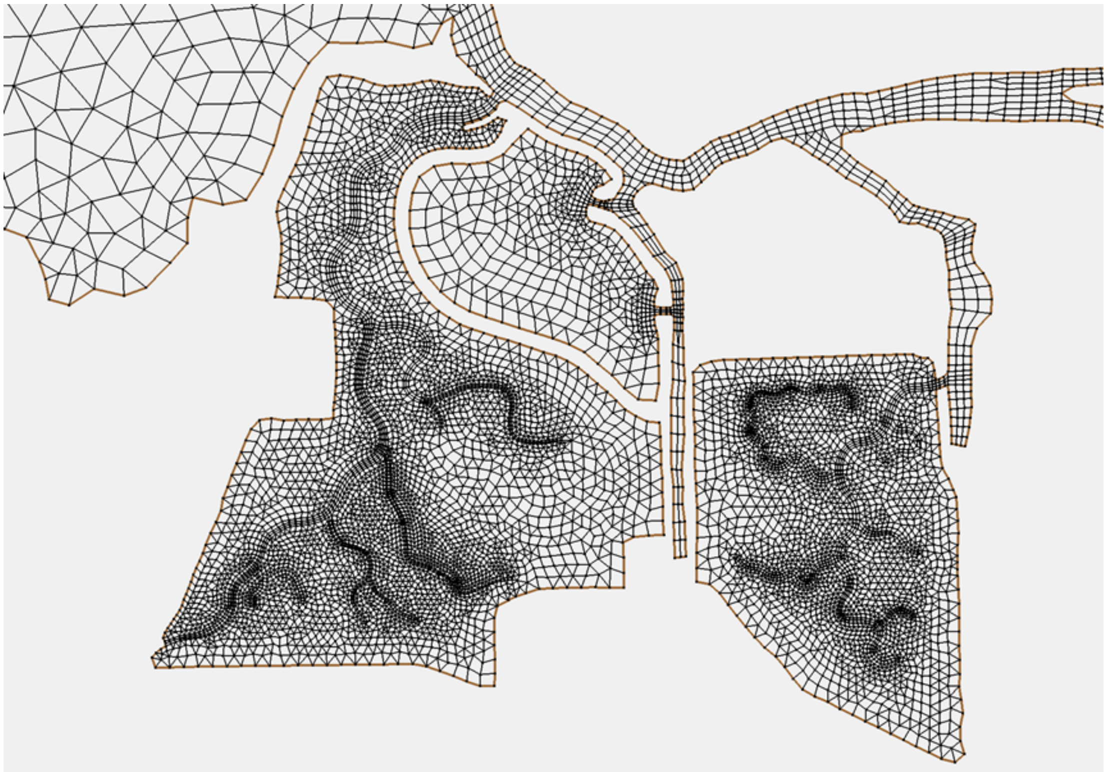

Note: Higher order channels are resolved, down to a width of approximately 6 meters.

Figure 44 is a change map of 14-day average specific conductance in early November that is analogous to Figure 32 but incorporates the three additional restoration areas. The spatial patterns of change are similar as those for Franks Tract alone, but skewed more toward increases. To clarify this point, Figure 45 illustrates the differences between the multiple restoration and single restoration cases, confirming that when compared to Franks Tract alone, the combined projects are saltier nearly everywhere. This is in evidence as well in the time series plots of Figure 33 through Figure 37, and is of particular importance at San Andreas Landing where the difference in tidally filtered salinity can be 100 µS/cm and the multiple projects impact D-1641 compliance. Over most of the middle and southern Delta, where Figure 44 is blue and Figure 45 is red, the Franks Tract is a compensating factor that offsets higher salinity from other projects.

Further work is underway by DWR to discern whether the changes shown in Figure 44 and Figure 45 represent a true interaction; i.e., whether the response to the combined projects is somehow greater than the sum of responses to the individual parts. This seems mostly likely along the main stem of the San Joaquin River and particularly at San Andreas Landing. There seems to be genuine interaction between projects. Franks Tract leads to a greater demand for Delta Cross Channel water and McCormack Williamson reduces the ability to supply it.

Figure 44 **14-Day Differences in Salinity in November, Multiple Restoration Case**

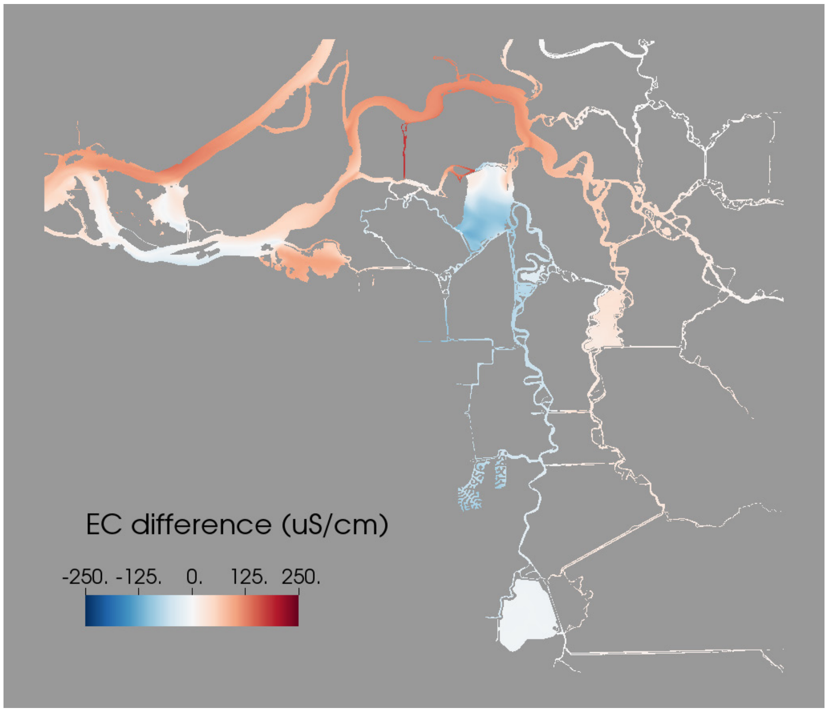

Notes: EC = electrical conductivity, uS/cm = micro-Siemens per centimeter
Salinity is converted to units of specific conductance between the restoration and base cases for the first 14 days of November. This image is comparable to Figure 32 but comes from the simulation with multiple restoration sites.

Figure 45 **Difference in November 14-Day Salinity between Multiple and Single Restoration Cases**

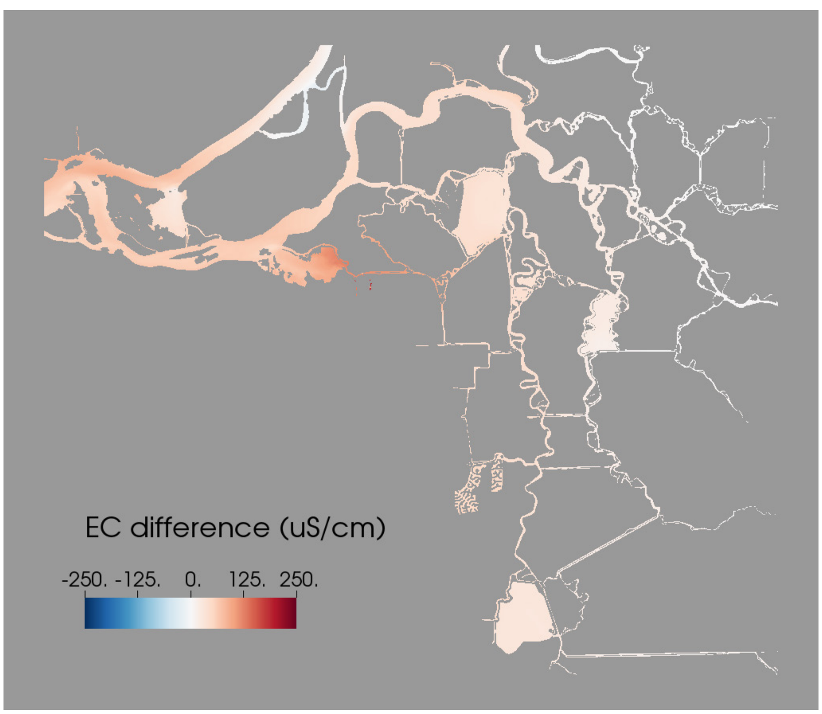

Notes: EC = electrical conductivity, uS/cm = micro-Siemens per centimeter
Salinity is converted to specific conductance. Differences are between the multiple restoration case and single restoration at Franks Tract.

3.5.3 Eastern Franks Tract Borrow Pit

Obtaining and delivering fill comprises a major cost for the project. One idea that was vetted to reduce costs was to borrow material from the east side of Franks Tract to fill the restoration area on the west side. The deepening required could be considerable because of the presense of peat in the borrow area. Based on data presented in *Franks Tract Engineering Feasibility Assessment* (Moffatt & Nichol 2017) for other parts of Franks Tract, it was expected the borrow pit might need to be as much as 25 feet deep. This was the value used in our investigation of the borrow pit impact.

The eastern borrow idea has many implications for navigation, aquatic weed control, and recreation.The main goal is to demonstrate that the borrow pit has a nearly negligible impact on regional salinity. Figure 42 is the change map between the case with and without a borrow pit. Changes are generally only a few micro-Siemens per centimeter.

Figure 46 Difference in August 14-Day Salinity Because of the Borrow Pit

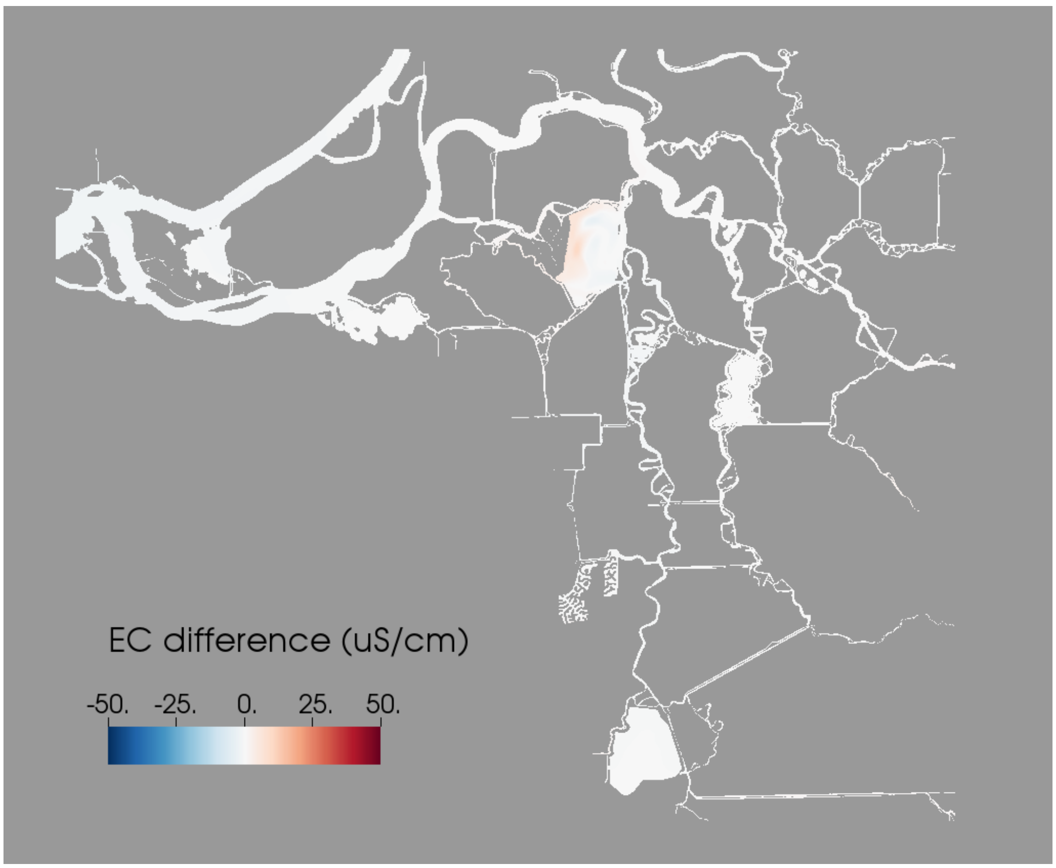

Notes: EC = Electrical Conductance (also referred to in text as specific conductance), uS/cm = micro-Siemens per centimeter.
Change is between restoration case with eastern borrow area and one without.

Chapter 4. Calibration

4.1 Summary

This section conveys how the model was tuned for the domain and to give an idea of its performance in 2009–2010, particularly in locations discussed in the report. DWR modelers have used 2009–2010 for studies and calibrations numerous times in the past, but the model was not spefically recalibrated for this project. The information presented here should be regarded as calibration level (evidence of performance on familiar hydrology data) rather than validation level (skill on entirely new periods and hydrology). Further information of validation performance within the Bay part of the model is available in Chao et al. (2017). A prior report on the full Bay-Delta model, in Ateljevich et al. (2014), includes spatial graphics characterizing systemwide performance on tidal and net flow characteristics. The report by Shu and Ateljevich (2017) on transit time in Clifton Court for the National Marine Fisheries Service describes model perforamnce in a shallow open water body.

Bay-Delta SCHISM has been calibrated for hydrodynamic variables (water surface, velocities, and cross-sectional flows) as well as salinity. Performance on temperature is reported for the Bay in Chao et al. (2017). A document on performance in 2015 during the EDB installation is in preparation within DWR and is due for release in January 2018. One plot has been included here that quantifies how the model responded at the critical Old River at Franks Tract (CDEC Code: OSJ) station that year.

The main items manipulated in a calibration were:

- Horizontal mesh configuration and density.
- Vertical mesh selection, configuration, and density.
- Roughness coefficients.
- The selection of turbulence closure.
- Algorithmic differences in the treatment of momentum advection.

There are results and rules of thumb in the literature to guide many of the selections, but these variables and decisions still represent a potentially large and intractable parameter space. To control this, only a global relationship between roughness and depth was allowed. In the present model, a roughness parameter between $z0=1e^{-4}$ in the shallows and $z0=1e^{-2}$ at depths of greater than 25 meters were assigned, with a linear transition in between. Physically, this assumes bottom roughness in deep areas is more affected by bedforms; also, numerically, it is believed form drag is lower overall in deep areas in models with terrain-following grids, but that the influence of numerical/form drag is proportionally greater in the shallows. These differences in roughness produce only a moderatly sensitivity in the model – it takes a factor between 2 and 5 change to make an appreciable difference in results.

The biggest contributor to error for salinity in the western Delta, and the biggest confounding factor in the calibration of any model, is uncertainty over outflow caused by Delta consumptive use by agriculture, and in particular, how this maps to channel depletions. It appears this point is well appreciated by Delta stakeholders. Successful qualitative modeling of transport in the western Delta requires that the salinity field be positioned roughly east-west along the main stem of the San Joaquin River. For instance, if salt hasn't arrived at Jersey Point, there won't be any gradient to support pumping in Franks Tract. Intrusion distance is controlled by Delta outflow, and the margin of error is probably 800 cfs to 1,500 cfs when

Delta outflow is low. Unfortunately, this figure is at times similar to the spread between various channel depletion estimates and flow gauge bias (Sandhu et al. 2016). This creates some sensitivity to technique around Jersey Point that confounds calibration in that region.

4.2 Locations

Figure 47 shows stations where metrics and plots are reported. These focus on the region of the study, but a small number of additional stations are included that are farther afield.

Figure 47 Map of Stations Included in Metrics Plots

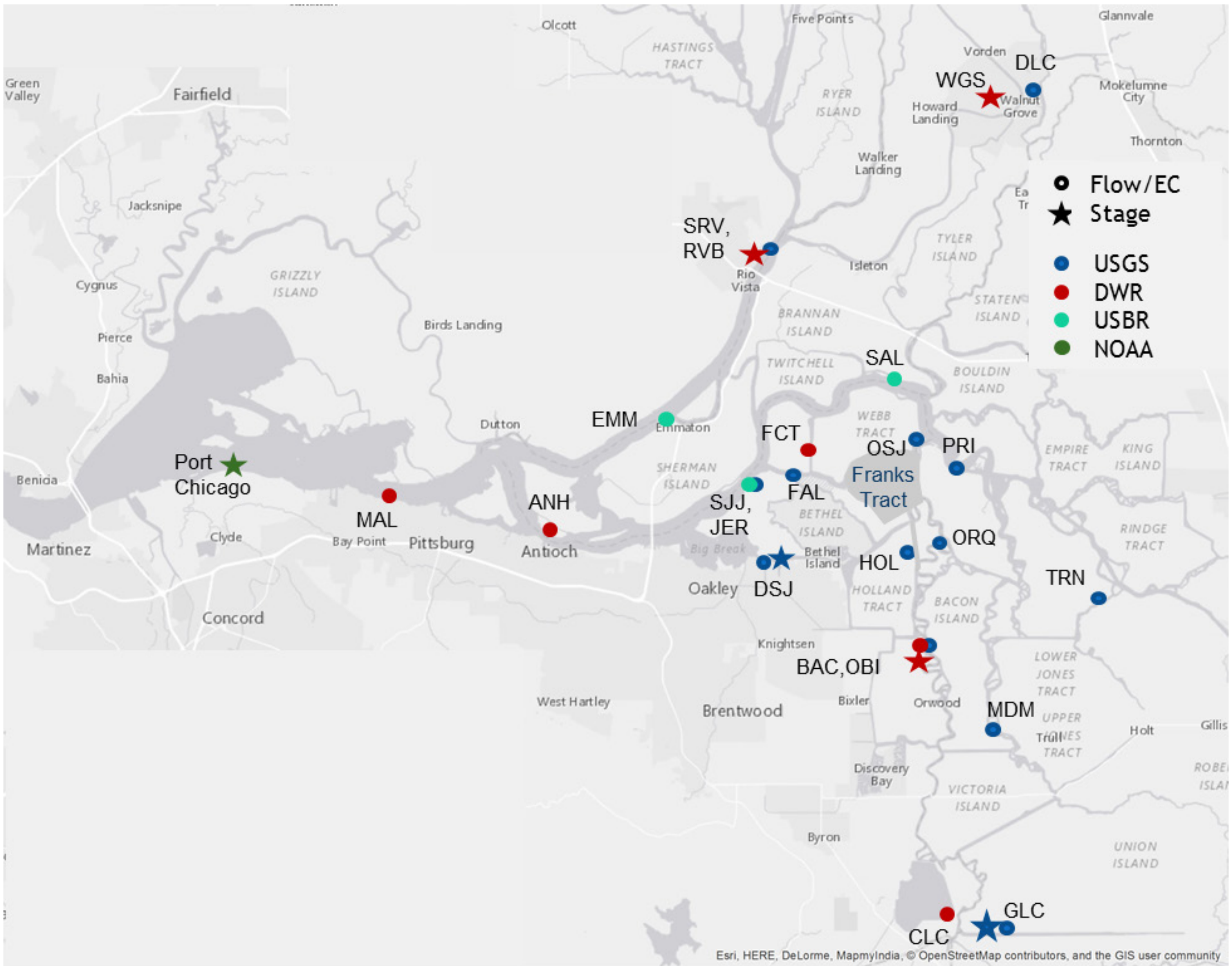

4.3 Skill Metrics for Scalar Station Data

For station data, model performance was evaluated based on both visual assessments of tidal and subtidal time series plots and quantitative fitness scores. The plots include a time series plot at tidal/instantaneous scales on top, a time series plot of tidally filtered ("net") quantities in the bottom left, and a scatter plot of observed versus modeled values on the bottom right. On the time series plots, the left axes labels are specified in metric units and the right axes labels are specified in U.S. customary units.

Observed data mostly come from DWR CDEC (California Department of Water Resources 2017) and Water Data Library (California Department of Water Resources 2016) websites, the USGS NWIS (U.S. Geological Survey 2016) website, and NOAA Tides and Currents (National Oceanic and Atmospheric Administration 2016) website. Data collected by DWR Operations and Maintenance, and Department of Environmental Services are sourced from CDEC. Model data marked “base” refer to model results under the base geometry.

The following statistics are reported where appropriate, computed from June 2009 to May 2010.

RMSE: Root mean square error, not phase-corrected.

Lag: An estimation of lag based on cross-correlation analysis, as described in Resource Management Associates (2005). The phase lag estimated here is used to shift the series for calculation of the remainder of the metrics. Note that in the case of stations labeled as having been obtained from CDEC, the timestamp is probably not accurate to better than one hour because of daylight saving time conversions that are either incorrect or that change over time.

Bias$_\varphi$ The median bias of phase corrected error (modeled - observed)

NSE$_\varphi$ The Nash-Sutcliffe efficiency for the phase-corrected error:

$$NSE\phi(f,r,x) = 1 - (MSE(f,x)/MSE(r,x))$$

where $MSE(f,x) = \frac{1}{n}\sum_{i=1}^{n}(f_i - x_i)^2$ is the mean squared error between a reference (f), and an observation (x); r represents the station mean.

R$_\varphi$ The correlation coefficient (the r in R^2) for the fit of the observations on the phase-corrected model values.

4.4 Water Level Calibration Plots and Metrics

Figure 48 through Figure 53 show plots and metrics for the stations starred in Figure 47. The model reproduces tidal and subtidal water level propagation throughout the domain. The main systematic drawback is the models tendency to funnel tidal energy so that tides are slightly amplified and sped up in the mid-Delta, which is an indicator that the model underestimates tidal prism mid-Delta; the effect is not exhibited upstream where the floodplain is discretized in some detail.

Figure 48 Water Level Performance Plots and Metrics at Port Chicago

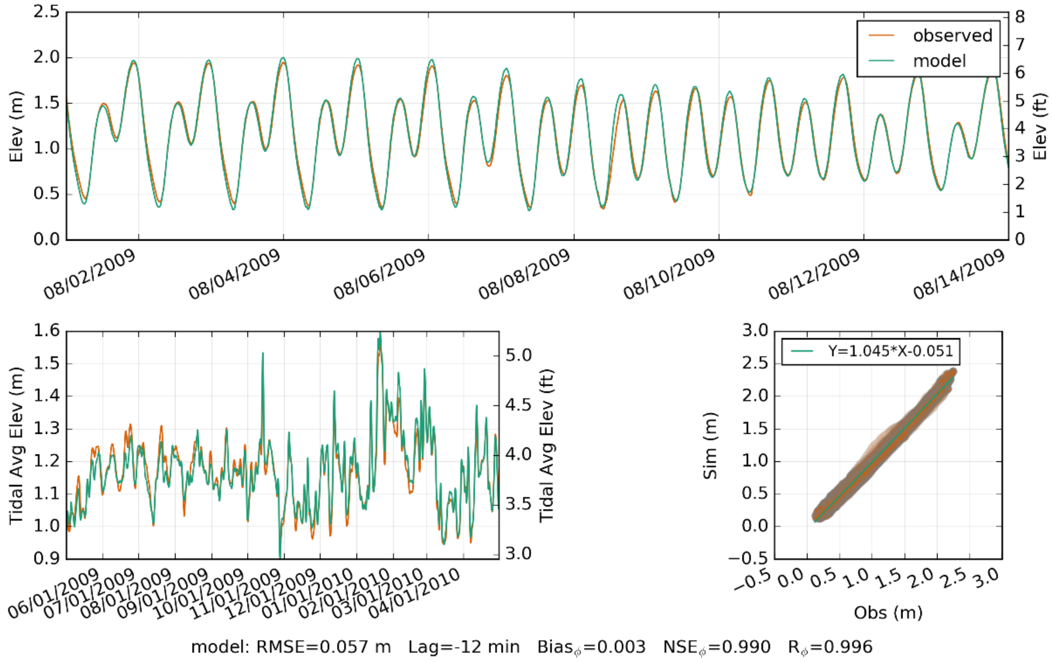

Source: National Oceanic and Atmospheric Administration, identification number: 9415144
Notes: Vertical datum is NAVD88. NSE = Nash-Sutcliffe efficiency, Obs = observed data,
R= correlation coefficient, RMSE = root mean square error, φ (subscript) indicates phase-corrected statistic.

Figure 49 Water Level Performance Plots and Metrics at Rio Vista (RVB)

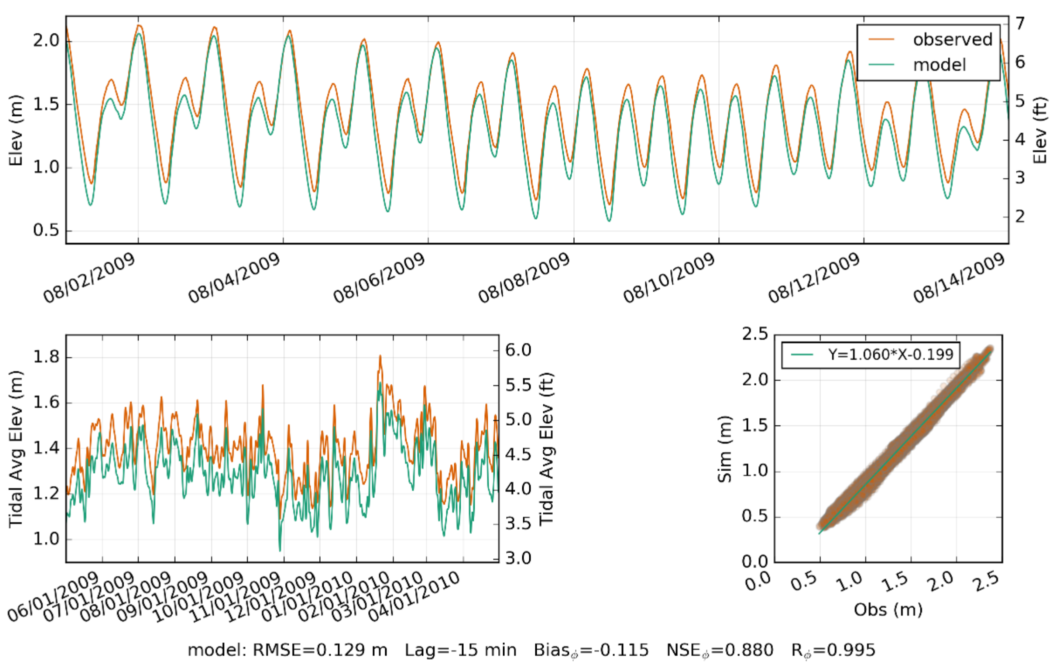

Source: California Department of Water Resources, Water Data Library identification number: B91212
Notes: Vertical datum is NAVD88. NSE = Nash-Sutcliffe efficiency, Obs = observed data, R= correlation coefficient, RMSE = root mean square error, φ (subscript) indicates phase-corrected statistic, RVB = California Data Exchange Center code for Sacramento River at Rio Vista

Figure 50 Water Level Performance Plots and Metrics at Walnut Grove (WGS)

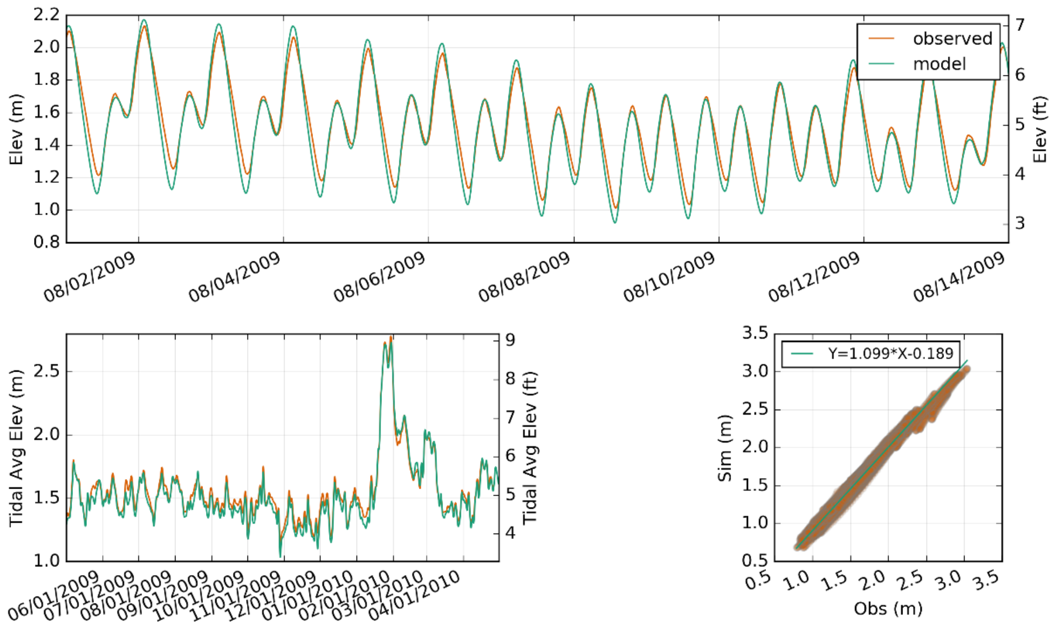

model: RMSE=0.077 m Lag=-24 min $Bias_{\phi}$=-0.032 NSE_{ϕ}=0.962 R_{ϕ}=0.992

Source: California Department of Water Resources Water Data Library, identification number: B91650

Notes: Vertical datum is NAVD88. NSE = Nash-Sutcliffe efficiency, Obs = observed data, R= correlation coefficient, RMSE = root mean square error, WGS = California Data Exchange Center code for Sacramento River at Walnut Grove, φ (subscript) indicates phase-corrected statistic

Figure 51 Water Level Performance Plots and Metrics at Dutch Slough (DSJ)

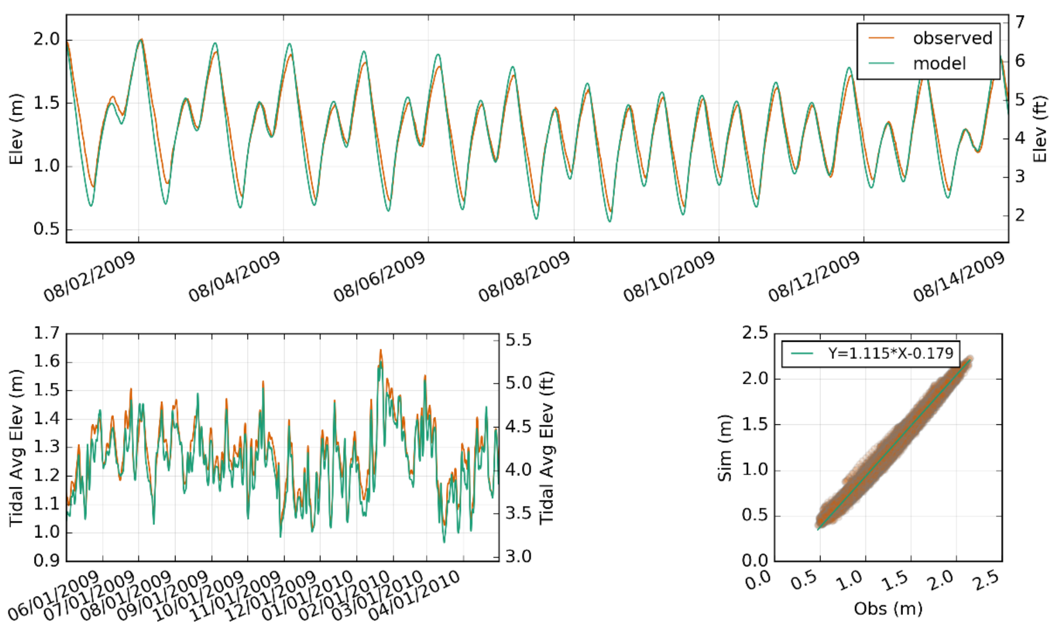

model: RMSE=0.078 m Lag=-20 min $Bias_{\phi}$=-0.030 NSE_{ϕ}=0.958 R_{ϕ}=0.993

Source: U.S. Geological Survey, identification number: 11313433

Note: Vertical datum is NAVD88. DSJ = California Data Exchange Center code for Dutch Slough below Jersey Island, NSE = Nash-Sutcliffe efficiency, Obs = observed data, R= correlation coefficient, RMSE = root mean square error, φ (subscript) indicates phase-corrected statistic

Figure 52 **Water Level Performance Plots and Metrics at Old River at Bacon Island (BAC)**

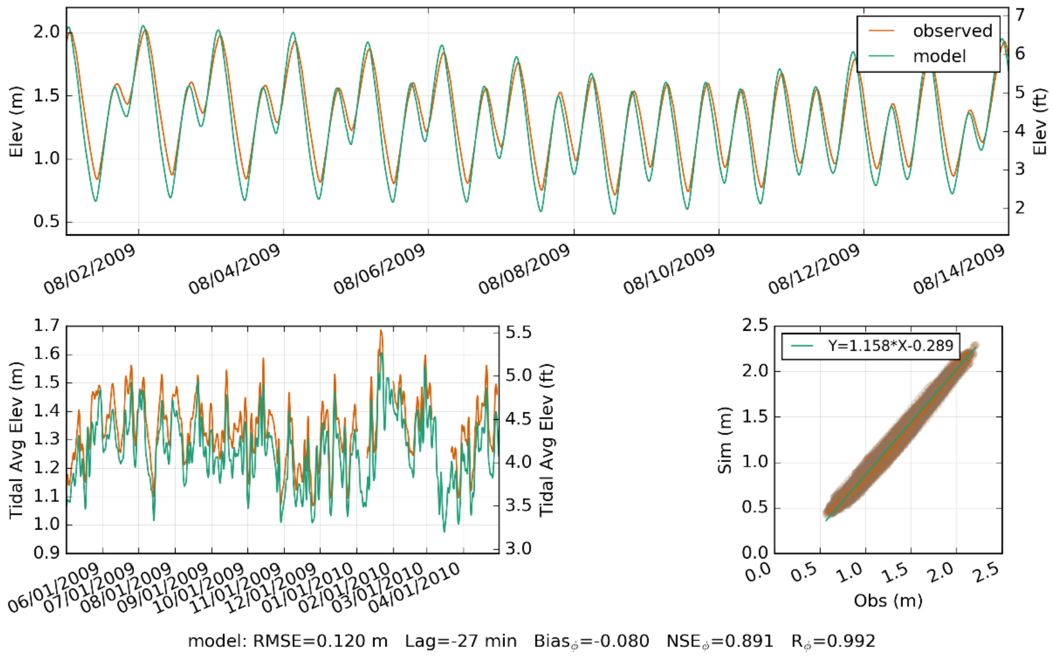

Source: California Department of Water Resources Water Data Library, identification number: B95250

Notes: Vertical datum is NAVD88. BAC = California Data Exchange Center Code for Old River at Bacon Island, NSE = Nash-Sutcliffe efficiency, Obs = observed data, R= correlation coefficient, RMSE = root mean square error, φ (subscript) indicates phase-corrected statistic

Figure 53 **Water Level Performance Plots and Metrics at Old River at Grantline Canal (GLC)**

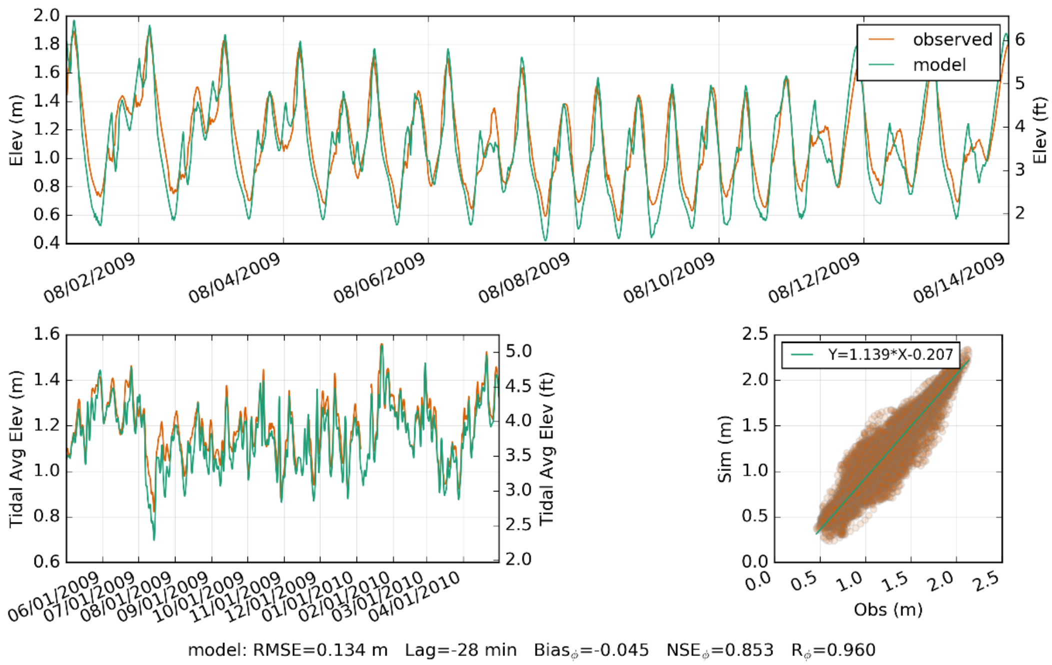

Source: U.S. Geological Survey, identification number: 11313200

Notes: Vertical datum is NAVD88. GLC = California Data Exchange Center code for Grantline Canal, NSE = Nash-Sutcliffe efficiency, Obs = observed data, R= correlation coefficient, RMSE = root mean square error, φ (subscript) indicates phase-corrected statistic

4.5 Flow Calibration Plots and Metrics

Flow metrics are given below for stations indicated with a circle in Figure 47, as well as for the Delta Cross Channel, which is relevant for assessing project interactions with McCormack-Williamson Tract. Overall, model skill on flow is strong at most stations. There are local examples of attenuation and minor phase lead. Net flow also matches observed data well. Figure 66 is a special case, a one-off map of USGS downward-looking Acoustic Doppler Current Profiler data used to calibrate the Old River at Franks Tract (CDEC code: OSJ) station while the 2015 EDB was in place. The modeling was completed in real-time, before the USGS data were received by modelers, so is of genuine validation quality and demonstrates the model did well capturing the doubling in tidal range following closure of the main berm. Because the Franks Tract restoration project produces similar changes as the drought barrier, this result is pertinent to the current work.

Figure 54 **Flow Performance Plots and Metrics at Rio Vista (SRV)**

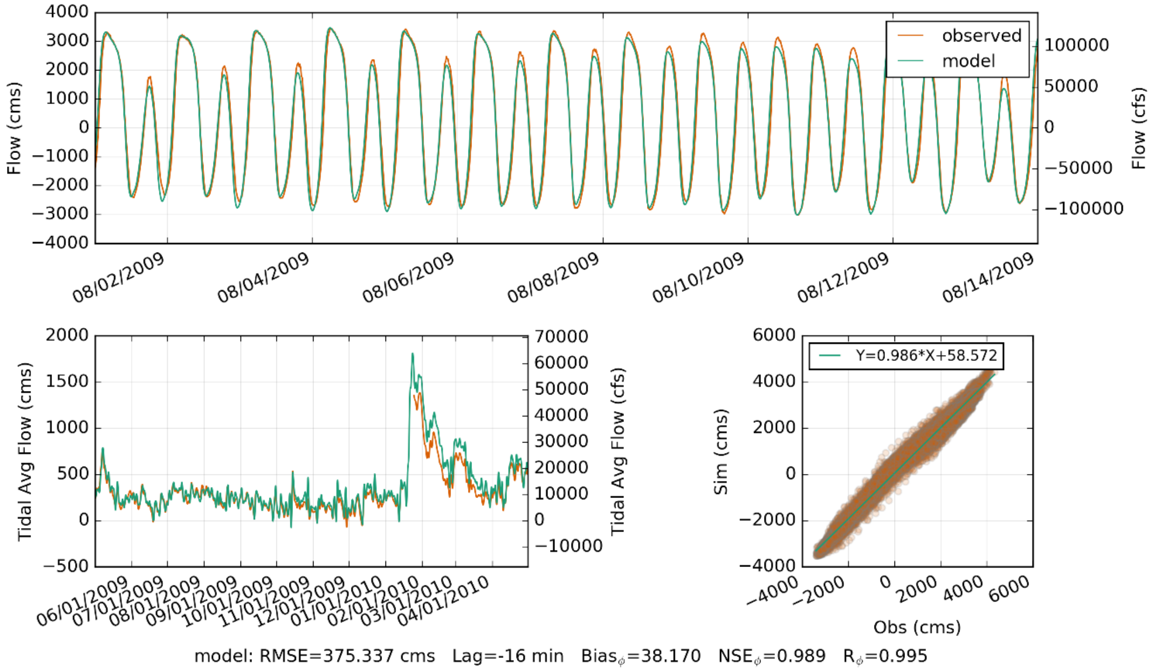

Source: U.S. Geological Survey, identification number: 11455420

Notes: NSE = Nash-Sutcliffe efficiency, Obs = observed data, R= correlation coefficient, RMSE = root mean square error, SRV = California Data Exchange Center code for Sacramento River at Rio Vista, φ (subscript) indicates phase-corrected statistic

Figure 55 **Flow Performance Plots on Dutch Slough (DSJ)**

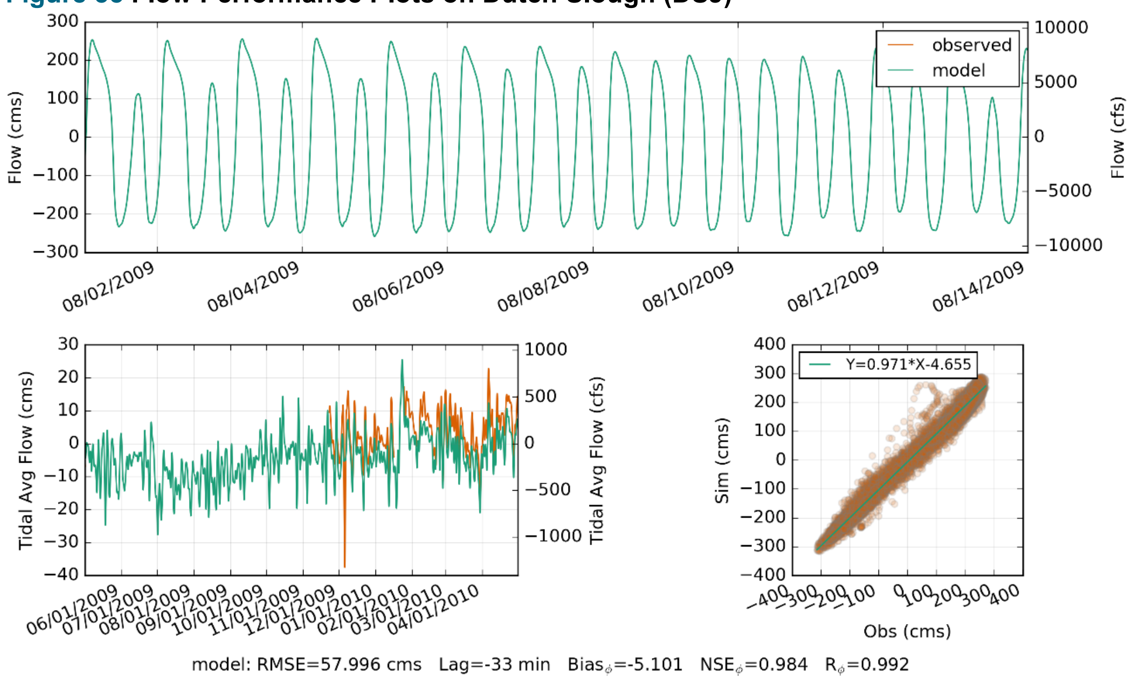

Source: U.S. Geological Survey, identification number: 11313433

Notes: DSJ = California Data Exchange Center code for Dutch Slough below Jersey Island, NSE = Nash-Sutcliffe efficiency, Obs = observed data, R= correlation coefficient, RMSE = root mean square error, φ (subscript) indicates phase-corrected statistic

Figure 56 Flow Performance Plots and Metrics at False River (FAL)

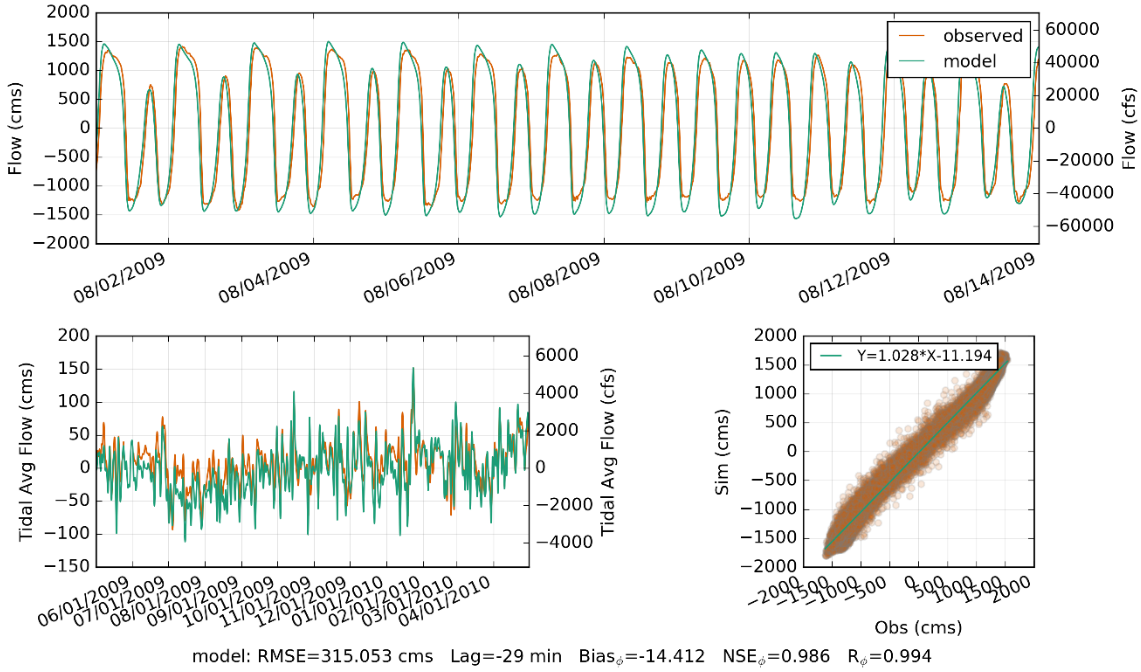

Source: U.S. Geological Survey, identification number: 11313440

Notes: FAL = California Data Exchange Center code for False River near Oakley, NSE = Nash-Sutcliffe efficiency, Obs = observed data, R= correlation coefficient, RMSE = root mean square error, φ (subscript) indicates phase-corrected statistic

Figure 57 Flow Performance Plots and Metrics on Old River at Franks Tract (OSJ)

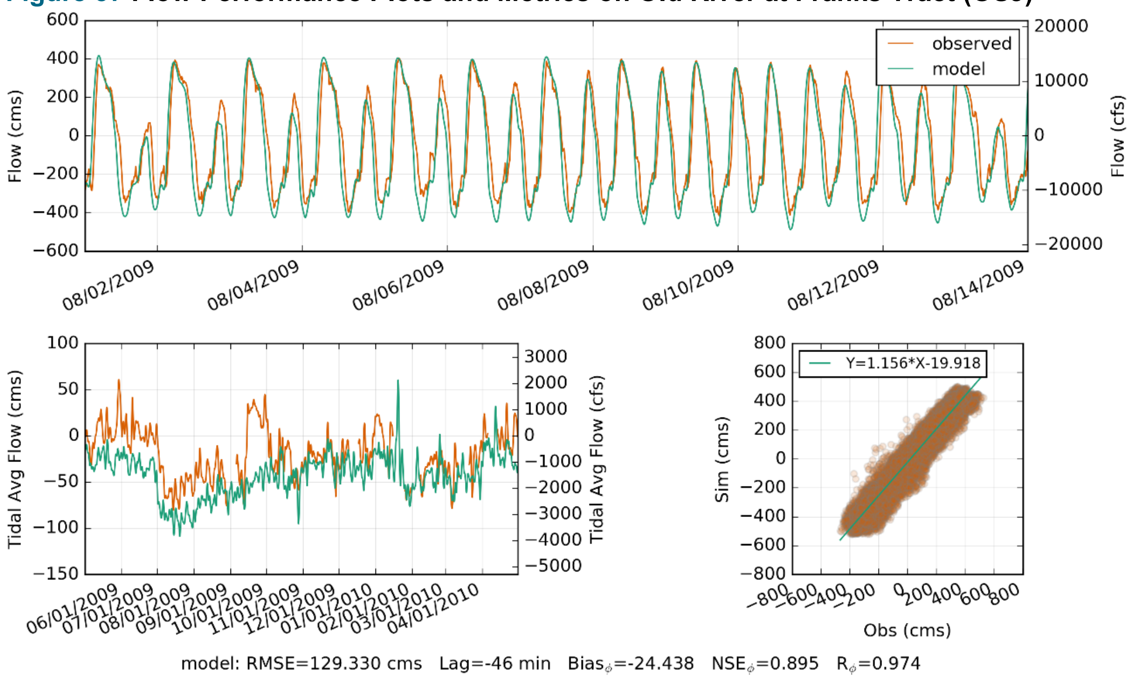

Source: U.S. Geological Survey, identification number: 11313452.

Notes: NSE = Nash-Sutcliffe efficiency, Obs = observed data, R= correlation coefficient, OSJ = California Data Exchange Center code for Old River at Franks Tract, RMSE = root mean square error, φ (subscript) indicates phase-corrected statistic

Figure 58 Flow Performance Plots and Metrics at Holland Cut (HOL)

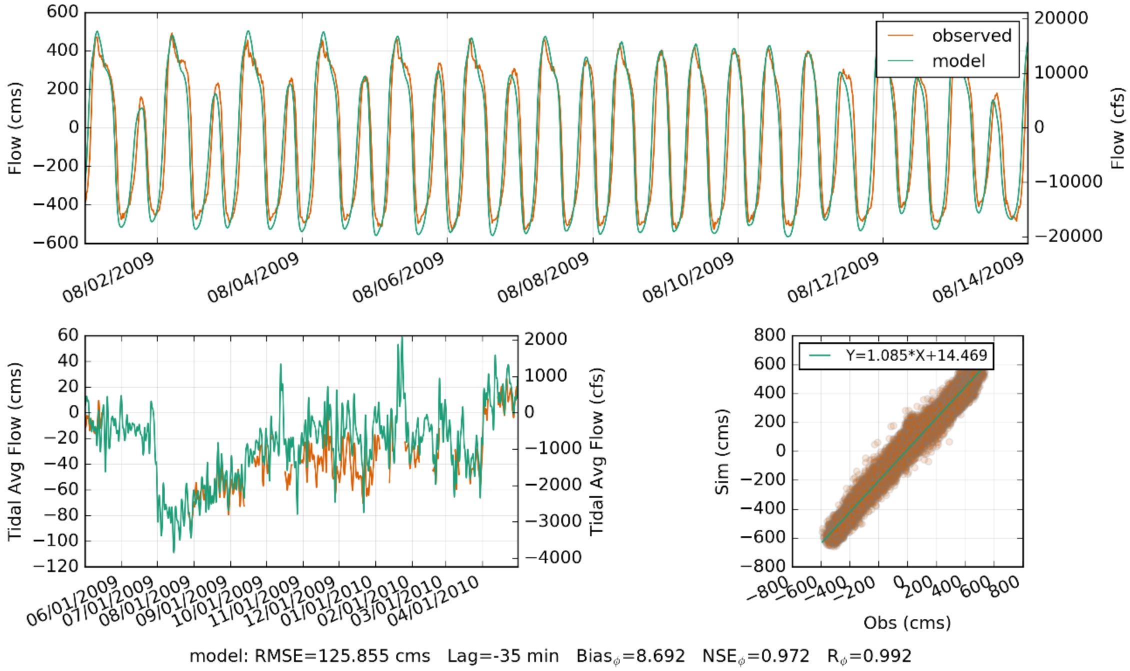

Source: U.S. Geological Survey, identification number: 11313431

Notes: HOL = California Data Exchange Center code for Holland Cut near Bethel Island, NSE = Nash-Sutcliffe efficiency, Obs = observed data, R= correlation coefficient, RMSE = root mean square error, φ (subscript) indicates phase-corrected statistic

Figure 59 Flow Performance Plots and Metrics at Old River at Quimby (ORQ)

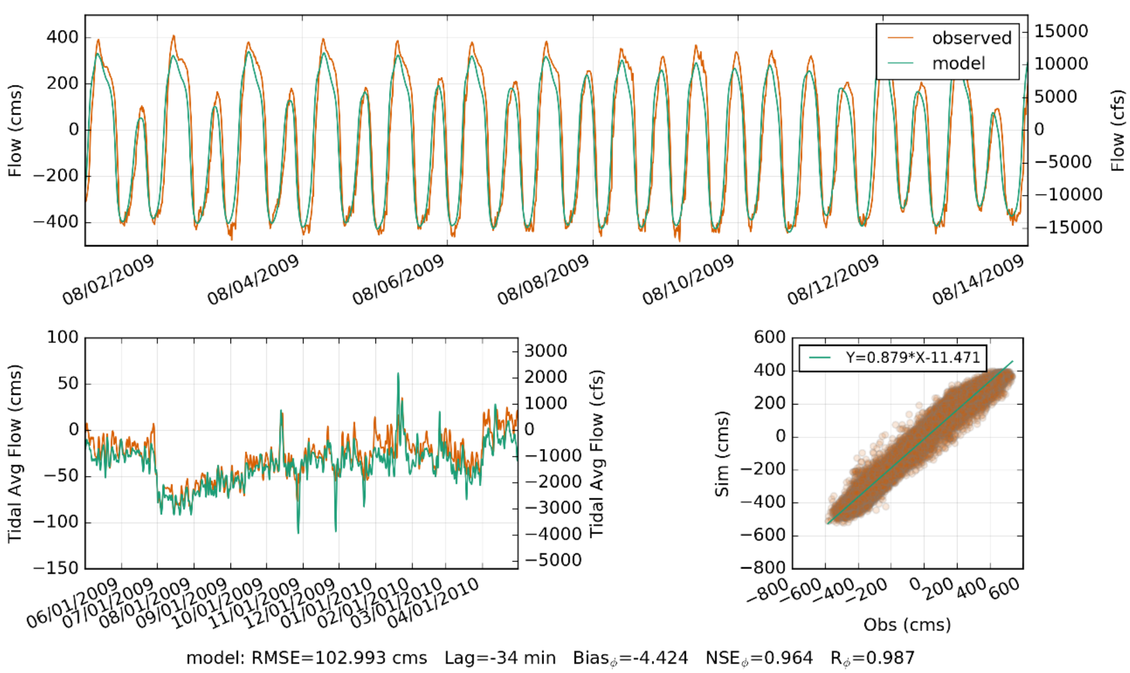

Source: U.S. Geological Survey, identification number: 11313434

Notes: NSE = Nash-Sutcliffe efficiency, Obs = observed data, R= correlation coefficient, RMSE = root mean square error, ORQ = California Data Exchange Center code for Old River at Quimby Island, φ (subscript) indicates phase-corrected statistic

Figure 60 **Flow Performance Plots and Metrics at Middle River (MDM)**

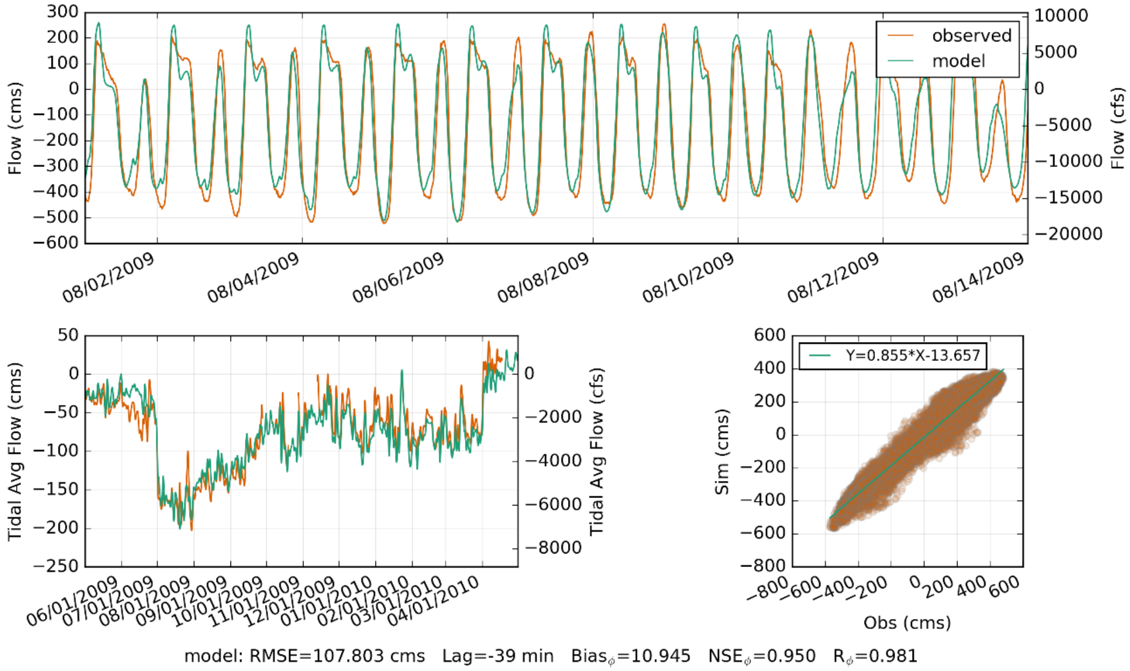

Source: U.S. Geological Survey, identification number: 11312676

Notes: MDM = California Data Exchange Center code for Middle River, NSE = Nash-Sutcliffe efficiency, Obs = observed data, R= correlation coefficient, RMSE = root mean square error, φ (subscript) indicates phase-corrected statistic

Figure 61 **Flow Performance Plots and Metrics for Old River at Bacon Island (OBI)**

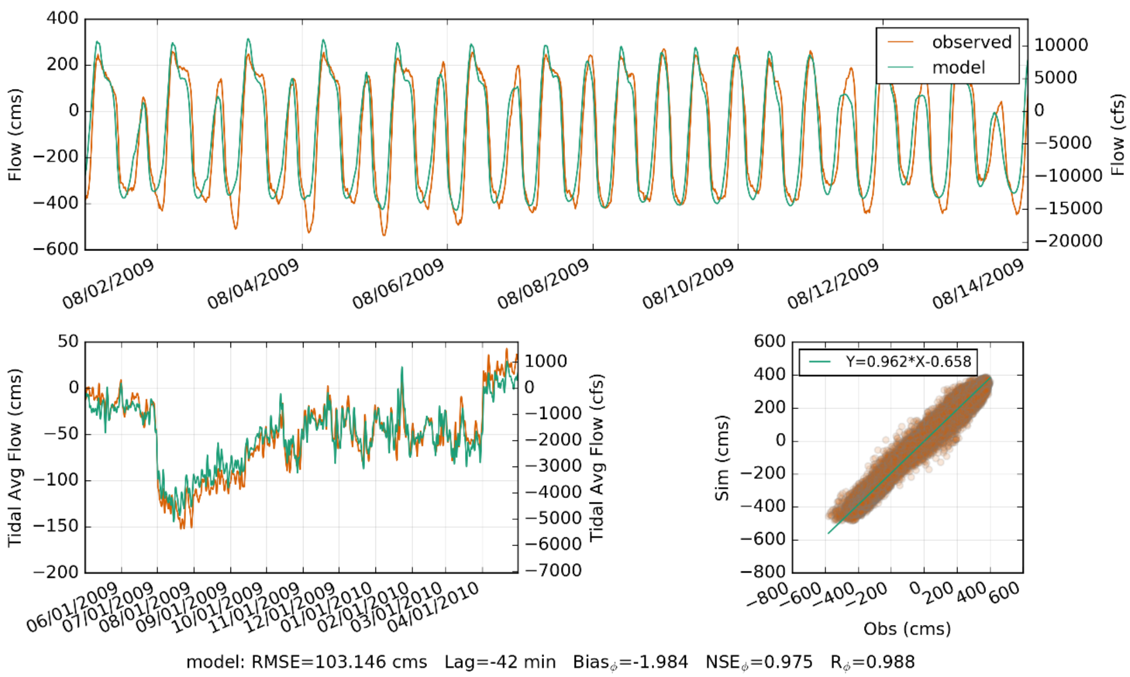

Source: U.S. Geological Survey, identification number: 11313405

Notes: NSE = Nash-Sutcliffe efficiency, OBI = California Data Exchange Center code for Old River at Bacon Island, Obs = observed data, R= correlation coefficient, RMSE = root mean square error, φ (subscript) indicates phase-corrected statistic

Figure 62 **Flow Performance Plots and Metrics at Grantline Canal (GLC)**

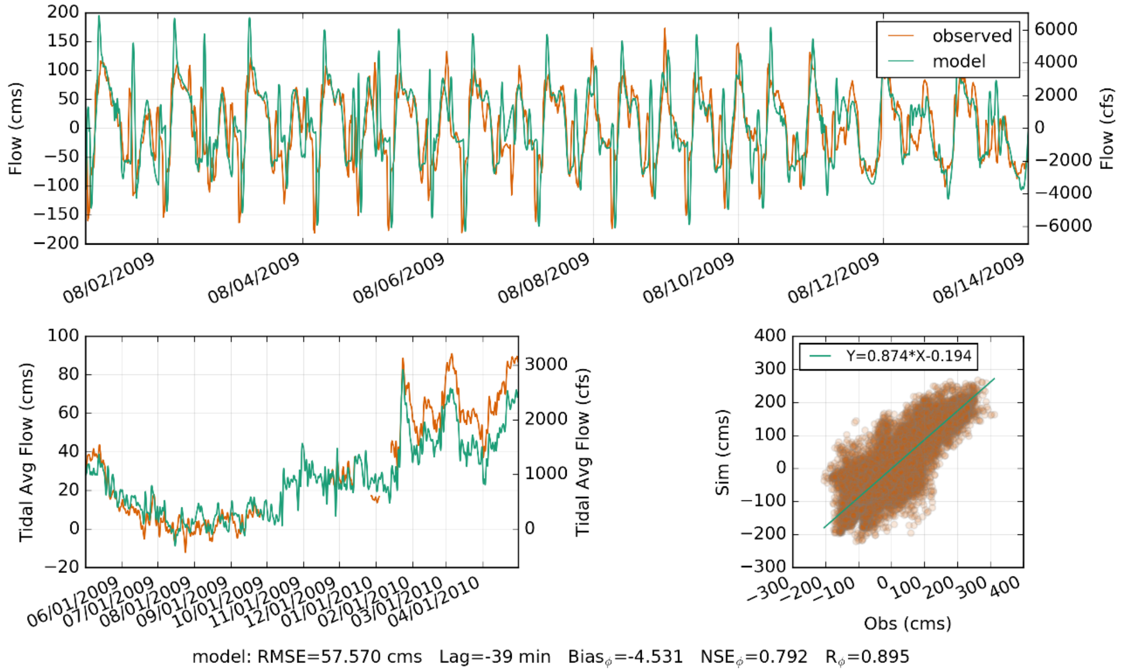

Source: U.S. Geological Survey, identification number: 11313200

Notes: GLC = California Data Exchange Center code for Grantline Canal, NSE = Nash-Sutcliffe efficiency, Obs = observed data, R= correlation coefficient, RMSE = root mean square error, φ (subscript) indicates phase-corrected statistic

Figure 63 **Flow Performance Plots and Metrics at Delta Cross Channel (DLC)**

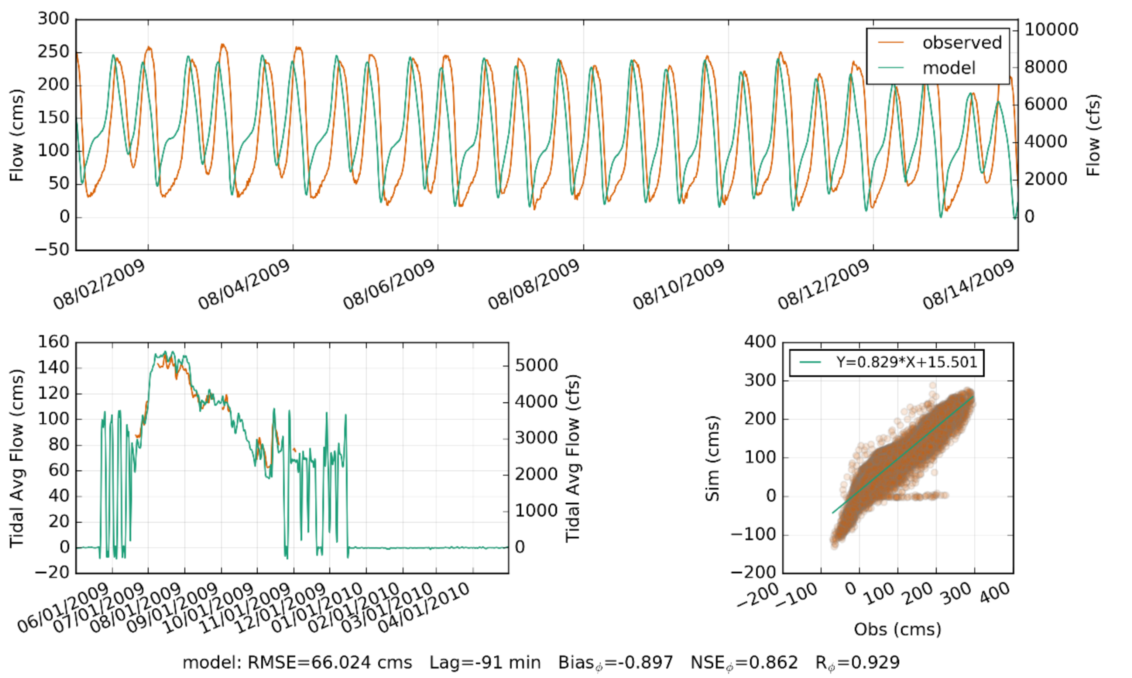

Source: U.S. Geological Survey, identification number: 11336600

Notes: base = model output with the base mesh, DLC = California Data Exchange Center code for Delta Cross Channel near Walnut Grove, NSE = Nash-Sutcliffe efficiency, Obs = observed data, R= correlation coefficient, RMSE = root mean square error, φ (subscript) indicates phase-corrected statistic

Figure 64 Flow Performance Plots and Metrics on the San Joaquin River at Prisoners Point (PRI)

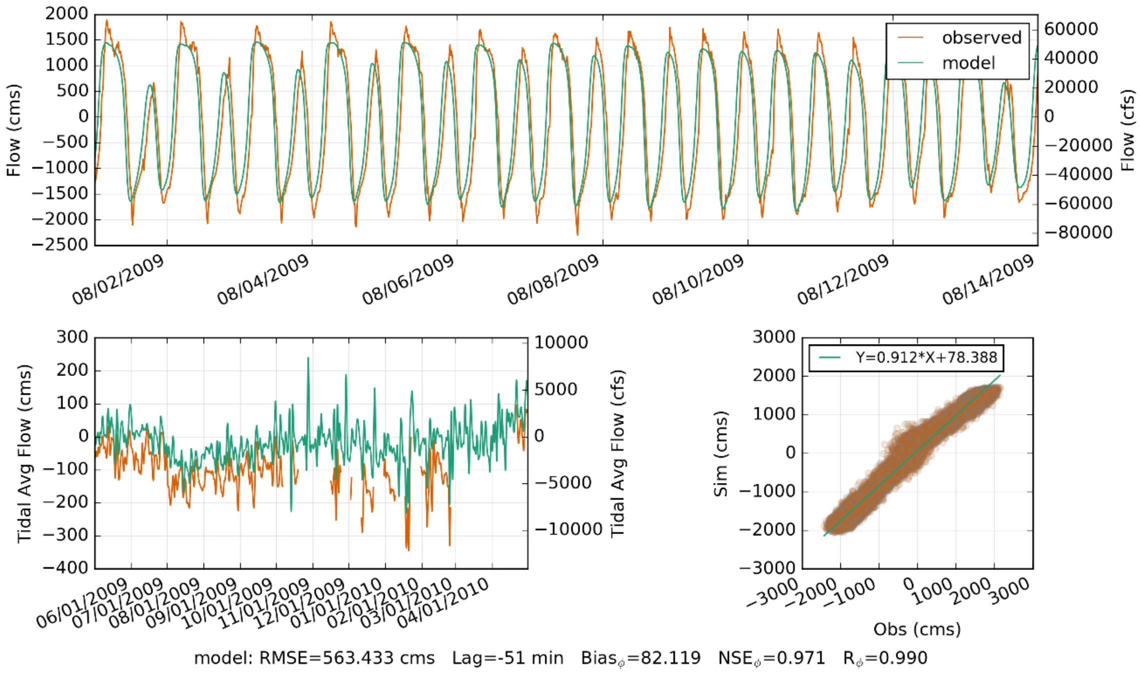

Source: U.S. Geological Survey, identification number: 11313460

Notes: NSE = Nash-Sutcliffe efficiency, Obs = observed data, PRI = California Data Exchange Center code for San Joaquin River at Prisoners Point, R= correlation coefficient, RMSE = root mean square error, φ (subscript) indicates phase-corrected statistic

Figure 65 Flow Performance Plots and Metrics at Turner Cut (TRN)

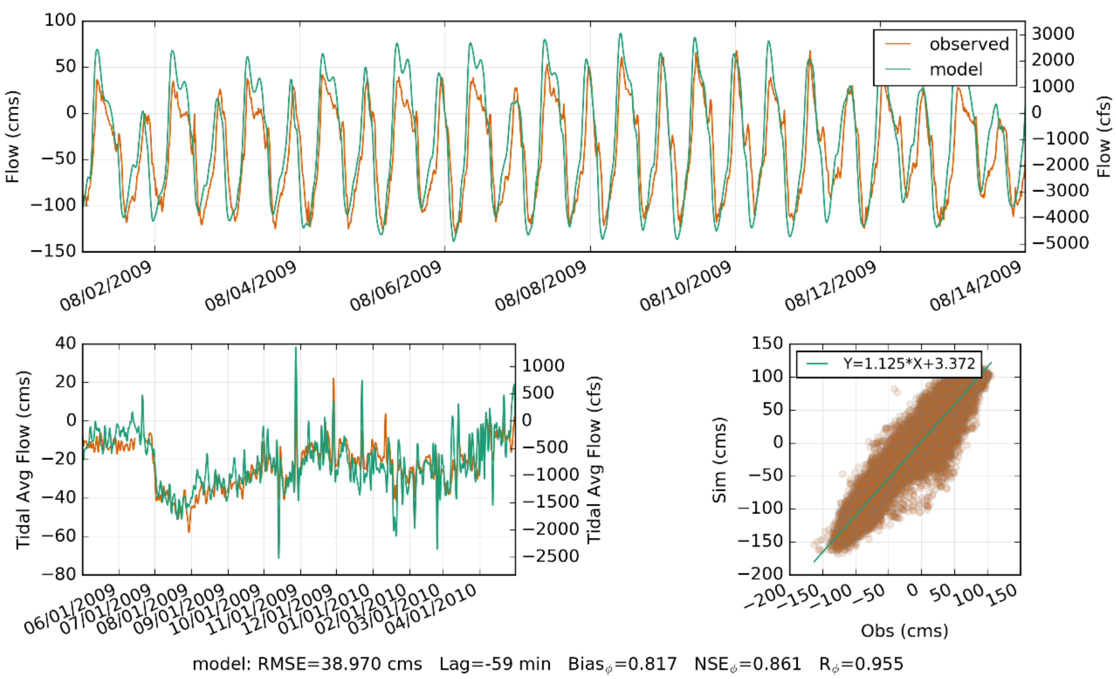

Source: U.S. Geological Survey, identification number: 11311300

Notes: NSE = Nash-Sutcliffe efficiency, Obs = observed data, R= correlation coefficient, RMSE = root mean square error, TRN = California Data Exchange Center code for Turner Cut near Holt, φ (subscript) indicates phase-corrected statistic

Figure 66 Flow Station Calibration Data and Model Output June 22, 2015, for Old River at Franks Tract

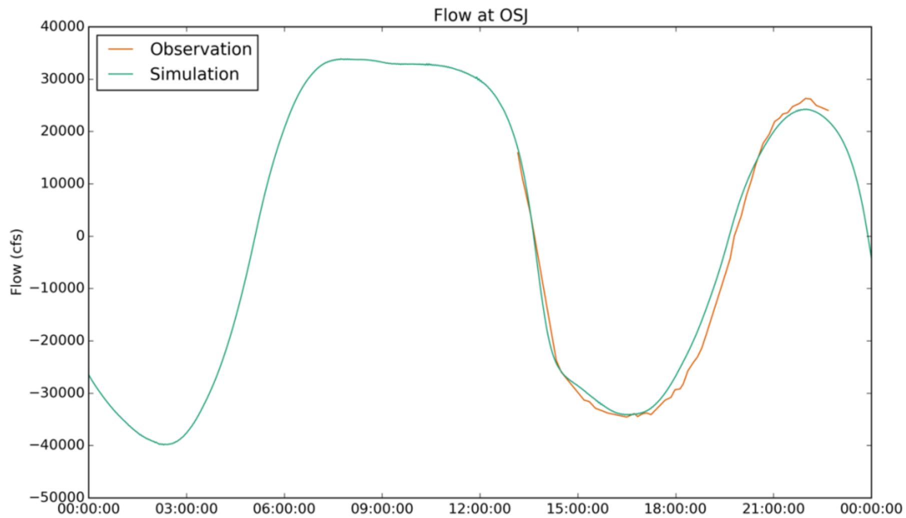

Note: Tidal range is double the normal because of the closure of the West False River Emergency Drought Barrier.

4.6 Salinity Calibration Plots and Metrics

Salinity metrics are given for the stations marked in Figure 47 with a circle. The units of the time series plots are in practical salinity units (psu) on the left axes and conductance (µS/cm) on the right axes. The label *EC* on the conductance label refers to electrical conductivity, which is a term often applied to observations of specific conductance in Delta technical and regulatory language.

From the bottom left plots, it seems the model is able to reproduce salinity intrusion and San Joaquin River influences sufficiently well, except in January 2010. At that point, it is believed there was an outflow reduction in the field that is not captured in the channel depletion/accretion estimates.

The tendency during the instantaneous plotting window is toward overestimation, but the error is small compared to tidal range and compared to uncertainties posed by outflow. Old River at Bacon Island has the highest overestimation during the fall period and instantaneous plot window (12 percent–18 percent), but the longer-term time trends at that station are still reproduced with sufficient accuracy. There is some phase lead in a number of the plots, including the ones with reliable time stamping. CDEC data have timestamps that can be incorrect by an hour or more because of practices surrounding daylight saving time conversions.

Figure 67 Salinity Performance Plots and Metrics at Mallard Island Upper Sensor (MAL)

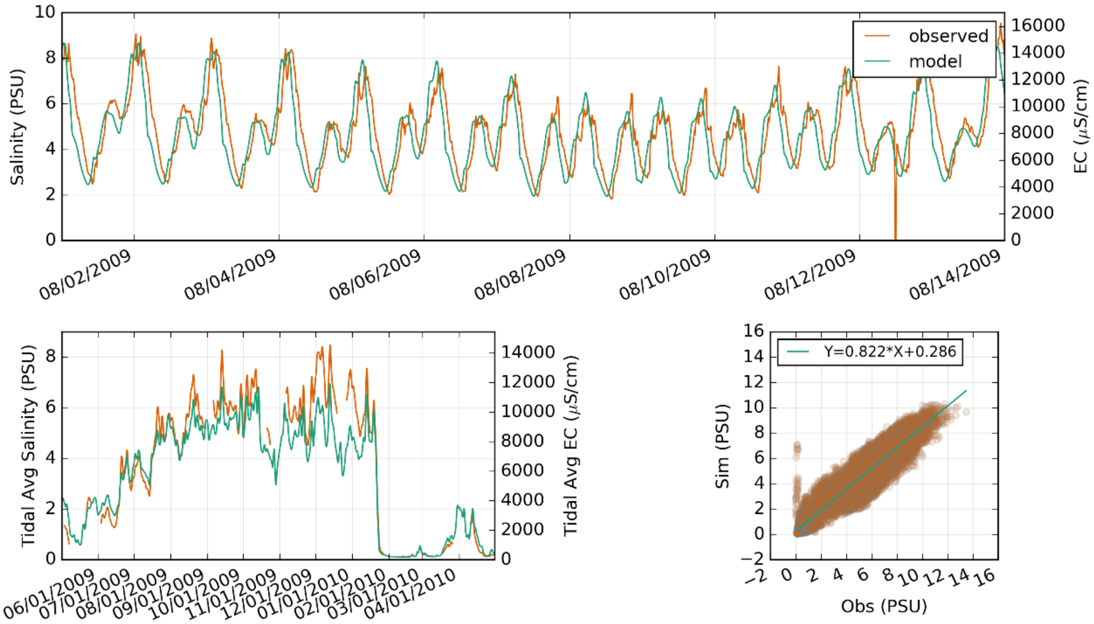

model: RMSE=1.066 PSU Lag=-63 min Bias$_{\phi}$=-0.105 NSE$_{\phi}$=0.898 R$_{\phi}$=0.962

Source: California Department of Water Resources

Notes: EC = electrical conductivity, MAL = California Data Exchange Center code for Mallard Island, NSE = Nash-Sutcliffe efficiency, Obs = observed data, R= correlation coefficient, PSU = practical salinity units, RMSE = root mean square error, φ (subscript) indicates phase-corrected statistic

Figure 68 Salinity Performance Plots and Metrics at Mallard Island Lower Sensor (MAL)

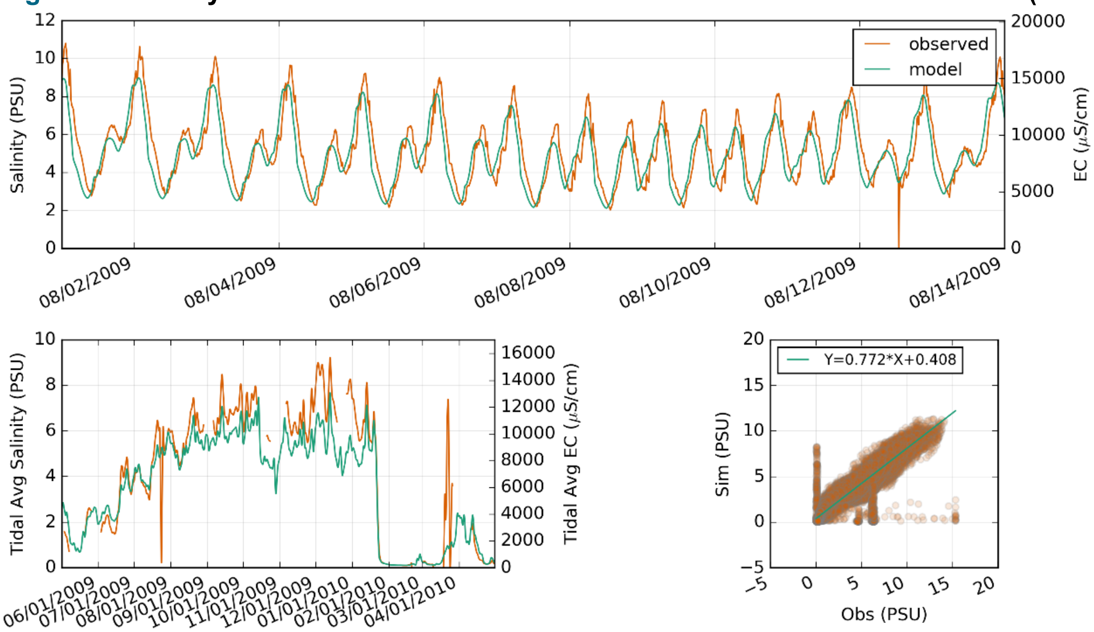

model: RMSE=1.371 PSU Lag=-45 min Bias$_{\phi}$=-0.226 NSE$_{\phi}$=0.834 R$_{\phi}$=0.934

Source: California Department of Water Resources

Notes: EC = electrical conductivity, MAL = California Data Exchange Center code for Mallard Island, NSE = Nash-Sutcliffe efficiency, Obs = observed data, R= correlation coefficient, PSU = practical salinity units, RMSE = root mean square error, φ (subscript) indicates phase-corrected statistic

Figure 69 **Salinity Performance Plots and Metrics at Antioch Upper Sensor (ANH)**

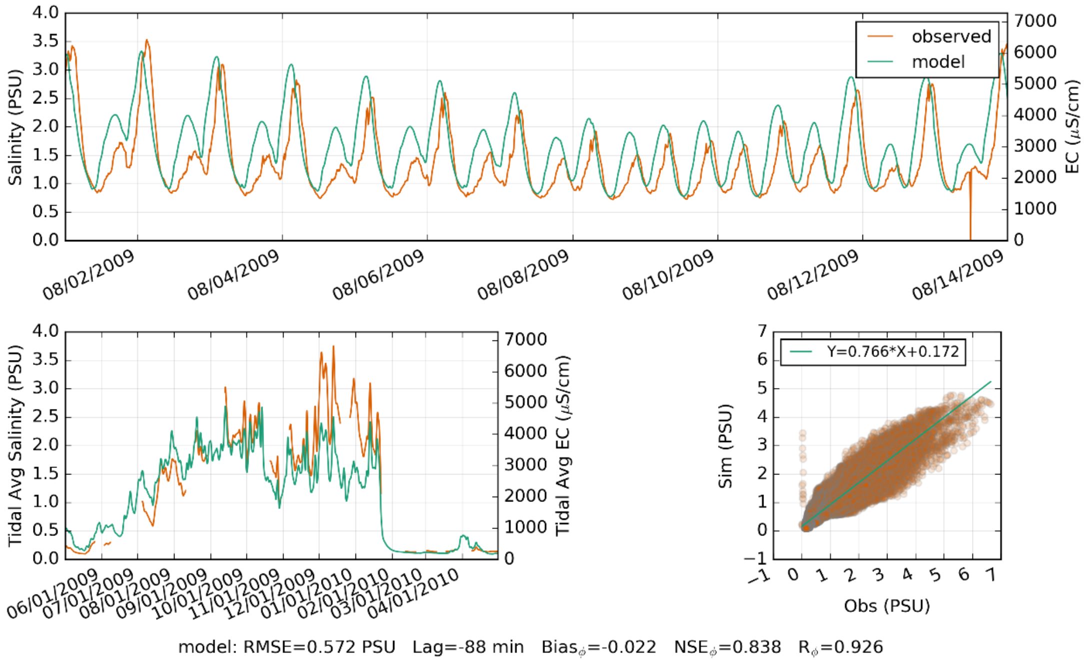

Source: California Department of Water Resources

Notes: ANH = California Data Exchange Center code for San Joaquin River at Antioch, EC = electrical conductivity, NSE = Nash-Sutcliffe efficiency, Obs = observed data, R= correlation coefficient, PSU = practical salinity units, RMSE = root mean square error, φ (subscript) indicates phase-corrected statistic

Figure 70 **Salinity Performance Plots and Metrics at Antioch Lower Sensor (ANH)**

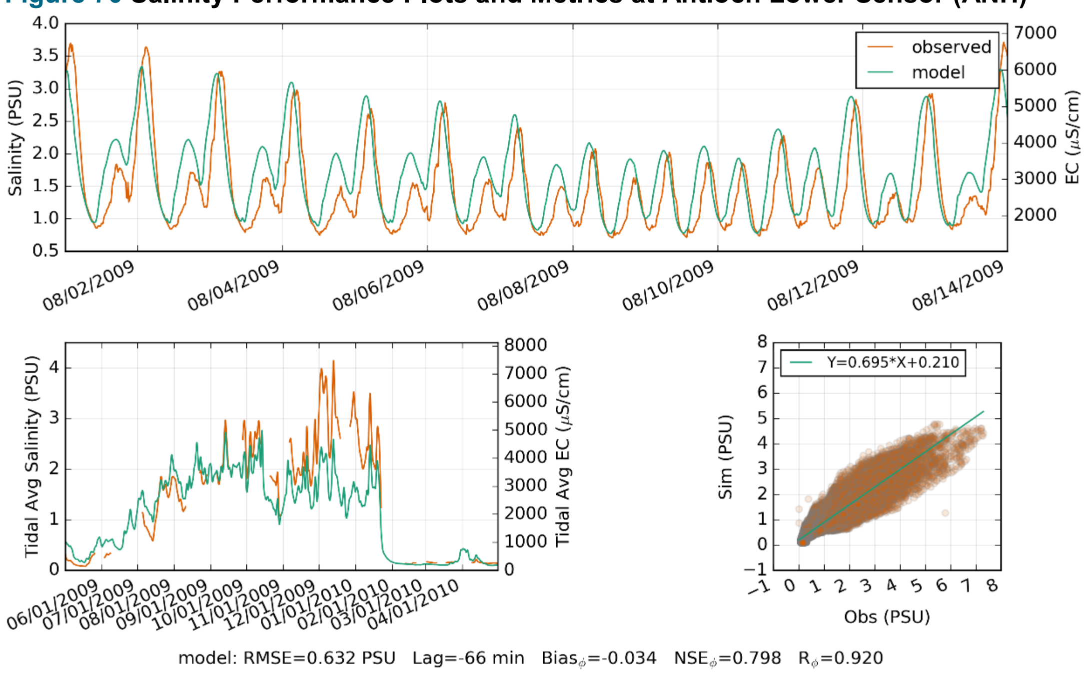

Source: California Department of Water Resources

Notes: ANH = California Data Exchange Center code for San Joaquin River at Antioch, EC = electrical conductivity, NSE = Nash-Sutcliffe efficiency, Obs = observed data, PSU = practical salinity units, R= correlation coefficient, RMSE = root mean square error, φ (subscript) indicates phase-corrected statistic

Figure 71 **Salinity Performance Plots and Metrics at Emmaton Upper Sensor (EMM)**

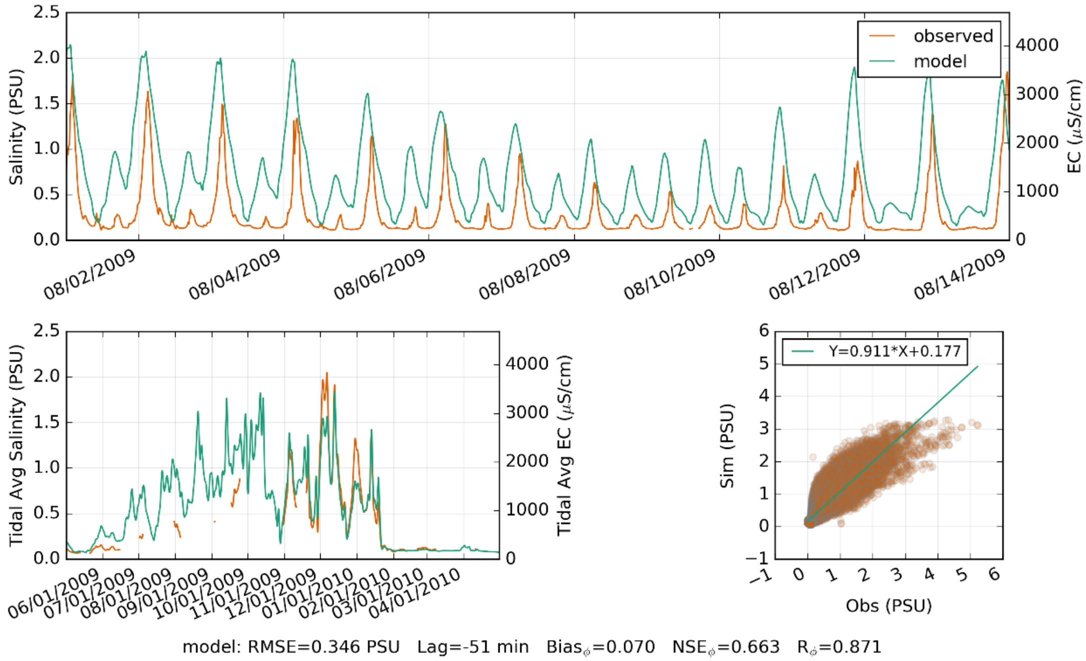

Source: California Department of Water Resources, Water Data Library identification number: B91120

Notes: EC = electrical conductivity, EMM = California Data Exchange Center code for Sacramento River at Emmaton, NSE = Nash-Sutcliffe efficiency, Obs = observed data, PSU = practical salinity units, R= correlation coefficient, RMSE = root mean square error, φ (subscript) indicates phase-corrected statistic

Figure 72 **Salinity Performance Plots and Metrics on the San Joaquin River at Jersey Point (JER)**

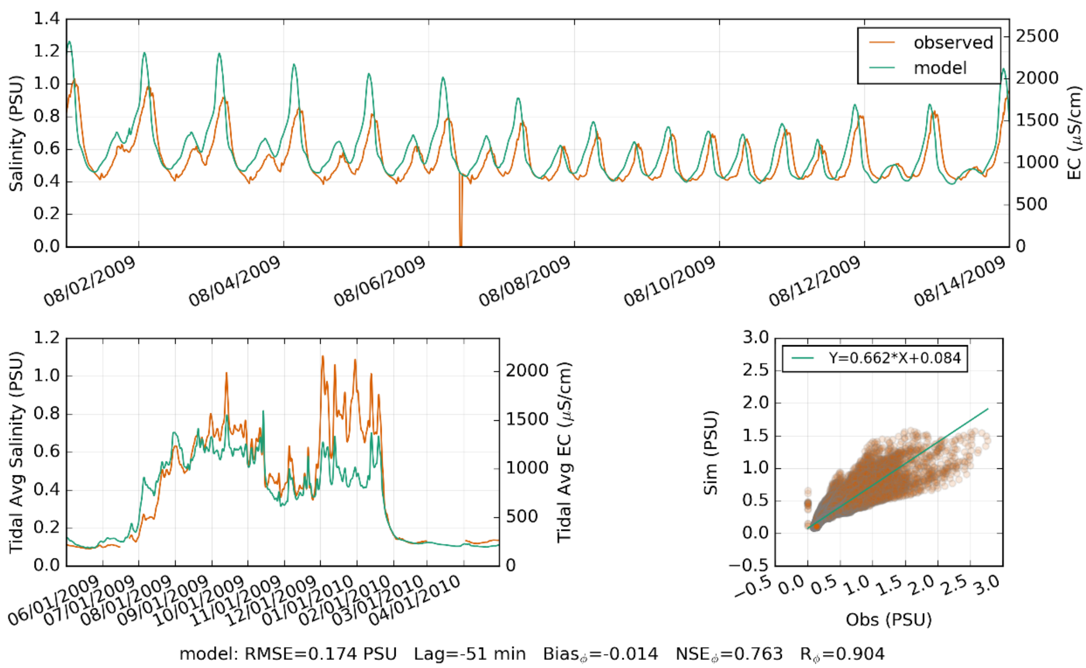

Source: U.S. Bureau of Reclamation

Notes: EC = electrical conductivity, JER = California Data Exchange Center code for San Joaquin River at Jersey Point, NSE = Nash-Sutcliffe efficiency, Obs = observed data, PSU = practical salinity units, R= correlation coefficient, RMSE = root mean square error, φ (subscript) indicates phase-corrected statistic

Figure 73 **Salinity Performance Plots and Metrics at Dutch Slough (DSJ)**

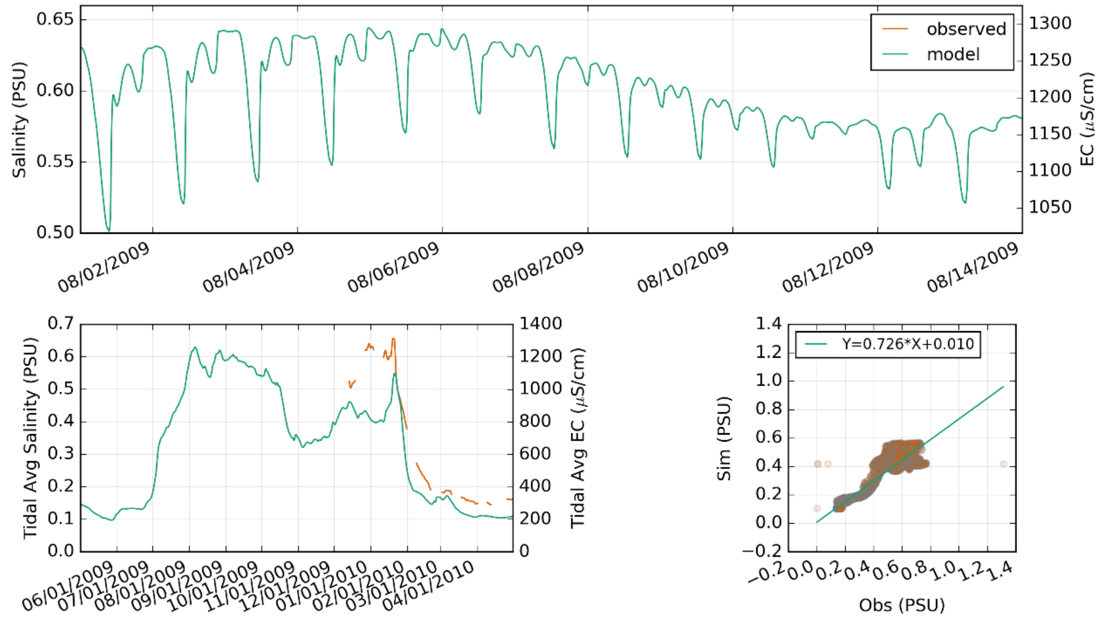

model: RMSE=0.106 PSU   Lag=-75 min   Bias$_{\phi}$=-0.052   NSE$_{\phi}$=0.701   R$_{\phi}$=0.956

Source: U.S. Geological Survey, identification number: 11313433

Notes: Station not available in 2009. DSJ = California Data Exchange Center code for Dutch Slough below Jersey Island, EC = electrical conductivity, NSE = Nash-Sutcliffe efficiency, Obs = observed data, PSU = practical salinity units, R= correlation coefficient, RMSE = root mean square error, φ (subscript) indicates phase-corrected statistic

Figure 74 **Salinity Performance Plots and Metrics at False River (FAL)**

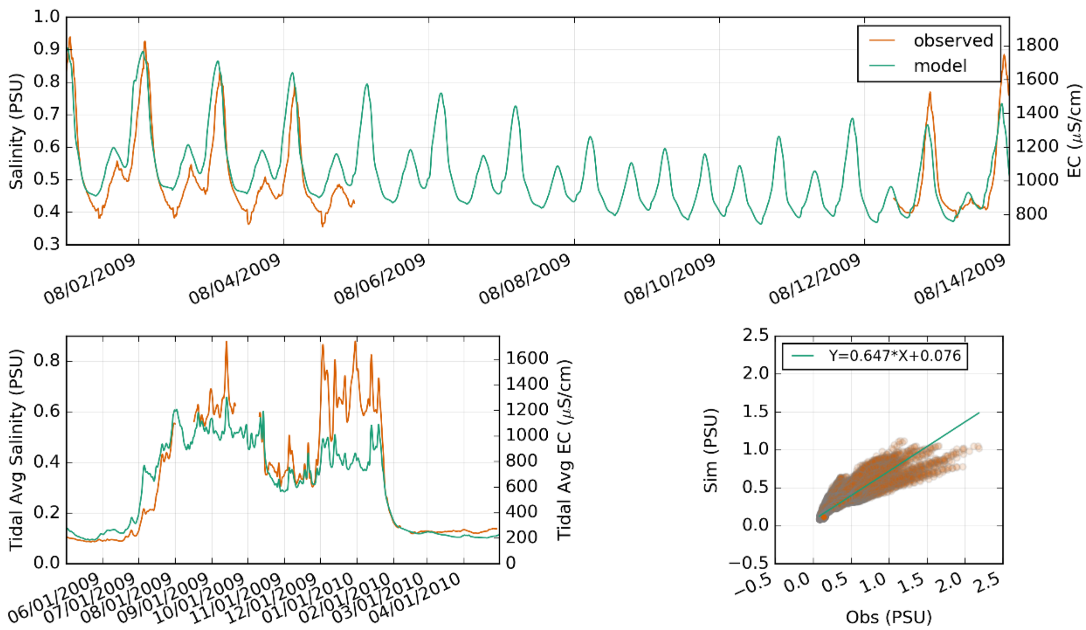

model: RMSE=0.134 PSU   Lag=-55 min   Bias$_{\phi}$=-0.013   NSE$_{\phi}$=0.767   R$_{\phi}$=0.914

Source: California Department of Water Resources, Water Data Library identification number: B9504400

Notes: EC = electrical conductivity, FAL = California Data Exchange Center code for False River near Oakley, NSE = Nash-Sutcliffe efficiency, Obs = observed data, PSU = practical salinity units, R= correlation coefficient, RMSE = root mean square error, φ (subscript) indicates phase-corrected statistic

Figure 75 **Salinity Performance Plots and Metrics at Holland Cut (HOL)**

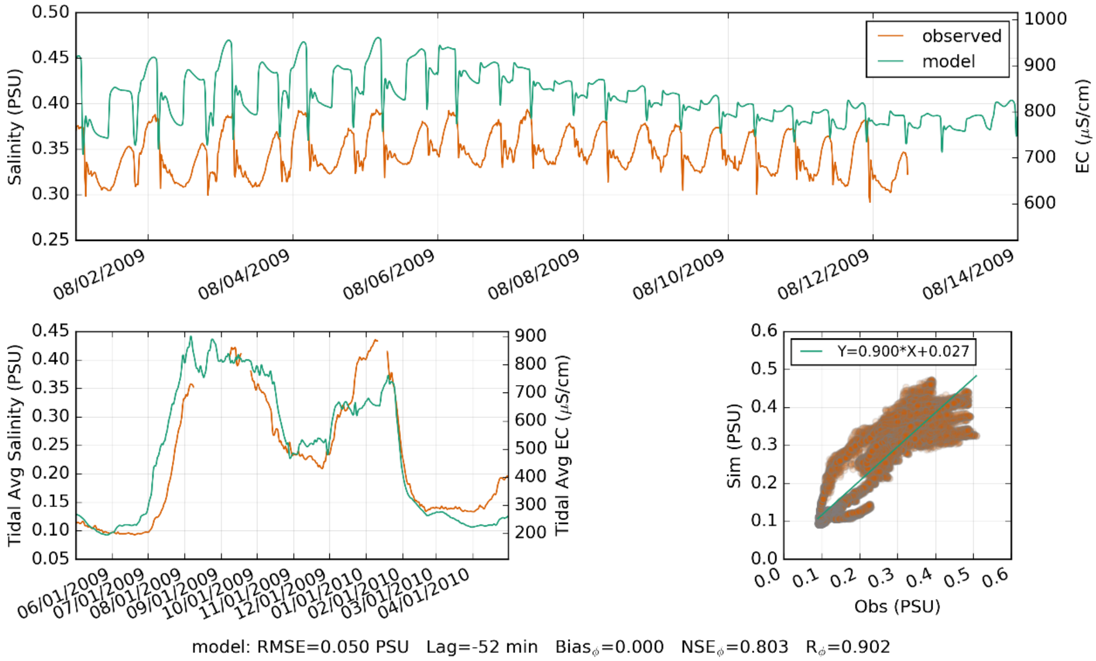

Source: California Department of Water Resources, Water Data Library identification number: B9512000
Notes: EC = electrical conductivity, HOL = California Data Exchange Center code for Holland Cut near Bethel Island, NSE = Nash-Sutcliffe efficiency, Obs = observed data, PSU = practical salinity units, R= correlation coefficient, RMSE = root mean square error, φ (subscript) indicates phase-corrected statistic

Figure 76 **Salinity Performance Plots and Metrics, Old River at Quimby Island (ORQ)**

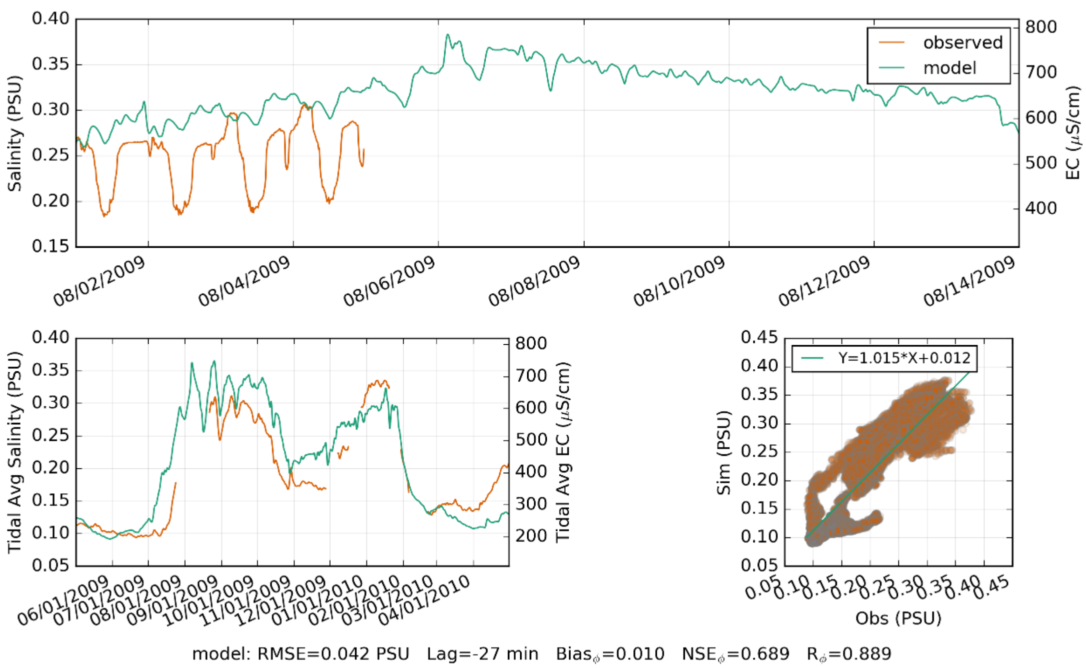

Source: California Department of Water Resources, Water Data Library identification number: B9520000
Notes: EC = electrical conductivity, NSE = Nash-Sutcliffe efficiency, Obs = observed data, ORQ = California Data Exchange Center code for Old River at Quimby Island, PSU = practical salinity units, R= correlation coefficient, RMSE = root mean square error, φ (subscript) indicates phase-corrected statistic

Figure 77 **Salinity Performance Plots and Metrics on Old River at Bacon Island (BAC)**

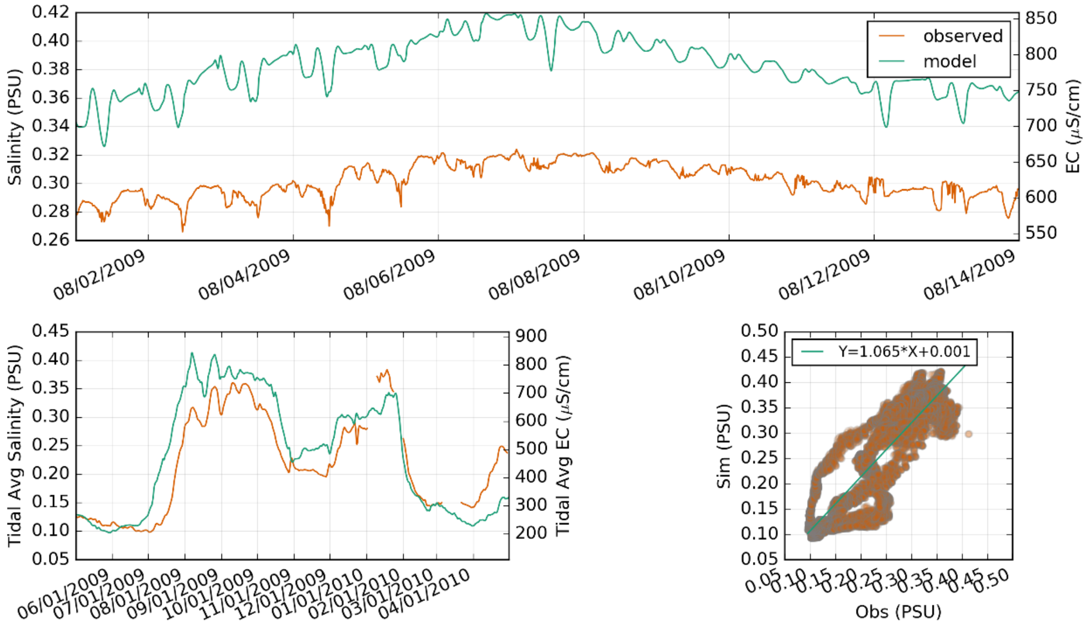

model: RMSE=0.049 PSU Lag=-63 min Bias$_\phi$=0.014 NSE$_\phi$=0.678 R$_\phi$=0.894

Source: California Department of Water Resources, Water Data Library identification number: B95250
Notes: BAC = California Data Exchange Center code for Old River at Bacon Island, EC = electrical conductivity, NSE = Nash-Sutcliffe efficiency, Obs = observed data, PSU = practical salinity units, R= correlation coefficient, RMSE = root mean square error, φ (subscript) indicates phase-corrected statistic

Figure 78 **Salinity Performance Plots and Metrics on Middle River (MDM)**

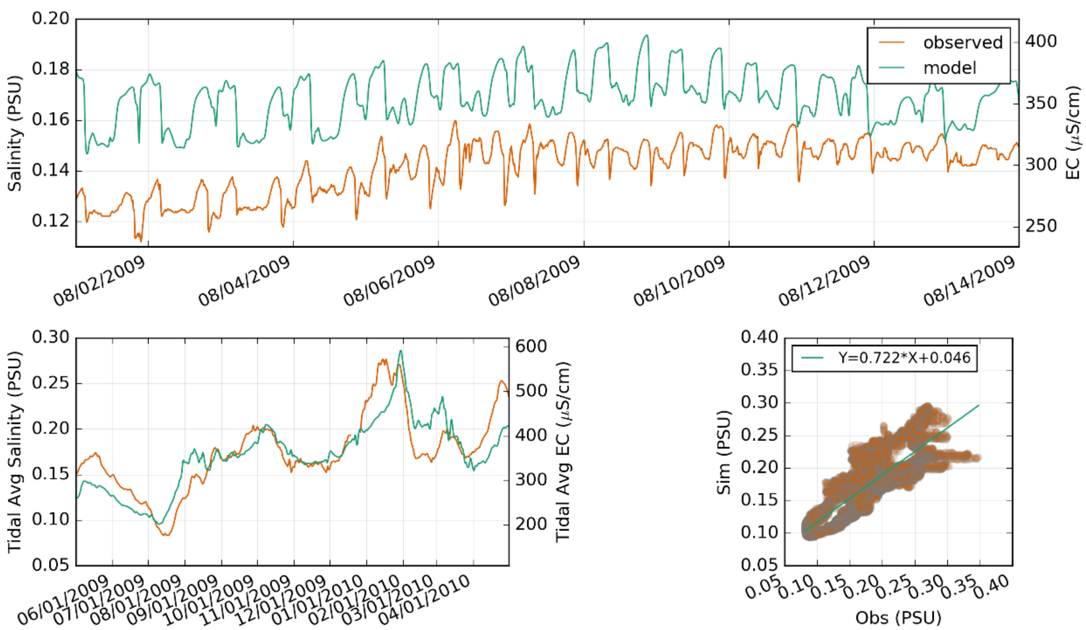

model: RMSE=0.025 PSU Lag=5 min Bias$_\phi$=-0.002 NSE$_\phi$=0.638 R$_\phi$=0.807

Source: California Department of Water Resources, Water Data Library identification number: B95468
Notes: EC = electrical conductivity, MDM = California Data Exchange Center code for Middle River at Middle River, NSE = Nash-Sutcliffe efficiency, Obs = observed data, PSU = practical salinity units, R= correlation coefficient, RMSE = root mean square error, φ (subscript) indicates phase-corrected statistic

Figure 79 **Salinity Performance Plots and Metrics on Old River at Franks Tract (OSJ)**

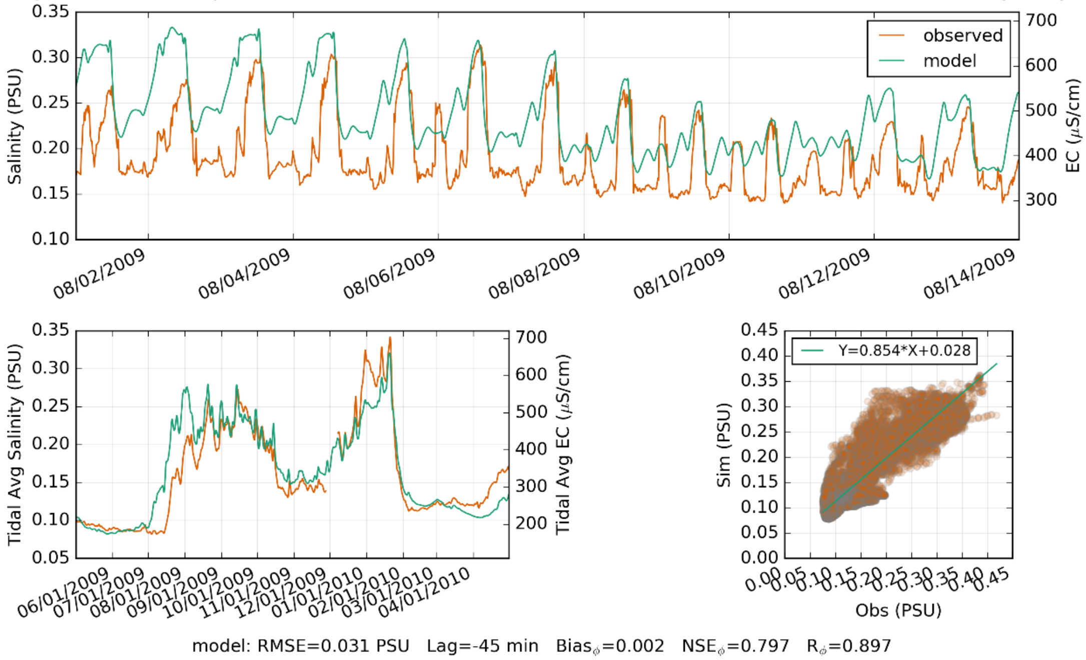

Source: California Department of Water Resources, Water Data Library identification number: B9510800

Notes: EC = electrical conductivity, NSE = Nash-Sutcliffe efficiency, Obs = observed data, PSU = practical salinity units, R= correlation coefficient, OSJ = California Data Exchange Center code for Old River at Franks Tract, RMSE = root mean square error, φ (subscript) indicates phase-corrected statistic

Figure 80 **Salinity Performance Plots and Metrics on the San Joaquin River at Prisoners Point (PPT)**

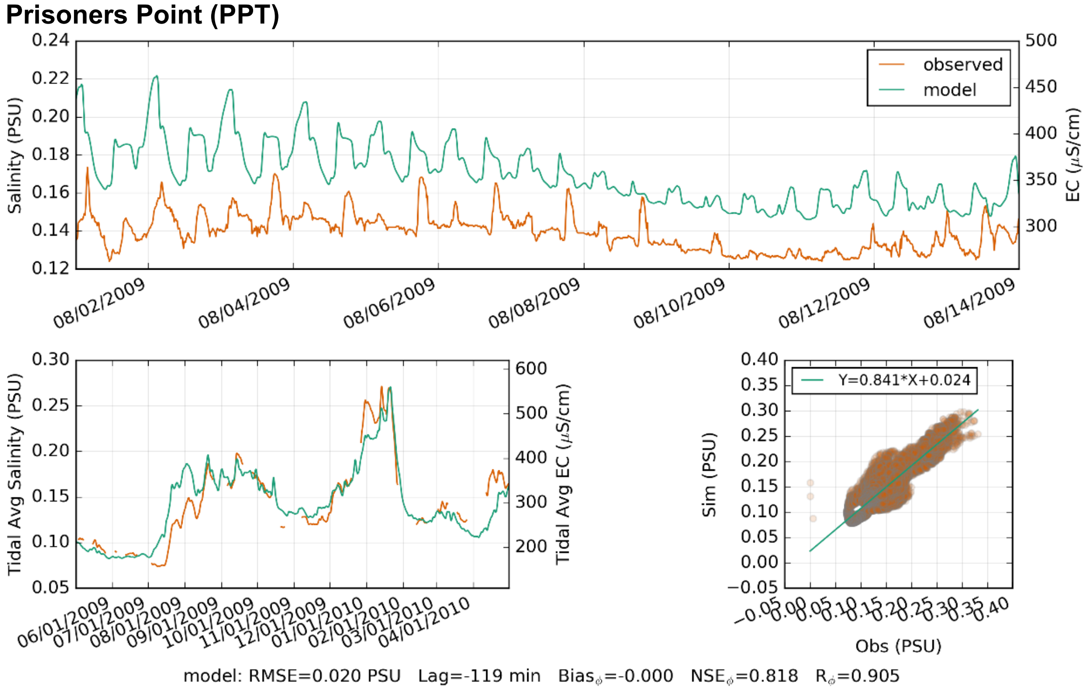

Source: California Data Exchange Center

Notes: EC = electrical conductivity, NSE = Nash-Sutcliffe efficiency, Obs = observed data, R= correlation coefficient, PPT = California Data Exchange code for San Joaquin River at Prisoners Point, PSU = practical salinity units, RMSE = root mean square error, φ (subscript) indicates phase-corrected statistic

Figure 81 Salinity Performance Plots and Metrics on the San Joaquin at San Andreas Landing (SAL)

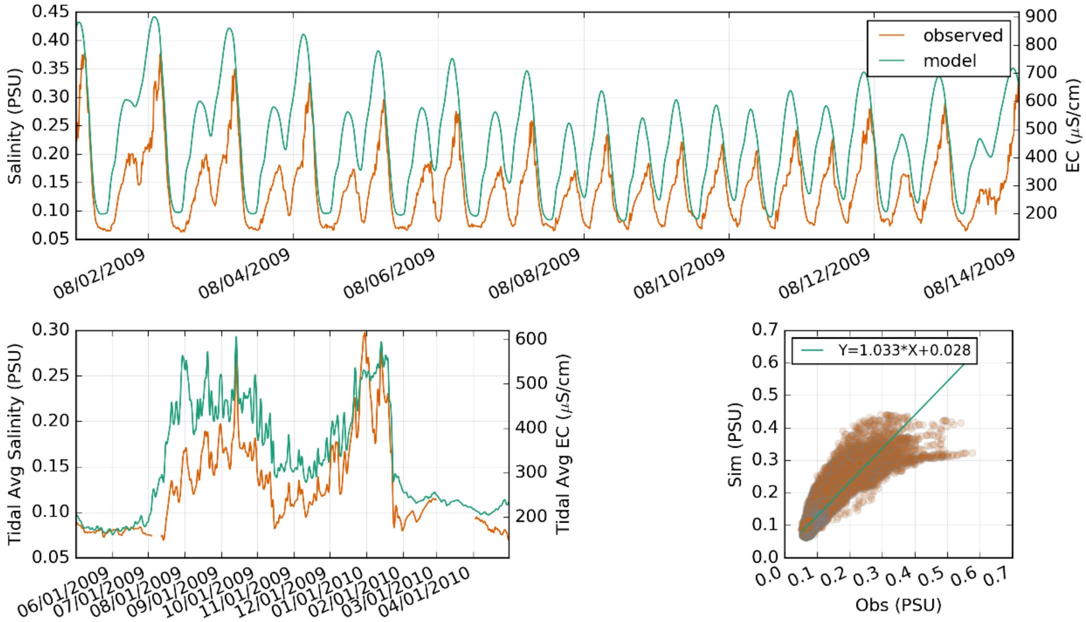

model: RMSE=0.050 PSU Lag=-57 min $Bias_{\phi}$=0.023 NSE_{ϕ}=0.407 R_{ϕ}=0.875

Source: California Data Exchange Center

Notes: EC = electrical conductivity, NSE = Nash-Sutcliffe efficiency, Obs = observed data, PSU = practical salinity units, R= correlation coefficient, RMSE = root mean square error, SAL = California Data Exchange Center code for San Andreas Landing, φ (subscript) indicates phase-corrected statistic

Figure 82 Salinity Performance Plots and Metrics at Turner Cut (TRN)

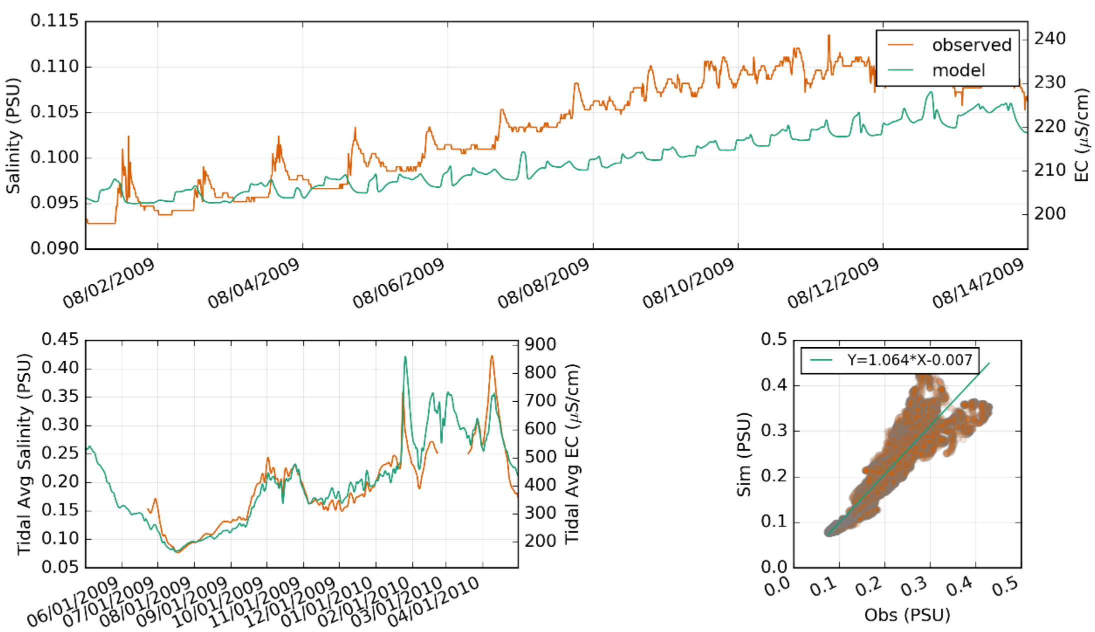

model: RMSE=0.033 PSU Lag=-45 min $Bias_{\phi}$=-0.001 NSE_{ϕ}=0.766 R_{ϕ}=0.914

Source: California Department of Water Resources, Water Data Library identification number: B9561600

Notes: EC = electrical conductivity, TRN = California Data Exchange code for Turner Cut near Holt, NSE = Nash-Sutcliffe efficiency, Obs = observed data, PSU = practical salinity units, R= correlation coefficient, RMSE = root mean square error, φ (subscript) indicates phase-corrected statistic

Chapter 5. References

Ateljevich E, Nam K, Zhang Y, Wang R, Shu Q. 2014. “Bay-Delta SELFE calibration overview.” In: Methodology for Flow and Salinity Estimates in the Sacramento-San Joaquin Delta and Suisun Marsh. 35th Annual Progress Report to the State Water Resources Control Board. Chapter 7. Sacramento (CA): Bay-Delta Office. Delta Modeling Section. California Department of Water Resources.

Ateljevich E, Tu M-Y, Le, K. 2015. “Calculation Clifton Court Forebay inflow and re-rating the forebay gates.” In: Methodology for Flow and Salinity Estimates in the Sacramento-San Joaquin Delta and Suisun Marsh. 36th Annual Progress Report to the State Water Resources Control Board. Chapter 6. Sacramento (CA): Delta Modeling Section. California Department of Water Resources.

Chao, Y., Farrara, J.D., Bjorkstedt, E., Chai, F., Chavez, F., Rudnick, D., Enright, W., Fisher, J.L., Peterson, W.T., Welch, G.F., Davis, C.O., Dugdale, R.C., Wilkerson, F.P., Zhang, H., Zhang, Y., Ateljevich, E. 2017. The origins of the anomalous warming in the California coastal ocean and San Francisco Bay during 2014-2016, J. Geophysical Research-Oceans. DOI: 10.1002/2017JC013120

California Department of Water Resources (in preparation) Efficacy Report: 2015 Emergency Drought Barrier (EDB) Project.

California Department of Water Resources. 2016, Water Data Library data available on the World Wide Web (WDL), accessed June 2016, at: http://www.water.ca.gov/waterdatalibrary/.

California Department of Water Resources. 2017, California Data Exchange Center data available on the World Wide Web (CDEC), accessed June 2016, at: http://cdec.water.ca.gov.

Kimmerer WJ, Nobriga ML. 2008. Investigating Particle Transport and Fate in the Sacramento-San Joaquin Delta Using a Particle-Tracking Model, San Francisco Estuary and Watershed Science: 6(11). Journal on the World Wide Web, at https://escholarship.org/uc/item/547917gn, accessed November 1, 2017.

Large WG, Pond S. 1981. Open Ocean Momentum Flux Measurements in Moderate to Strong Winds, Journal of Physical Oceanography:11(3), pp. 324-336.

MacWilliams, Michael L.; Ateljevich, Eli S.; Monismith, Stephen G.; & Enright, Chris. (2016). An Overview of Multi-Dimensional Models of the Sacramento–San Joaquin Delta. San Francisco Estuary and Watershed Science, 14(4). jmie_sfews_33445. Retrieved from: http://escholarship.org/uc/item/31r7x1js

MacWilliams, Michael L.; & Gross, Edward S. (2013). Hydrodynamic Simulation of Circulation and Residence Time in Clifton Court Forebay. San Francisco Estuary and Watershed Science, 11(2). jmie_sfews_11167. Retrieved from: http://escholarship.org/uc/item/4q82g2bz National Oceanic and Atmospheric Administration. 2016.

Moffatt & Nichol. 2017. *Franks Tract Engineering Feasibility Assessment.* Walnut Creek [CA]: Prepared by: Moffatt & Nichol. Prepared for: Metropolitan Water District of Southern California. 78 pp.

National Oceanic and Atmospheric Administration Tides and Current Data available on the World Wide Web, accessed June 2016 at URL https://tidesandcurrents.noaa.gov/.

Research Management Associates. 2005. Flooded islands pre-feasibility study RMA delta model calibration report. Technical report, Prepared For: California Department of Water Resources For Submittal To California Bay-Delta Authority.

Sandhu N, Suits B, Ateljevich E, Zhong L, Kadir, T. 2016. “On Estimating Net Delta Outflow (NDO): Approaches to estimating NDO in the Sacramento-San Joaquin Delta.” DWR.

Schraga T, Cloern J. 2017.Water Quality Measurements in San Francisco Bay by the U.S.Geological Survey, 1969-2015. Scientific Data 4:170098 doi:10.1038/sdata.2017.98.

Shu Q, Ateljevich E. 2017. Clifton Court Forebay Transit Time Modeling Analysis. DWR report prepared for the National Marine Fisheries Service.

Smith, P. 2011. Notes on Estimating Flow through the Clifton Court Forebay Radial Gates. Memo from P. Smith, USGS to Katherine Kelly, DWR Bay-Delta Office.

Song Y and Haidvogel DB. 1994. “A semi-implicit ocean circulation model using a generalized topography-following coordinate.” Journal of Computational Physics. 115(1). pp. 228-244.

Umlauf L and Burchard H. 2003. “A generic length-scale equation for geophysical turbulence models.” Journal of Marine Research. 61(2)6. pp. 235–265.

U.S. Geological Survey. 2016, National Water Information System data available on the World Wide Web (NWIS), accessed June 2016, at URL http://waterdata.usgs.gov/nwis/.

Ustin, S, Khanna S, Bellvert J, Boyer JD, Shapiro K. 2016. Impact of drought on Submerged Aquatic Vegetation (SAV) and Floating Aquatic Vegetation (FAV) using AVIRIS-NG airborne imagery. California Department of Fish and Wildlife.

Wang R, Ateljevich E. 2012. A Continuous Surface Elevation Map for Modeling (Chapter 6). In Methodology for Flow and Salinity Estimates in the Sacramento-San Joaquin Delta and Suisun Mars, 23rd Annual Progress Report to the State Water Resources Control Board. California Department of Water Resources, Bay-Delta Office, Delta Modeling Section.

Zhang Y, Ateljevich E, Yu HS, Wu CH, Yu J. 2015. “A new vertical coordinate system for a 3D unstructured-grid model.” Ocean Modelling. 85. pp. 16-31.

Zhang Y, Baptista AM. 2008. “SELFE: A semi-implicit Eulerian-Lagrangian finite-element model for cross-scale ocean circulation.” Ocean Modelling. 21(3-4). pp. 71-96.

Zhang Y, Ye F, Stanev EV, Grashorn S. 2016. “Seamless cross-scale modeling with SCHISM. Ocean Modelling.” 102. pp. 64-81.

DEPARTMENT OF WATER RESOURCES
STATE OF CALIFORNIA